Graz University of Technology

Thesis to get the degree of a Diplomingenieur, equivalent to a

Master of Science

Development of a Risk Estimation Model of Motorcycle Accidents on Rural Roads

by

Ewald Benes

This master's thesis has been conducted at the Vehicle Safety Institute, a member of Frank Stronach Institute at Graz University of Technology

Head of the Department: Univ.-Prof. Dipl. Ing. Dr. techn. Hermann Steffan

Supervisors: Dipl. Ing. Dr. techn. Wolfgang Sinz, Heinz Hoschopf

October 2012

VSI
Vehicle Safety Institute

Deutsche Fassung:
Beschluss der Curricula-Kommission für Bachelor-, Master- und Diplomstudien vom 10.11.2008
Genehmigung des Senates am 1.12.2008

EIDESSTATTLICHE ERKLÄRUNG

Ich erkläre an E ides statt, dass ich die vorliegende Arbeit selbstständig verfasst, andere als die angegebenen Quellen/Hilfsmittel nicht benutzt, und die den benutzten Quellen wörtlich und inhaltlich entnommenen Stellen als solche kenntlich gemacht habe.

Graz, am 30.10.2012 ……..
(Unterschrift)

Englische Fassung:

STATUTORY DECLARATION

I declare that I have authored this thesis independently, that I have not used other than the declared sources / resources, and that I have explicitly marked all material which has been quoted either literally or by content from the used sources.

10/30/2012 ……..
date (signature)

Acknowledgment

I wish to thank, first and foremost, my Professor Hermann Steffan, my supervisors, Wolfgang Sinz and Heinz Hoschopf, to make this thesis possible. By means of their deep knowledge and the great attitude they brought to me I was able to carry out this study and to keep on working when times were hard.

I am indebted to my parents who have always been showing sympathy for my studies and paved the way to achieve to be here. Furthermore it gives me great pleasure to acknowledge the help of my colleagues and friends, especially Michael Haderspock, during my career.

Contents

Abstract

This master's thesis studies the capability of predicting single-vehicle accidents of motorcycles on rural roads in Austria by an easy-to-use hybrid statistical and physical model. Over the years, motorcycle accident counts in Austria decreased slightly. Particular countermeasures such as adapted road design, infrastructure or restraint systems at certain locations might be necessary to further decrease those accident counts. The locations where countermeasures might be carried out efficiently are not always apparent when roads are going to be designed. Therefore it can save costs being able to anticipate those accident locations and eventually prevent accidents before they actually take place. Accident statistics of well-known high-risk motorcycle roads are used to extract significant risk variables that form the base of the forecast. The calculated prediction is cross-checked with the accident location at the existing high-risk roads. A simple physical motorcycle model is taken to discuss the statistical part by comparing the roll angle, speed and friction at the simulated and real accident locations. At the end some open questions, improvements and extension approaches are raised that might be the scope for further studies.

Zusammenfassung

Diese Diplomarbeit beschäftigt sich mit der Vorhersage von Motorradalleinunfällen auf Freilandstraßen in Österreich mithilfe eines einfachen statistischen und physikalischen Modells. Die Motorradunfallzahlen in Österreich sind in den letzten Jahren leicht sinkend. Um diese Zahl in der Zukunft weiter zu verringern, sind weitere Maßnahmen wie angepasste Straßenführung, Infrastruktur oder Rückhaltesysteme notwendig. Für neue Straßenabschnitte kann es effizient und kostensparend sein, Unfallorte vorhersagen zu können und damit Unfälle im Vorhinein schon mit einer risikoverminderten Straßenführung zu verhindern. Unfallstatistiken von Hochrisikostrecken werden verwendet und daraus riskobeeinflussende Parameter isoliert, die die Grundlage für das Model bilden. Die simulierte Prognose der Unfallstellen wird mit den realen Unfällen auf den vorher gewählten Hochrisikostraßen verglichen. Ergänzend wird ein einfaches physikalisches Motorradmodell ausgearbeitet und dessen Ergebnisse aufgrund von Vorgaben mit dem statistischen verglichen. Als letztes werden offene Fragen und Ansätze für Verbesserungen und Erweiterungen aufgeworfen, die als Grundlage für weitere Untersuchungen dienen können.

1. Introduction

Accidents, may it be a car, a motorcycle or any other vehicle, is a tragedy for any human that suffers from it. At the beginning of vehicle ownership and until the eighties of the 20^{th} century, accident mortality rates were high compared to these days. A lot of effort has been put into making roads safer for motorcycles and to decrease accident counts and fatalities over the past decades. Statistics reflect the effort and accident counts fell. Also the count of dead persons in motorbike accidents declined. An overall stagnation of fatality counts has occurred in the last decade. The count of injured persons in accidents is slightly falling in the last three years [5].

Nonetheless, according to statistics [3, cf. p. 3] the motorcycle remains one of the most dangerous vehicles and the risk being killed in an accident is several times higher than being killed in a car accident. The non-existing crush zone, high performance-mass-ratios, in many cases little riding experience and the labile equilibrium make the riding behavior of a motorcycle totally different but also more experiencing compared to a car.

A mixture of different actions are done to make motorcycle riding safer on Austrian roads. Riders are more sensitized for the risk when doing the driving test and compulsory programs to enhance the riders' capabilities on their bikes are appended after getting the driver's license. Those active countermeasures are very important to show up the main differences to a car. The environment is another essential variable. Different roads may imply varying risks because of sharp curves or non-existing free space to damper the kinetic energy of a vehicle. When an accident happens passive systems such as restraint systems or even just a free zone can make the difference between life and death. Many keywords mentioned may point out the complex interacting aspects of having an accident or even worse getting killed in it.

1.1 Conceptual Formulation

Currently, from 2007 to 2011, more than 3.000 motorcycle crashes are registered anually in Austria. Around 100 of them die in an accident or from the causes of it. Although the death rate has been declining slightly in the last three years, a further decrease may not be the case in the future as oscillating death rates had shown in the years before [5].

As stated, the effort that is put into road safety issues from the authorities is high. Many experts are involved. They assess the necessity of the countermeasures and actions with respect to many aspects including financial ones. Funds are limited and certain countermeasure may not achieve the goal that was expected. In some cases there may lack profound knowledge about motorcycle risks to do the right for adding security.

For this reason a model that predicts potential risk sites should be proposed. The model should fill the gap between simple factors that may lead to an accident and the actual countermeasure that is going to be evaluated after detecting high-risk locations for motorbikes. Upon the basis of the output of the model, actual countermeasures should be able to be decided easier and in a more cost-effective manner. At the same time a few variables only should be necessary to keep it simple to use and easy to understand. Simple future maintainance of the model without profound knowledge should be possible since non-motorcycle-experienced persons should be able to make decisions based on the forecast.

1.2 Motorcycle Accident Statistics

Statistics about motorcycle accidents and road accidents in general are well available. By means of those statistics, an overview about the dimension and the importance of this topic might be illustrated.

Total accident counts (not only motorcycle accidents) in Austria are compared with other countries being members of the EU. Austria is average in the area of accident numbers. 60 to 80 fatalities per one million inhabitants spread over all vehicle types take place in Austria according to figure 1.1. Countries where this measure is less, under 40 fatalities per one million inhabitants, exist like Great Britain, Sweden and

Netherlands. Germany, Spain, Finnland, Ireland, Slovakia and Estonia have also less accidents than Austria ranging between 40 and 60 fatalities per one million inhabitants. Approximately the same fatality ratio have the countries Portugal, France, Italy, Czech Republic, Hungary, Belgium, Luxembourg, Slovenia and Cyprus including Austria. The countries that lie above are Poland, Lithuania, Latvia, Rumania, Bulgaria and Greece with 80 and above fatalities per one million inhabitants [4, p. 11].

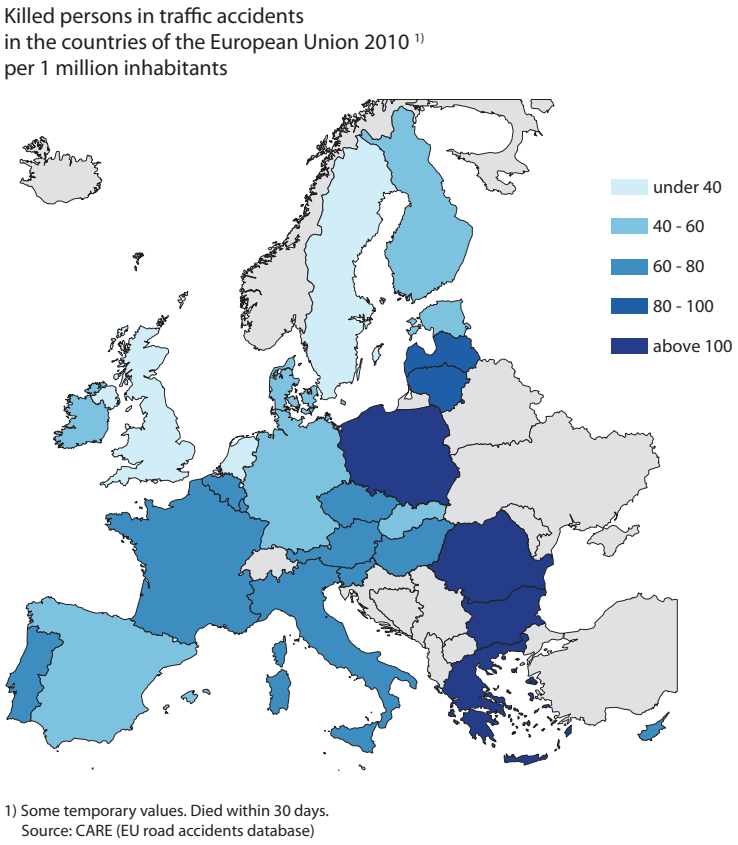

Figure 1.1: Overview of the total fatality rate per one million inhabitants in the EU [4, p. 11] in 2010.

Effort has been put into decreasing the accidents in the EU and aims were defined in the past. In figure 1.2 the decrease in percent of the total accident rate is itemized for each country of the EU. The actual average decline of all countries and the aim are shown as dotted lines. With respect to the country count, Austria's accident rate decrease is below the average. Statistics of Austria are also slightly under the European average and the EU's aim was not reached lacking 10 percent points with an actual 40

percent decrease.

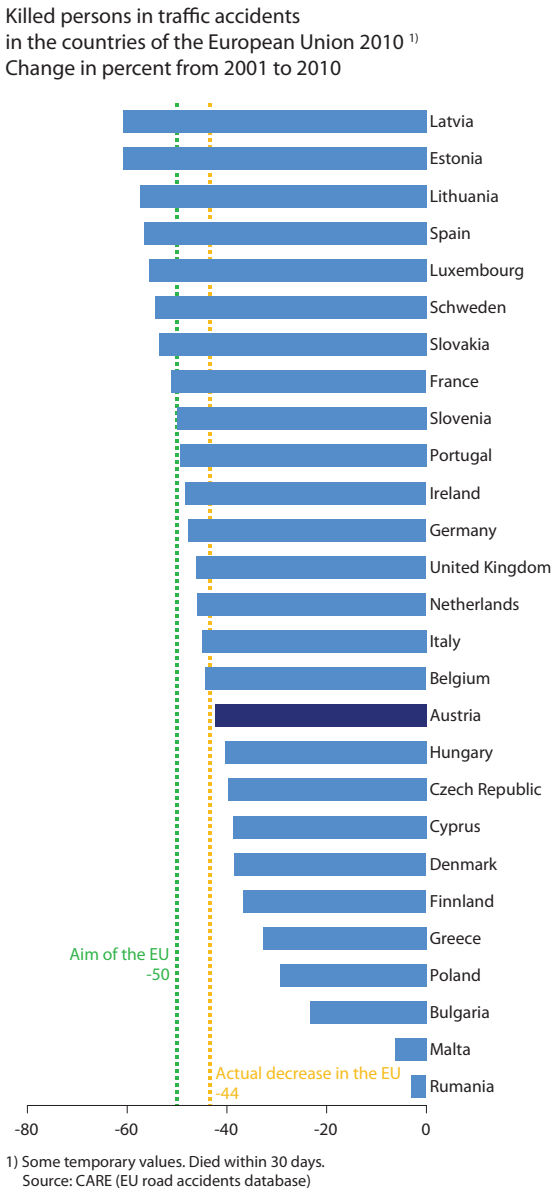

Figure 1.2: Overview of the actual accident decrease in the EU [4, p. 13] from 2001 to 2010 compared to the aim.

Having a look at the motorcycle accident development especially in Austria, figure 1.3 gives the overview about the total happened accidents using the measure on the left side and the diamonds. The killed riders amount in accidents is shown with the squares using the measure on the right side. The total accident count declined about more than 400 accidents starting from 2007 to 2010 and in 2011 finally shot up to nearly the same value as in 2007. Opposing to that, the amount of killed riders decreased continuously from 96 in 2007 to about 67 in 2011. It is a 30 percent decrease in five years.

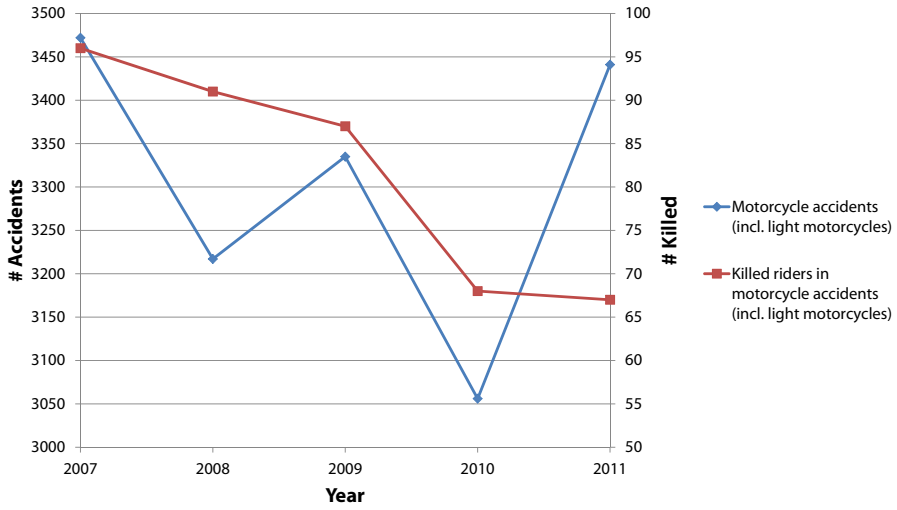

Figure 1.3: Development of motorcycle accidents from 2007 to 2011 in Austria [5].

For comparision of motorcycle and car accident counts, also statistics of car accidents are presented in the same period from 2007 to 2011. The total accident amount and the count of killed occupants in accidents are displayed in figure 1.4. The diamonds with the measure on the left side represent the total car accident count. An approximate linear fall from 33,315 in 2007 to 27,974 accidents in 2011 took place where the decrease is about 16 percent. The amount of killed occupants in car accidents is described by the squares and right side measure. Here also an overall decrease of about 23 percent was the case. When in 2007 378 persons died in car accidents it fell down to 290 persons in 2011.

To summarize between motorcycle and car accidents for the year 2011, 27,974 car accidents face 3,441 motorcycle accidents and 290 killed occupants in car accidents face 67 killed riders. Roughly one percent of the persons that have a car accident are killed. Nearly two percent of the motorcycle riders are killed in an accident and is approximatly twice as high as the risk of suffering death. Although the accidents in general as well as the killed persons in car and motorcylce accidents decreased, it can be seen that the motorcycle remains dangerous if comparing the mortality when having an accident.

An important factor of an accident is the type. It means in which circumstances the accident occurred. In figure 1.5 the accident types of motorcycle accidents are broken down into five and represent the state in 2011 in Austria. One third of all accidents

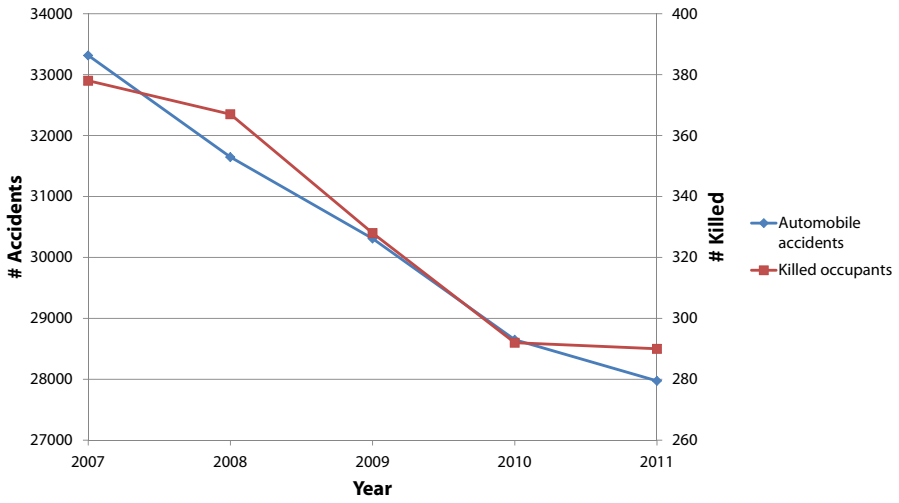

Figure 1.4: Development of car accidents in Austria from 2007 to 2011 [5].

are junction crashes. 25 percent form crashed with other vehicles on the same lane or with the oncoming traffic. The single vehicle accidents compose the highest part with 42 percent. Those accidents occur without the evident involvement of another vehicle.

The single vehicle accidents are addressed in this study. By trying to reduce this type of accidents the a potential is about 28 fatalities per year [5].

1.3 Infrastructural Countermeasures

Two types of countermeasures, active and passive ones, can be distinguished. Infrastructurally seen, in order to lower the risk of accidents for motorcycle riders different actions are available requiring different effort put into. Such actions might be

- restoring the road surface.
- removing environmental influences that soil the road.
- optimizing the road run (might not be possible due to the terrain).
- removing obstacles that hinder the view of the rider.

Those countermeasures are active ones that can avoid accidents in advance.

Passive countermeasures are those that can reduce the severity of injuries. They act when accidents are about to occur and are not avoidable anymore. Those can be

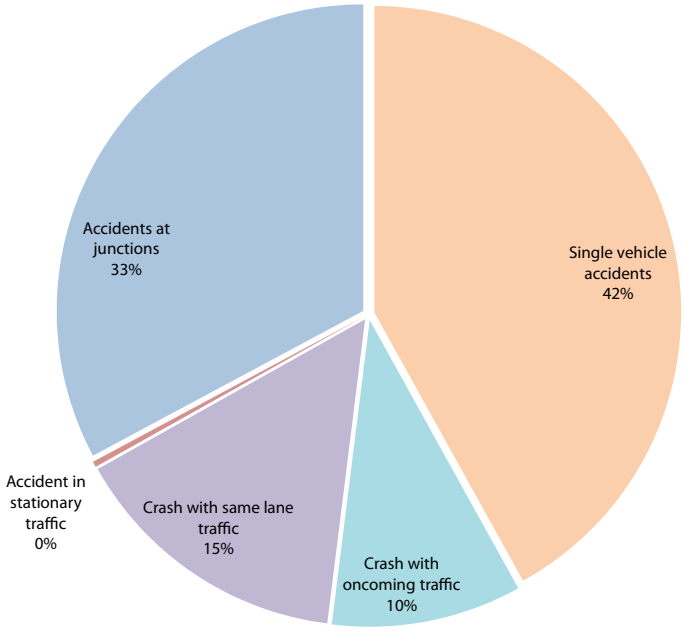

Figure 1.5: Motorcycle collision types in percent in Austria in 2011 [5].

- restraint systems to hinder motorbikes getting off the street.
- walls.
- crash damping elements.
- intentional free zones that allow the motorcycle getting off the street.

Whether an action of the mentioned types is feasible depends heavily on the location. In some cases one or the other is easier to take but anyway requires specific inspection at the risky location [1, p. 37].

1.4 Existing Accident Prediction Models

Transportation aims to ship goods and persons from one destination to the other. It has high significance for the economy and the wealth of the civilization. But unforeseen incidents meaning a random event that cause injury to human-beings, death and/or property damage may happen while being on a vehicle. Those can be collisions with other road users, crashes with animals or loss of control over the vehicle that someone

drives. To lower accident counts by applying countermeasures, traffic security studies have been conducted by researchers. They also consist of models that may predict accident numbers for roads or road sections.

An approach [8, p. 3] to capture the cause and result of accidents is reached by using multivariate linear or non-linear regression analysis. Research that has been done in the accident field try to find causal factors on accident counts. The mapping from the causal factor to the accident count is the function that is seeked after.

Fault tree analysis is one of the most important logic and probalistic techniques used in Probabilistic Risk Assessment (PRA) and system reliability assessment today. It is originated in US aerospace and missile programs in the early 1960s as a logical, systematic and comprehensive approach to assess the risk in probabilistic systems based on factors that have direct influence onto it [17].

The finding of causal factors for statistical regression analysis can be supported by building a fault tree based on the influencing variables. Figure 1.6 illustrates such a fault tree. The rectangles contain the category the accident is associated to. The rounded rectangle below the bigger one indicates the how many accidents fall into that category. The root node sums up all accidents that are looked at. The fault tree provides an overview about the classification of the accidents and may also give an easier insight into the corresponding causalities.

[9] state that nearly all modern accident prediction models can be written as

$$E = \alpha \cdot Q^{\beta} \cdot e^{\sum \gamma_i p_i} \tag{1.1}$$

where the expected number of accidents is E, the traffic volume Q in vehicles per time unit, α and γ_i are conversion factors. An elasticity is applied on the traffic volume's function by raising it with β. p is a causal accident factor. They also listed three major points explanatory variables should fullfill.

- They have been proved to exert a major influence on the number of accidents.
- They can be measured reliably.
- They do not correlate with other causal factors.

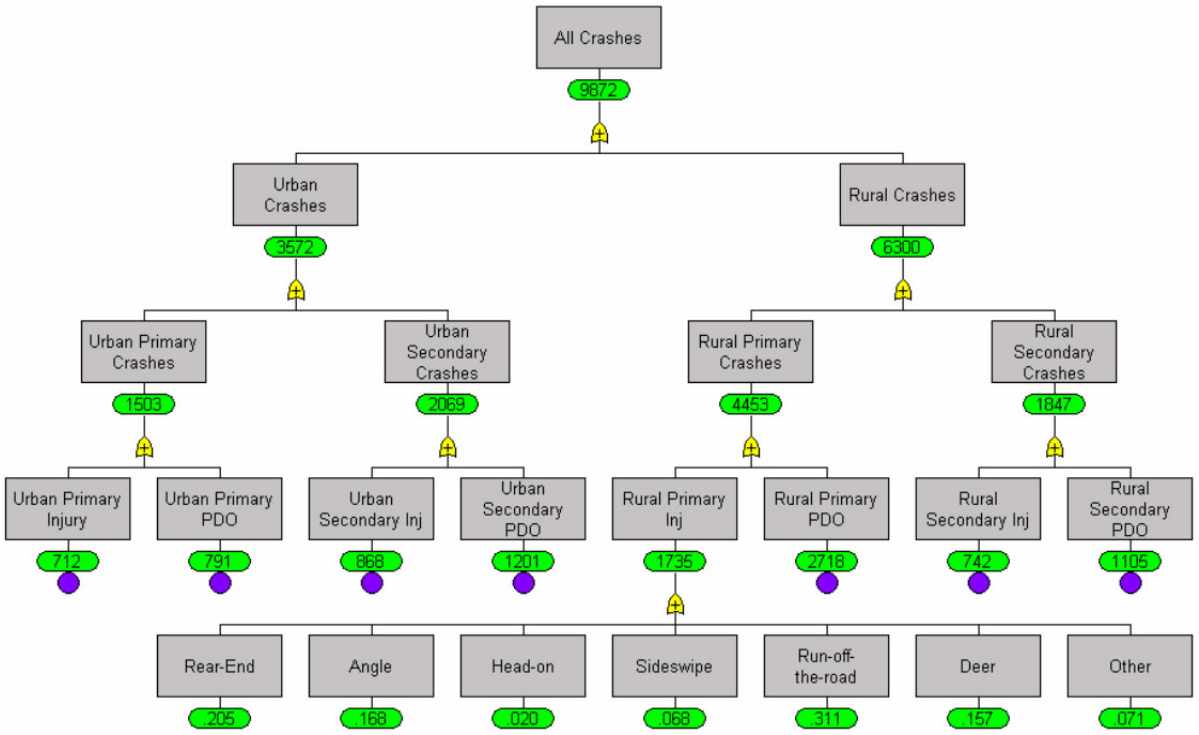

Figure 1.6: Example branches for run-off-the-road crashes on rural secondary sites [15, p. 8].

For the identification of dependencies on related variables the use of artificial neural networks can be useful. An artificial neural network consists of neurons distributed to different layers as shown in figure 1.7. In a multilayer perceptron (MLP, a feedforward artificial neural network) the input values enter the network at the input layer. The signal is distributed through the network until it reaches the output layer. So called "weight coefficients" determine the behaviour of a neural cell. Each neuron calculates it signal output upon the weight coefficients and the activation function and is then forwarded to the next neuron. By training the neural network the weight coefficients are determined in that way that a certain input function leads to a desired output function. Learning methods provide different ways to achieve a trained neural network.

Basically every non-linear function can be approximated by a multilayer perceptron (MLP) with high accuracy [11, p. 42-43].

Existing accident prediction models try to forecast the number of accidents that are likely to occur on a certain road section. In general, they are based on equation 1.1 and output a number of accidents that is likely to happen per year on the road section

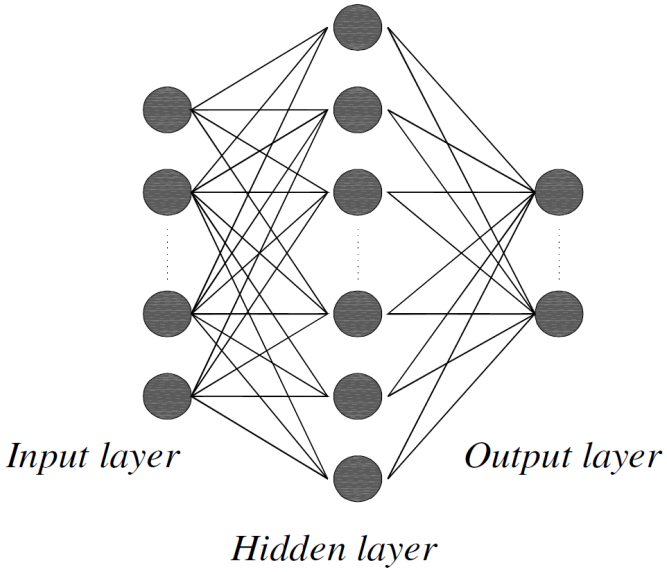

Figure 1.7: An artificial neural network made up of three layers [11, p. 42].

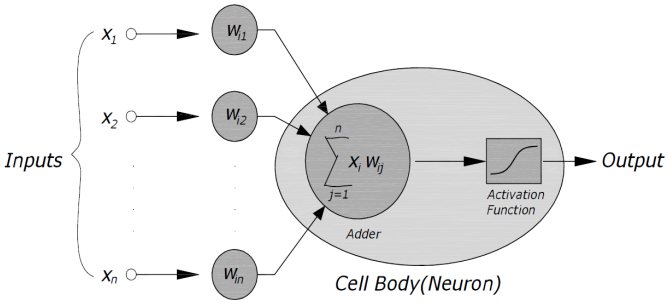

Figure 1.8: A neural cell with inputs, corresponding weight coefficients, an adder and an activation function [11, p. 42].

that is simulated. In contrast to existing models, this study aims to predict specific accident sites to take measures against hazardous points on road sections. Anyway, the approaches of those existing models can be seen as a source of ideas and can be adopted partly to the needs of this study.

2. Motorcycle Physics

2.1 Basics

The dynamics of the motorcycle system are more complex than the dyanamics of a car. A car is a self-stable system that cannot tilt over without an extraordinary high lateral force applied on. This makes the description of a car as a physical system simpler compared to those of a motorcycle.

In contrast, a motorbike tilts over automatically if nothing prevents it from tumbling down. Initially when the rider starts the ride on his motorcycle he takes care of balancing it. After a certain speed threshold value is passed the motorbike self-stabilizes and it gets easy for the rider to do a straight-running ride. Physically this phenomenon may be considered as an inverted pendulum with an acceleration applied at the vehicle's base.

Gyroscopic effects enable that a two-wheeler gets maneuverable in a wide velocity range. A simplified model of a two-wheeler shown as a gyro may be taken in order to illustrate the basics of the self-stabilizing mechanism. A single wheel rolling on the floor is analyzed. It suffices to consider a one-wheel model as a simplification of a two-wheeler and it can be demonstrated that a locomotion is possible with one wheel.

The Euler's equations for the rigid body in vector form [7, p. 177] are

$$\vec{M} = \frac{d\vec{L}}{dt} = \frac{d^*\vec{L}}{dt} + \vec{\omega} \times \vec{L} \tag{2.1}$$

where $\vec{M}$ is the applied torque, L is the angular momentum and ω is the angular velocity. $\frac{d\vec{L}}{dt}$ is the derivative of the angular momentum in a fixed coordinate frame and $\frac{d^*\vec{L}}{dt}$ is the derivative of the angular momentum in a floating coordinate frame.

For the shown system in figure 2.1 and using δ as the control variable, equation 2.1 results in

$$\vec{M} = -\dot{\delta} \cdot I_{yy} \cdot \frac{v}{R_{dyn}} \cdot \vec{e}_x \tag{2.2}$$

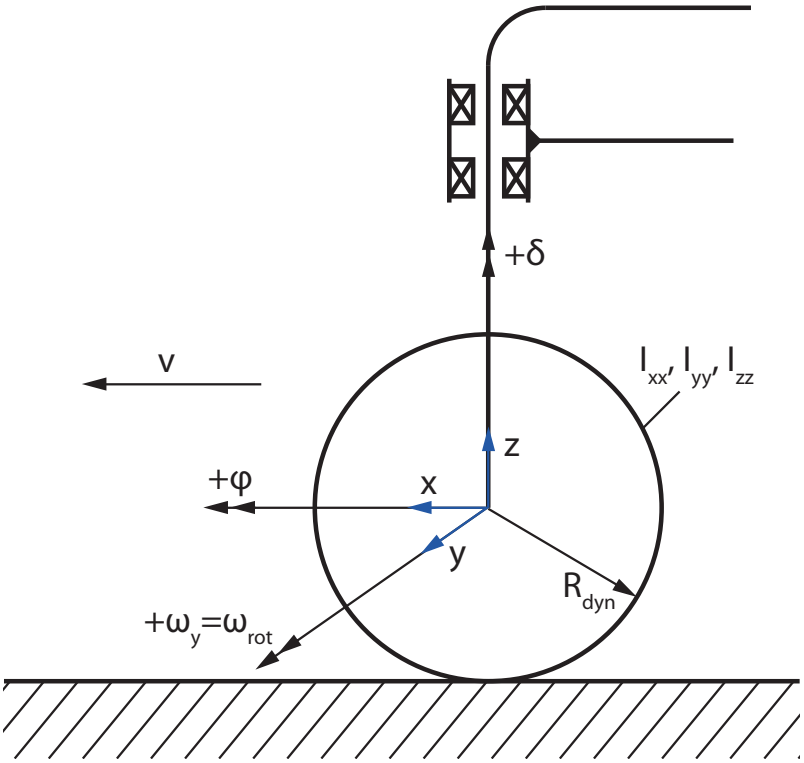

Figure 2.1: Simplified model of the front wheel system [16, p. 10].

The resulting torque is the reaction torque that arises if the z-axis of the gyro would be prevented from tilting over. The free not retained gyro receives the torque reaction of the opposite direction thus it can written

$$\vec{M}_r = -\vec{M} = \dot{\delta} \cdot I_{yy} \cdot \frac{v}{R_{dyn}} \cdot \vec{e}_x \tag{2.3}$$

Contemplating equation 2.3 it demonstrates that an induced steering action to the left ($\dot{\delta} > 0$) causes rolling to the right ($M_x > 0$) as a positive torque about the x-axis turns the wheel right and vice versa.

Using the φ as the control input of the system, the Euler's equations can be transformed to the following form for the z-axis

$$\vec{M}_r = -\dot{\varphi} \cdot I_{yy} \cdot \frac{v}{R_{dyn}} \cdot \vec{e}_z \tag{2.4}$$

where $\dot{\delta}$ is exchanged by $\dot{\varphi}$ and a negative sign.

The last equation can be interpreted in the way that tilting over to right side ($\dot{\varphi} > 0$) the torque about the z-axis causes a steering action to the right ($M_z < 0$) and vice versa.

An external interference like e.g. wind may cause the vehicle to roll to the right then the resulting torque forces the steering wheel and the rigidly connected handle bar to

turn right. The steering action also reinduces a torque that tries to tilt the vehicle over to the left and those superpose that the motorcycle sits up. The roll action crosses the neutral upright position and starts the same mechanism at the left side. This opposing gyroscopic effects and the additional control actions of the rider let the vehicle oscillate about the neutral position.

At low speeds the self-balancing mechanism takes place at a low frequency and the rider has to stabilize the vehicle without those counteractions the two-wheeler would fall since the torques are of low magnitude. If the vehicle increases its speed the torques increase and the frequency of rolling to the right and the left increases too. The vehicle gets self-stable [6, p. 42].

However at higher speed, a low-frequency oscillation (2-3 Hz), an oscillation over the roll, yaw and steer axis, may not be well dampered and can force the rider to loose control over his vehicle and in the most adverse case it can lead to a crash. This phenomenon is better known under the term "weave" [6, p. 53] and the higher-frequency (typically 7-9 Hz) steering oscillation under "wobble" [6, p. 50].

2.2 Motorcycle Models

The basic findings in motorcycle physics can be applied and put into creating dynamic motorcycle models. Those models make transient simulations possible and may be used in different areas of investigation.

Motorcycle physics is an interdisciplinary field of investigation. Many variables influence each other and can decrease the running behavior in a negative way.

Straight running stability is one of the fundamental aspects to be able to drive a two-wheeler. It shows the characteristics on navigating the vehicle straight ahead at a certain velocity. The vehicle stabilizes itself after passing a certain speed threshold and keeps being self-stable without regulative actions.

Vertical and lateral dynamics are the two other main fields of interest when looking at going through a curve and taking into account that streets are uneven and cause the vehicle to bounce up and down. Street and other environmental conditions interfere with the driver-motorcycle-system and apply wave motions on it. Those disturbances

can downgrade the curve and straight running stability and make the control of the motorcycle more difficult.

Different motorcycle models regarding grade of detail [see in this chapter] exist to mathematically describe the behavior of a two-wheeler. Investigational effort has been put into developing control systems based on those models and led to distinct degrees of complexity regarding the independent parameters. The grade of complexity of a model can be described by the degrees of freedom (DOF).

Such models range from minimum three DOF to high developed model that consist of even more than 11 DOF. Detailed information can be gained from such models but in these days cannot replace real-life riding tests.

Two - the simplest and a more sophisticated - models are going to be described in the following sections.

2.2.1 Three DOF Point-Mass Model

The simplest approach is to describe a two-wheeler with a three DOF model [6, p. 40]. Figure 2.2 shows the two-wheeler with the three independent parameters and the geometric constraints.

A cartesian coordinate system placed into the rear-wheel contact point is used for locating the object in the space where the Society of Automotive Engineers (SAE) sign convention is applied. The positive x-axis is directed towards the forward running direction, the positive y-axis is directed towards the right-looking side of the rider and the z-axis points to the ground. The roll angle φ describes the rolling of the object and is counted positively clockwise. The amount of steering is indicated through the parameter δ and is counted positively clockwise. The yaw angle ψ describes the angular position compared to the coordinate frame. The whole mass m is concentrated in a single point h above the ground and b in front of the rear wheel contact point. The distance between the rear and front wheel contact point, denoted as the wheelbase, is w long.

The front fork, the handlebar and the rear frame are considered to be rigid and pinned together non-flexibly and the rider is rigidly connected with the frame. No

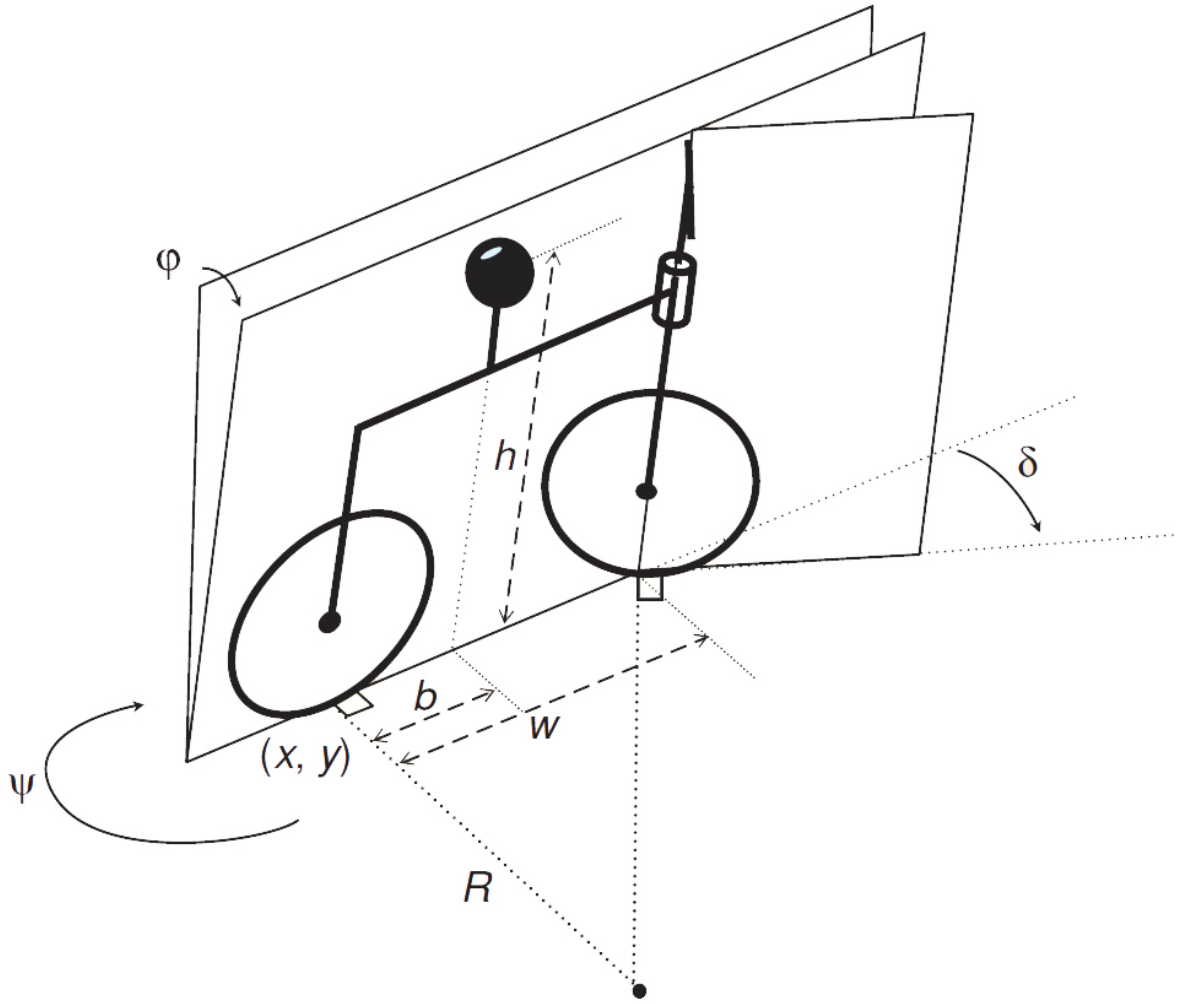

Figure 2.2: Three DOF motorcycle model as a point-mass model [6, p. 40].

aerodynamic drag, no propulsion, no frame flexibility, no slipping between the wheels and the ground and no rider control is taken into account.

These assumptions lead to a three degrees of freedom model where φ, ψ and δ are the independent variables.

Since no side- nor longitudinal-slipping occurs between the wheels and the ground the kinematics of the planar motion of the center-of-mass point can be described by

$$\dot{x} = v \cdot \cos\psi \tag{2.5}$$

$$\dot{y} = v \cdot \sin\psi \tag{2.6}$$

$$\dot{\psi} = \frac{v \cdot \tan\delta}{w \cdot \cos\varphi} \tag{2.7}$$

where v is the forward speed. The speed does not need to be constant and can also be a function. The speed v and the yaw rate are linked by the curvature σ or $1/R$, the reciprocal value of the curve radius, and is written as

$$v \cdot \sigma = \frac{v}{R} = \dot{\psi} \tag{2.8}$$

The roll dynamics are the same as those of the inverted pendulum with an acceleration applied at the vehicle's base. The momentum equilibrium equation about the x-axis can be written as

$$h\ddot{\varphi} = g\sin\varphi - \left[\left(1 - h\sigma\sin\varphi\right)\sigma v^2 + b\left(\ddot{\psi} + \dot{v}\left(\sigma - \frac{\dot{\varphi}}{v}\right)\right)\right]\cos\varphi \tag{2.9}$$

where the curvature and the vehicle's speed are linked by the curvature σ. $\ddot{\psi}$ can be replaced by using equation 2.7 and yields

$$h\ddot{\varphi} = g\sin\varphi - \tan\delta\left(\frac{v^2}{w} + \frac{b\dot{v}}{w} + \tan\varphi\left(\frac{vb}{w}\dot{\varphi} - \frac{hv^2}{w^2}\tan\delta\right)\right) - \frac{bv\dot{\delta}}{w\cos^2\delta} \tag{2.10}$$

The latter equation represents a simple nonholonomic model of a two-wheeler with the input variables δ, the steering angle, and v, the vehicle's speed. The response of the system is the roll angle. The equation is nonlinear and is general with respect to speed change or high roll or steering angles. The model could be linearized about zero

	DOF
1	yaw angle
2	roll angle
3	steering angle

Table 2.1: Itemizes every degree of freedom of the three DOF model.

roll angle for small perturbations. In a curve roll angles can reach values of various 10 degrees. Hence linearizing the model about small roll angles is not appropriate for this study.

Because of its few parameters and variables this model is used for the physical variables study and serves as a comparision basis to the statistical model.

2.2.2 11 DOF Model

A more complex model of a two-wheeler is shown in figure 2.3. Six connected bodies form this system. It has 11 DOF where the rear assembly center of mass, the yaw angle, the roll angle, the pitch angle, the steering angle, the travel of front and rear suspension and the spin rotation of both wheels are associated with it.

As in the previous model in chapter 2.2.1 the rider is rigidly attached to the rear frame. The model allows to retrieve more details about the riding behavior compared to the simple 3 DOF model. It is useful when deeper insight in responses of vehicle parts is necessary. For this study the 11 DOF model provides too high grade of detail, requires to much computational effort and is not feasible due to many vehicle specific parameters [19, p. 424].

In this case a more generalized approach is taken - the three DOF model - to be able to abstract for many different types of motorcycles and to check the usefullness of it.

2.2.3 Comparision

The two motorcycle models have some basic differences. The three degrees of freedom model describes the rolling behavior in the most basic manner how a two-wheeler can be mapped to virtuality. It forms a simple control system that consists of the steer angle

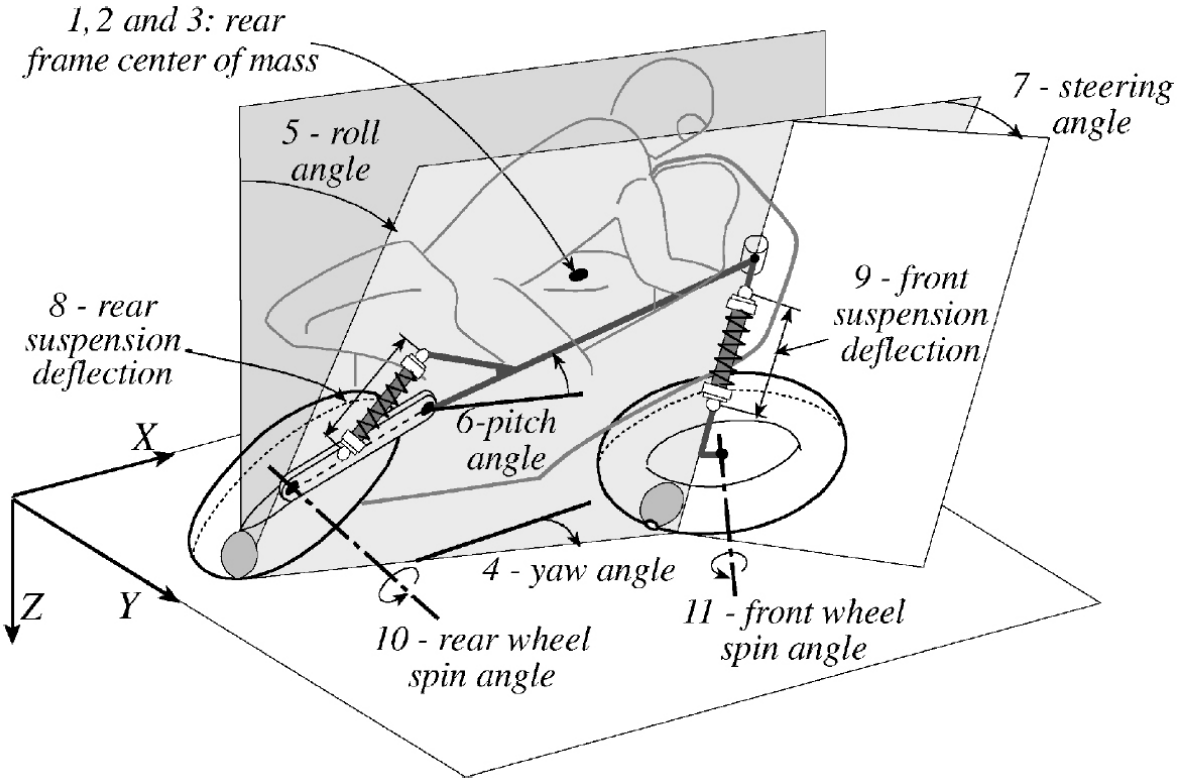

Figure 2.3: 11 DOF motorcycle model [19, p. 424].

	DOF
1, 2, 3	rear frame center of mass
4	yaw angle
5	roll angle
6	pitch angle
7	steering angle
8	rear suspension deflection
9	front suspension deflection
10	rear wheel spin angle
11	front wheel spin angle

Table 2.2: Itemizes every degree of freedom of the 11 DOF model [19, p. 424].

Comparision	
3 DOF Model	**11 DOF Model**
requires 5 mechanical properties	requires 56 mechanical properties
1 momentum equation	34 independent constraint equations

Table 2.3: Shows the most important characteristics of both models.

as the input parameter and the roll angle as the system response [see equation 2.9].

In contrast, the 11 degrees of freedom model is a more sophisticated approach to cover more details about vertical, horizontal and lateral dynamics of a motorcycle including the suspension. It does not only map the rolling mechanism but also the street influence through uneveness of the underground which is then transfered by the wheels to the suspension system and furthermore to the frame with the rider on it.

Table 2.3 summarizes in short the differences between the simple three DOF and the more complex 11 DOF model.

Every additional degree of freedom that is specified increases the difficulties to be able to solve the system. For the first one a quick solution can be found without putting much effort into it. Little information about the motorbike type itself must be known compared to the latter one.

This means that the level of abstraction sinks with the degrees of freedom increasing. Detailed studies about specific performance of a motorcycle system implies more detailed models. More complex models allow to simulate real-life comportment in certain situations and thus need to be provided more geometric and mechanic input parameters.

The following section simplifies the transient three DOF motorcycle model and works out a steady-state derivation of it that shows furthermore the roll angles of certain curve radii as a result.

2.3 Apply Physical Model to Road

Chapter 2.2.1 describes the 3 DOF motorcycle model. Due to the simplicity of this model it is used for calculating the key parameters when riding a motorcycle through a curve.

More complex models introduce a lot of additional parameters that must be known to solve the system. Not enough existing data is available in this study to assert the output of those complex models. They are also far more exhaustive for computational treatment. Since the aim of the risk simulation should be an easy handling and maintenance for end-users, this leads to the conclusion that the 3 DOF model fits perfectly the needs for this task.

2.3.1 Side Forces

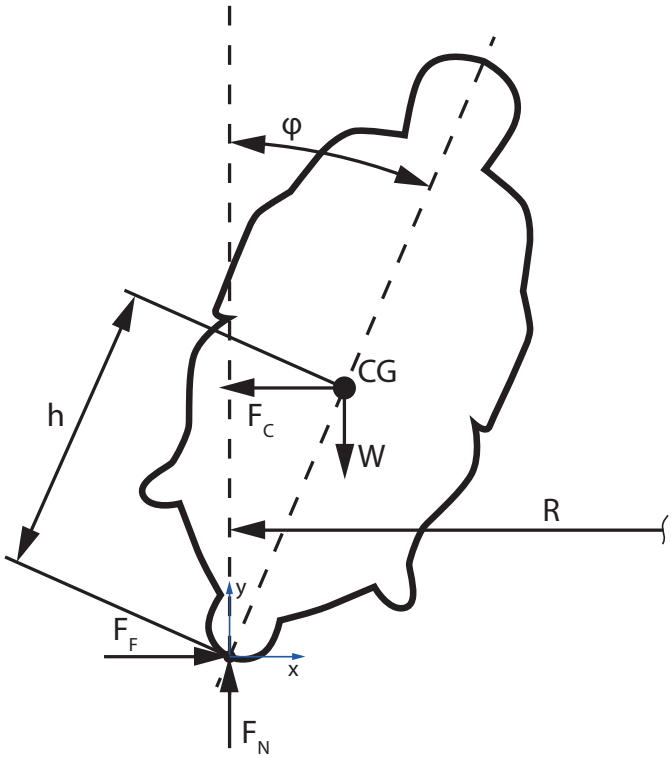

Figure 2.4: Acting side forces on a motorcycle in a curve.

The side forces acting in a turn are shown in figure A.15. According to Newton's second law of motion the force equilibrium in the x-axis direction is

$$m\ddot{x}_c = \sum F \tag{2.11}$$

where m is the body's mass, $\ddot{x}_c$ the second derivative of the center of mass' displacement in x-direction as seen in figure A.15 and $\sum F$ denotes the sum of all external forces acting

on the body. With the introduction of the inertial force [7, p. 191] the previous equation can be rewritten to

$$F_i = \sum F \tag{2.12}$$

where F_i is the inertial force in x-direction. Assuming a steady-state turn with a constant roll angle a constant inertial force, the centrifugal force, acts on the body's center of mass. Latter equation is rewritten to

$$F_C = F_F \tag{2.13}$$

with F_C as the centrifugal force acting from the rotation center outwards and F_F is the friction. The two forces can be replaced by

$$m\frac{v^2}{R} = mg\mu \tag{2.14}$$

where m is the mass of the body, v is the tangential speed, R is the instantaneous turning radius, g the gravitational acceleration and μ the friction coefficient. The equation can be reduced to

$$v = \sqrt{g\mu R} \tag{2.15}$$

and v is the maximum possible speed where static friction is still present. Exceeding this speed means that the motorcycle starts to slide and control over it might be lost. In general, for the speed can be written

$$v = f\left(\mu, R\right) \tag{2.16}$$

No motorcycle physics specific assumptions have been met so far. In this model the roll angle does not influence the force equilibrium in the x-direction and so the derived equations are not special for the case of a motorcycle and are also valid for the simplest case of a car or any other vehicle that uses the friction of the underground to keep the track. The friction coefficient may change depending upon the vehicle.

2.3.2 Rolling and Steering

The equations needed to describe the dependency between rolling and steering, have been deduced in chapter 2.2.1, are taken to discuss a steady-state turn of a motorcycle. It is assumed that a state with a constant roll angle is going to be reached in a curve. It is the state where the motorbike starts to sit up again. This condition is only valid for slow changes of φ. The index s stands for "steady-state" and describes a constant value. It is introduced to be able to distinguish the values from the time-dependent functions. Therefore the equation 2.10 and 2.7 are reduced to the form

$$g \cdot \sin \varphi_s - \frac{v_s^2}{w} \cdot \tan \delta_s + \frac{h v_s^2}{w^2} \cdot \tan^2 \delta_s \tan \varphi_s = 0 \tag{2.17}$$

$$-\dot{\psi}_s + \frac{v_s}{w} \frac{\tan \delta_s}{\cos \varphi_s} = 0 \tag{2.18}$$

The angular yaw rate is defined by the track the motorcycle runs and can be retrieved from the curve. The equations can be linearized around small steering angles. Solutions of the non-linearized equations showed that the steering angle ranges between zero and two degrees and thus is able to be simplified. The error of linearizing the Tangent function between zero and five degrees is 0.25%. Equation 2.7 shows the relation of the angular yaw rate and further it can be used to replace the latter equation to

$$g \cdot \sin \varphi_s - \frac{v_s^2}{w} \cdot \delta_s + \frac{h v_s^2}{w^2} \cdot \delta_s^2 \tan \varphi_s = 0 \tag{2.19}$$

$$-\frac{v_s}{R} + \frac{v_s}{w} \frac{\delta_s}{\cos \varphi_s} = 0 \tag{2.20}$$

Those equations form a system of two coupled non-linear equations with the two variables φ_s and δ_s that need to be solved. The interesting value of the system is the roll angle φ_s as a function of the speed or vice versa. It can be written

$$\varphi_s = f(v) \tag{2.21}$$

and since the speed v is a function too, it is replaced and put into the form

$$\varphi_s = f(v) = f(\mu, R) \tag{2.22}$$

It can be concluded that the friction and the curve radius influence the roll angle. Different combinations of the parameters friction coefficient μ and speed v are contemplated.

Two different scenarios are investigated. The friction coefficient as a parameter for the road surface and a crucial value for the security, is given to look at the highest possible speeds in a curve. It starts from 0.2 to 0.8 in 0.1 steps. The highest possible velocity is calculated upon the friction. Supposing that speed limits exist on a road section, the speed is given and the maximum roll angles are derived from. Greater roll angles drive the system into more extreme situations since a greater roll angle requires more friction and changes on the road surface can lower radically the friction coefficients. Common speeds in curves ranging from 40 km/h to 120 km/h in 10 km/h steps are investigated. The output, the roll angle φ_s, is used to classify the curve. A assumption is made that values above 30 degrees are considered as risky. In further studies this assumption might be refined.

As different friction values in the above mentioned range are taken to calculate the roll angle in a curve as many result roll angles are gathered. The roll angles above 30 degrees are counted and are compared relatively to all the others. A threshold values is introduced. If the count of the roll angles above 30 degrees exceeds the threshold then the curve is marked. The results are presented in chapter 5.

3. Risk Parameters to Accidents

As the physics of a motorcycle show, a two-wheeler is not self-stable and can be destabilized easily through outer influences like street conditions, wind, rapid and/or wrong riding maneuvers. High velocities, a motorcycle can reach through higher power-per-mass ratios, amplify the risk loosing control over it. The accident statistics reflect the higher risk by higher crash rates compared to cars.

Parameters that influence the risk directly can be divided into three main parts. The rider is the heart of every vehicle and also for a motorcycle it is the dominant factor. He decides the movements, steering actions and running speeds with its respective accelerations. Every vehicle is embedded into its environment and thus interacts with it. The environment affects the rider but also the motorcycle and the bike gives the feedback to the rider. The third part is the bike itself. A lot of different types of motorcycles are on the market

3.1 Rider

The rider is the major factor of a motorcycle and so in accident situations. Without the steering actions of the human a motorcycle is not able to move. See physics in chapter 2. Errors might be committed by the rider due to many reasons. Inattention to surrounding traffic, disobedience of traffic laws including speed limits, improper behavior in hazardous situations are common errors. In general, human behavior and attitude are complex factors and are complex to isolate because of their temporary nature. Influences are given by sensory capabilities, riding skills, attitude, consciousness and age to mention some. Using a motorbike under the influence of alcohol or drugs is also considerably dangerous like driving any other vehicle.

Motorcyclists often go for a ride in groups. Especially when riding motorcycles in groups peer pressure may be existent [12, p. 526] [1, p. 7].

3.2 Vehicle Associated Parameters

The vehicle is the instrument that a rider uses. Therefore it needs to fullfill the technical conditions so that the security of the rider is guaranteed. It means that essential parts of the motorcycle must not break under stress or disfunction. Tire failure, break failure or the breaking of stressed parts may lead to crashes with obstacles or other vehicles.

Worn tires or other wearing parts can cause disfunction or breaking of themselves as well as manufacturing errors. Statistics [14, p. 16] report that 0.5% of all accidents are caused by technical defects of the vehicle. Anyway the amount of accidents caused by those factors may be considered as a matter of minor significance [13, p. 119].

3.3 Road and Environmental Conditions

Motorcycles and its riders interact with their environment. Curves, road conditions, weather and its couplings impact on the behavior of the rider-motorbike system.

The risk parameters implied by the road are discussed in section 4.2 and are further used in the simulation model.

4. Accident Prediction Model

Upon the facts that were discussed in the previous chapters a model for estimating the risk of an accident is going to be derived. The risk is increased and decreased by many factors. In order to make the solution approach clearer, a step-by-step introduction to every hypothesis is going to be carried out.

When the individual factors are contemplated many of them are hard facts but there are also a lot "soft facts" in it that affect the risk of an accident taking place in a certain way. What is meant by distinguishing by those two terms? The first ones are those that can be qualified with numbers. That means that physical and geometric parameters like friction or curve radii can be denoted as hard facts. Such values can be determined easily by measurements.

On the other hand, especially where humans are involved in, many parameters such as human behavior and the source for it are difficult to be put into numbers. The mood of somebody, reactions in dangerous situations, peer pressure and characters are not easily determinable.

These two contrasting factor families lead to different solution approaches regarding the modelling of an adequate accident risk estimation model. Statistic reports of accident injuries and fatalities over years contain those "soft facts" implicitly. An accident happens when a combination of certain circumstances arises. A motorcycle rider may get to the physical limits of his vehicle and environmental conditions regardless of his skills then a dynamic simulation depending on pure physics may highlight risky points for motorcycle riders. Figure 4.1 summarizes the setup of the statistical modelling approach.

Based on it a statistical model and a physical model is going to be looked at.

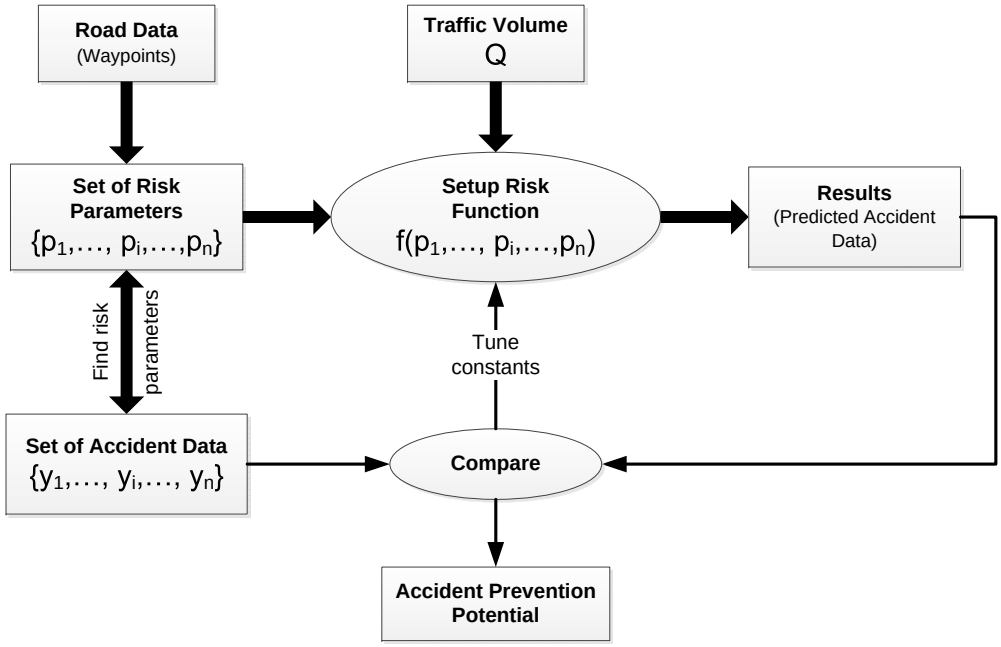

Figure 4.1: The setup of the statistical model with its interactions.

4.1 General

The simulation needs input data. Since the scope of this work is to generate prediction values for tracks on rural roads, geometric data of the streets is essential. In case an overall prediction model of accident counts is carried out, that is not going to be assigned to geographic locations, these steps can be skipped. For the retrieval of street data there are some sources out there. Today the internet is the most convenient and it is also a very rapid method to get the data someone seeks for. Spatial databases provide geographic data and metadata. The data is saved in a vectorized structure so that it is possible to serve for different application fields. That speaking the data is resolution independent.

Different providers of geographic information systems exist. In this work geographic information is extracted from Google Earth, but any other system that disposes extractable street data can be used too. It is free to use and can be downloaded from the internet. The usage of the application requires an established internet connection because the geographic data is fetched on demand from the internet. The programm only visualizes the vector and pixel data.

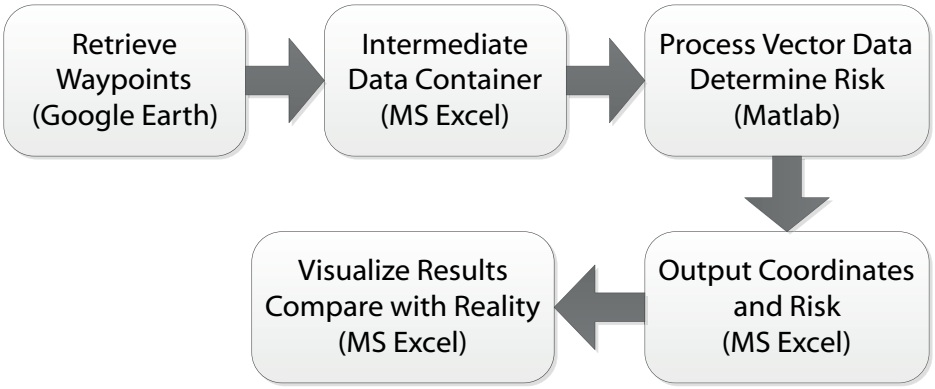

Figure 4.2: The calculation process steps of the model.

The flow inside the simulation is visualized in figure 4.2. Five main steps are carried out. The data retrieval process collects road data from an spatial database. Additional input parameters are specified to feed the model with arbitrary risk variables. After the calculation the coordinates with the results are backwritten into a file to be later visualized in a map.

4.1.1 Querying of the Street Data

Figure 4.3 shows the start screen of the application after opening it.

The screen is splitted into three areas. The black background area with the earth embedded is the navigation canvas where rotating, zooming, north-south orientation of the view onto the earth can be adjusted. On the left side are two vertically aligned tree views. In the lower one, layers are outlined that allow the user to switch between visible and non-visible items. Streets, country borders, cities marks can be made visible or hidden from the earth's surface. The upper tree view contains the data the user added in his workspace context. The toolbox above the navigation canvas provides the capabilities of adding location points, paths, polygones, bitmap overlays and virtual tours. Those can be persisted locally and show up in the left upper tree view.

To get the street data the path tool is the one that is going to be used. As the name suggests it gives the ability to define multiple connected lines that form a path object. Just a click on the "Add Path" icon in the upper toolbox pops up the dialog. The cursor will change its look and is ready for being clicked in every waypoint. The name of the path will later show up in the left upper tree view and so many different path objects

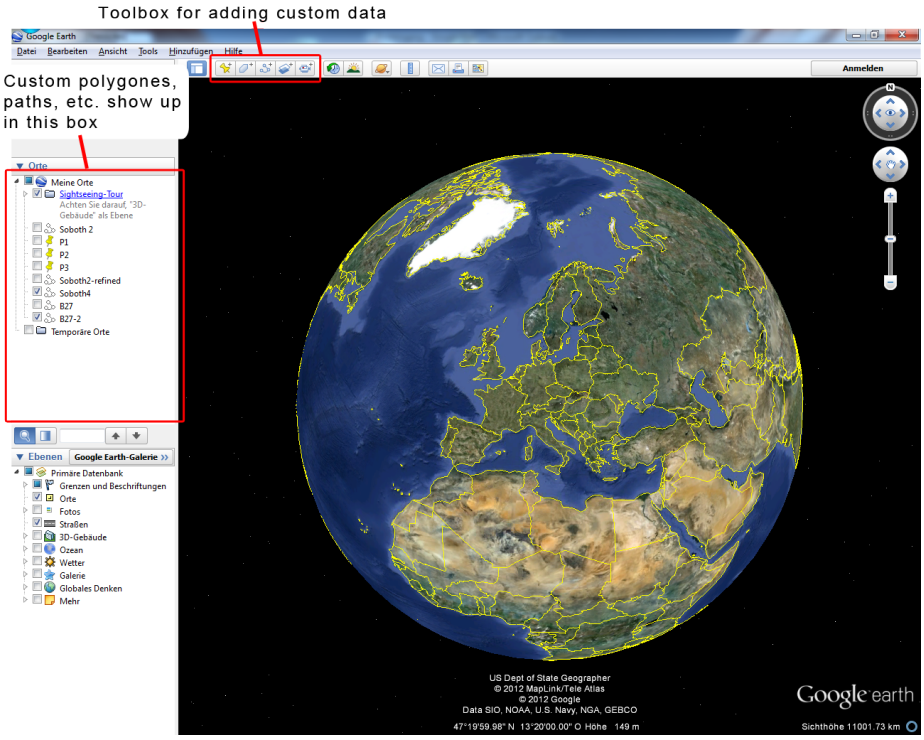

Figure 4.3: The start screen of Google Earth.

may be managed.

In figure 4.4 the creation of such a path around a curve is demonstrated. Besides appears the dialog to set the properties (e.g. name) of the path. For better visibility the path is marked red with points at the junctions.

The whole road track needs to be covered by the path points and requires some careful work. In real life, a road track is a three-dimensional curve. In this study a road track is represented by a planar curve. Google Earth does not provide three-dimensional road track coordinates. The elevation cannot be exported. Little data with apparent minor influence on the risk of motorcycle accidents is available for this study. That means that for simplicity the roads are looked at in a two-dimensional manner and the elevation coordinate is omitted.

After the scanning of the road track has been done, the path data needs to be exported. Google Earth provides the export of the path data in the *Keyhole Markup Language (KML)* format. It is human-readable text format that follows the XML specification.

The data from listing A.1 can be retrieved by copying the saved path object shown

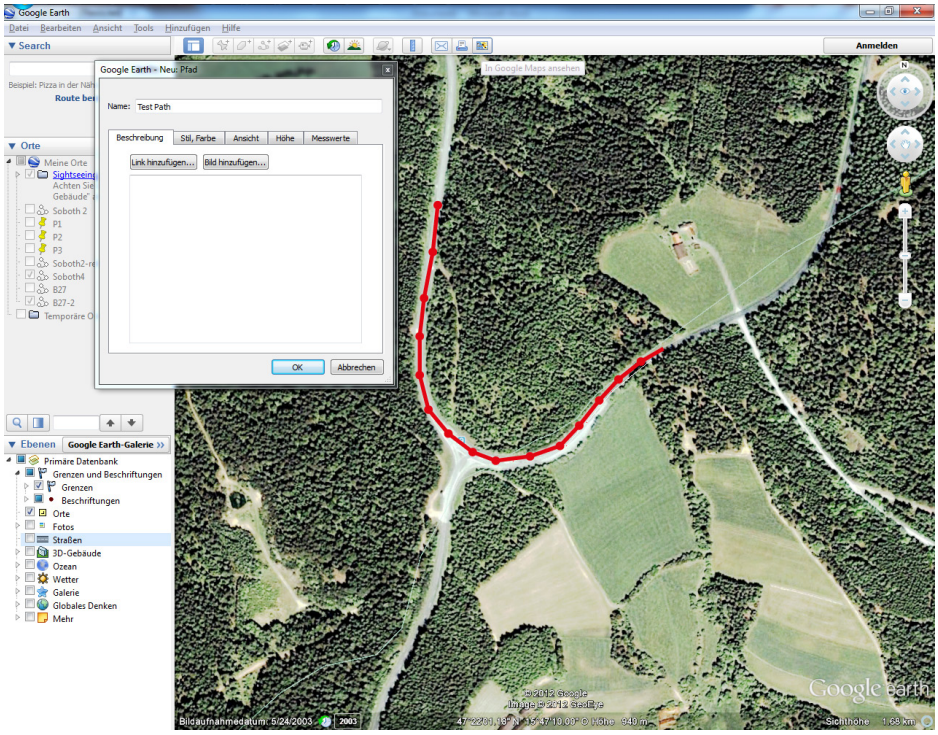

Figure 4.4: Add a new path to the Google Earth's user interface to trace the road.

in left upper tree view to the clipboard. It is a pure text representation in the clipboard and can be easily pasted into some text editor application. Since all the data in the clipboard is text no more actions have to be done.

The KML file holds the point coordinates of every junction of the path in geographic coordinates by longitude, latitude and elevation. This part can be found at the bottom of the file between the `<coordinates>` tag. As many coordinate triples separated by coma show up as has been defined in Google Earth and therefore can vary from this listing. Every coordinate triple is separated by a whitespace character or a carriage return. Exporting the waypoints into the simulation program can be automated and might be considered for future enhancements.

The coordinates must be converted into meters. They correspond to the *World Geodetic System (latest revision WGS 84)* coordinate frame for the Earth and is the reference used by the *Global Positioning System (GPS)*. It is based on an ellipsoid and by this means the length of one degree on the Earth's surface depends on longitude and latitude respectively. An approximative solution is to measure the length of one degree longitude and latitude in the area where the road track is situated.

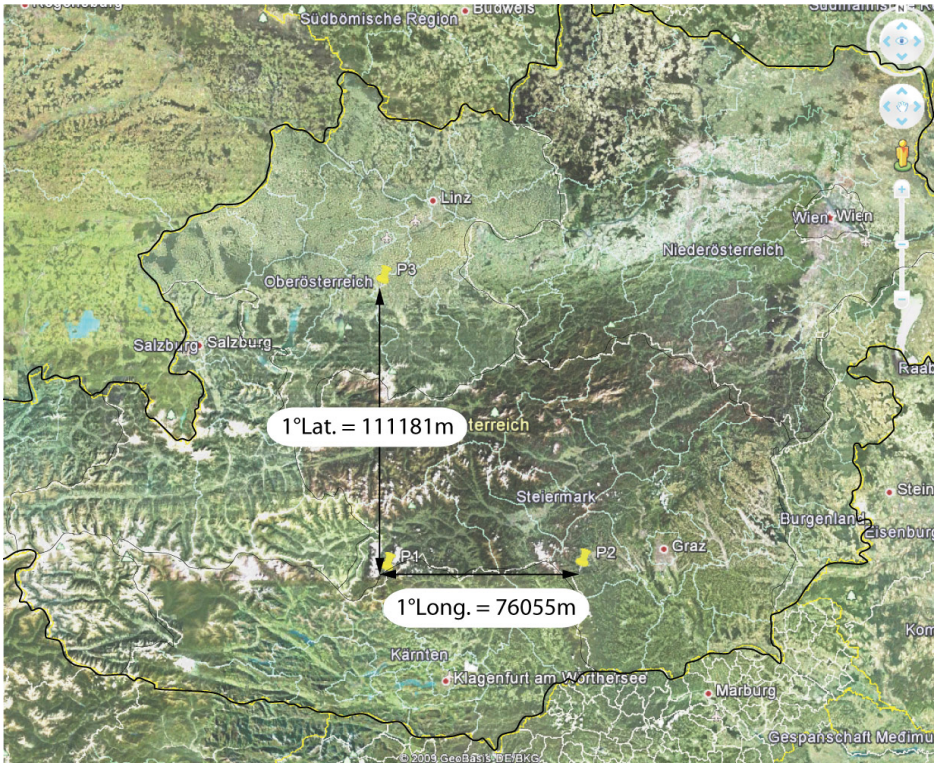

Figure 4.5: Measuring the length of one degree longitude and latitude.

Three location points are placed into the center of Austria. Many road tracks that are looked at in this study are closely located to those points and guarantee the minimum error possible in this case. The distance between the left bottom point 1 (P1) and the right bottom point 2 (P2) is the length of one degree longitude. Measuring the distance between point 1 (P1) and the upper point 3 (P3) determines the length of one degree latitude. The measurement can be done directly in Google Earth by placing two path segment between the respective points mentioned. The unit of the distance is provided in the last tab of the "Add New Path" dialog embedded in figure 4.4 on the left side in the navigation canvas. Different units are available for output and meters is the one that is used.

$$P1\,\{47°0'0.00"N|14°0'0.00"E\} \tag{4.1}$$

$$P2\,\{47°0'0.00"N|15°0'0.00"E\} \tag{4.2}$$

$$P3\,\{48°0'0.00"N|14°0'0.00"E\} \tag{4.3}$$

$$1°Long. \equiv 76055m \tag{4.4}$$

$$1°Lat. \equiv 111181m \tag{4.5}$$

Longitude	**Latitude**	**x [m]**	**y [m]**
15,72930425	47,78782292	0	0
15,7297131	47,78763236	31,09483755	-21,18608251
15,73013374	47,78751225	63,08669582	-34,54010373
15,73068699	47,78741797	105,1641282	-45,02252149
15,7314123	47,78738559	160,3277298	-48,62267579
15,73175375	47,787388	186,2963462	-48,35438229
15,73215484	47,7874827	216,80148	-37,82613476
15,73258363	47,78764229	249,4131163	-20,08259023
15,732942	47,78777128	276,6689838	-5,7416591
15,73324601	47,78779249	299,7900623	-3,382745998
15,73344148	47,78772241	314,6568024	-11,17429567
15,73353584	47,78760894	321,8336032	-23,79013132

Table 4.1: Example showing the transformation from *WGS 84* into custom coordinate frame.

The lengths of one degree longitude and one degree latitude can be seen in equation 4.4 and 4.5. A new cartesian coordinate frame for one road track is created using these values for transformation and looks as shown in figure 4.6.

The positive x-axis points from west to east and the positive y-axis points from south to north. The transformed coordinates of the initial part of a rural road is plotted in table 4.1. The two left columns are the original tuples in the *WGS 84* system.

4.1.2 Curve Detection Algorithm

The road track data is a finite tuple of coordinates and represent the location of each. Curves are lines with an infinite count of points. To be able to calculate parameters in an arbitrary point of the track it is necessary to map the track coordinates onto a curve that is continuously second order differentiable. The calculation of the curvature requires the first and second derivative of the curve.

Different ways are available to map points to a curve. Interpolation overlays a curve

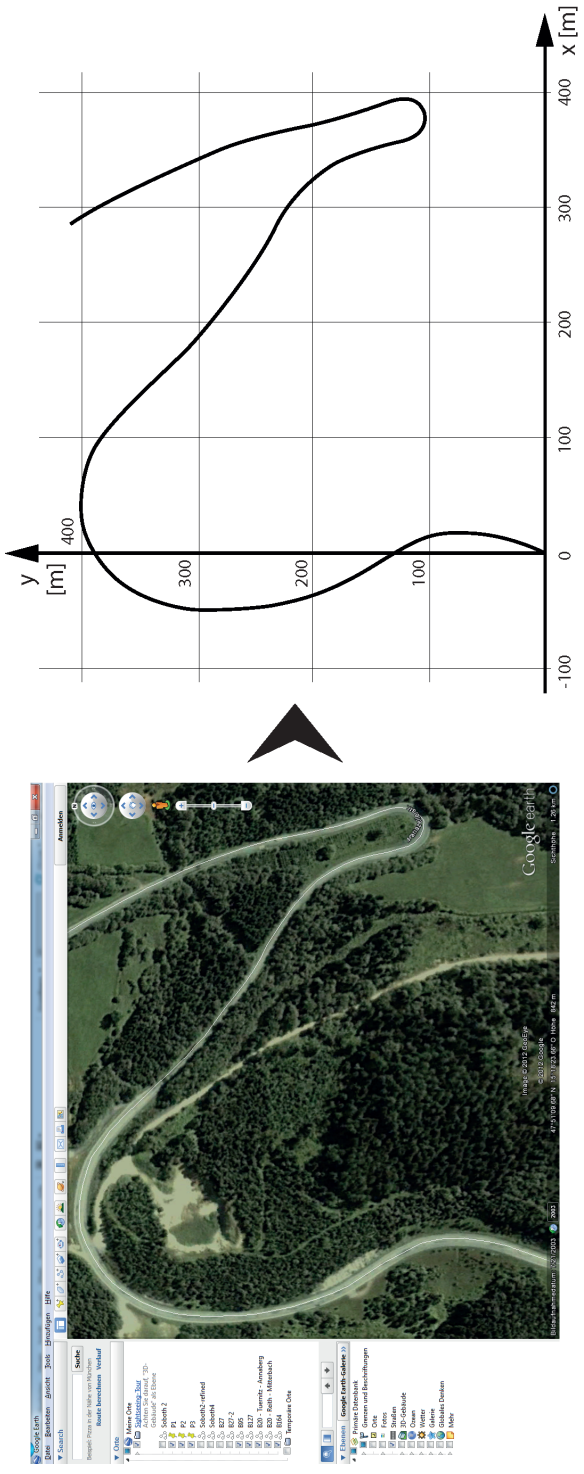

Figure 4.6: The road embedded into the newly defined coordinate frame.

exactly through every point and results in a zero deviation error. The interpolated curve goes through every way point.

Unlike interpolating a curve into points, fitting approximates a curve into points within a certain deviation error. That said, the points need not to be parts of the curve. The points are located in a certain distance range off the curve.

Basically every type of curve can be interpolated or fitted into a set of points.

Interpolation and Fitting

Pieces of straight lines are the simplest way to approximate a curve. Figure 4.7 shows the piecewise linear interpolation of a road section. This has the drawback that the tangent in a waypoint cannot be determined since it has a discontinuity in the junction. In order to be able to calculate the curvature radius in an arbitrary point, the curve needs to be continuous throughout the section that needs to be simulated.

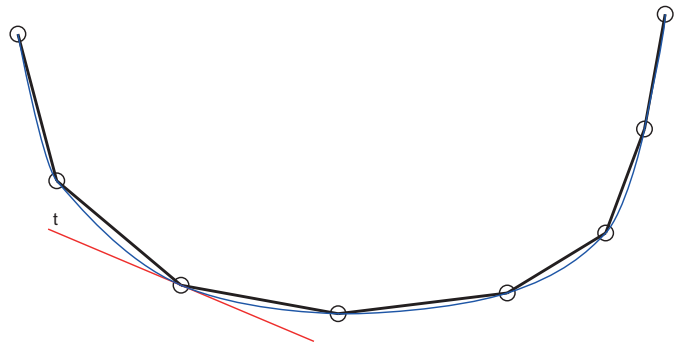

Figure 4.7: Interpolating a road with straight lines.

A polynom is the next interpolation approach to be looked at. A curve that is defined by three points can be interpolated by a polynom of second degree. In order that every point of the road is part of the polynom, the degree of the polynom increases by the count of the points. One hundred points would require a polynom degree of the amount of points minus 1 ($n = 100 - 1 = 99$) and so on. High degree polynomes tend to oscillate. In figure 4.8 the dotted line illustrates the principle of a polynom interpolation with higher order oscillations occurring and is only a symbolical illustration of the effect. In the case shown there might not be any noticable oscillations.

More usable, in the case of approximating a road track by a curve, are splines. Splines are piecewise defined polynoms of arbitrary degree and may have some boundary

conditions applied at the junctions. Such a boundary condition might be the necessity of being two times continuously differentiable. According to the degree of the polynom quadratic, cubic, etc. splines exist.

Taking a hermetic cubic spline it is possible to closely map the real road track into a mathematical representation. It is a spline that is of third order and merge continously differentiable into the next polynom at the connection node. The tangents of the two neighbour polynomes are equal. A symbolic illustration of interpolating a hermetic cubic spline into road coordinate points is shown in figure 4.8. Comparing to the dotted line in figure 4.8 it can be seen that a spline represents the supposed run of the road well assuming a case dependent adequate junction spacing.

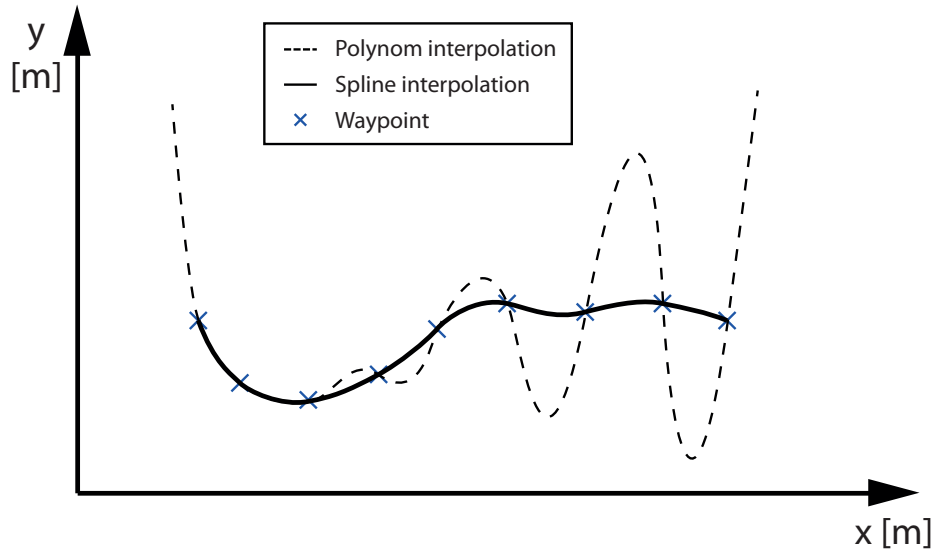

Figure 4.8: Interpolating road waypoints with a hermetic cubic spline vs. a polynom.

The process of manually traversing the road track and setting the points on the road is error-prone. It is likely that the point coordinates do not match exactly the road coordinates and thus inject a coordinate drift. The curvatures in the sketch 4.9 do not equal closely anymore to the real curvatures if a spline is interpolated in those erroneous points. A curve fit can remedy this effect induced by human definition of the street coordinate points.

In figure 4.9 a schematic illustration of a curve fit is shown. The red mark shows where a smoothing effect between two points is reached. It dampers subtle oscillations of the curvature.

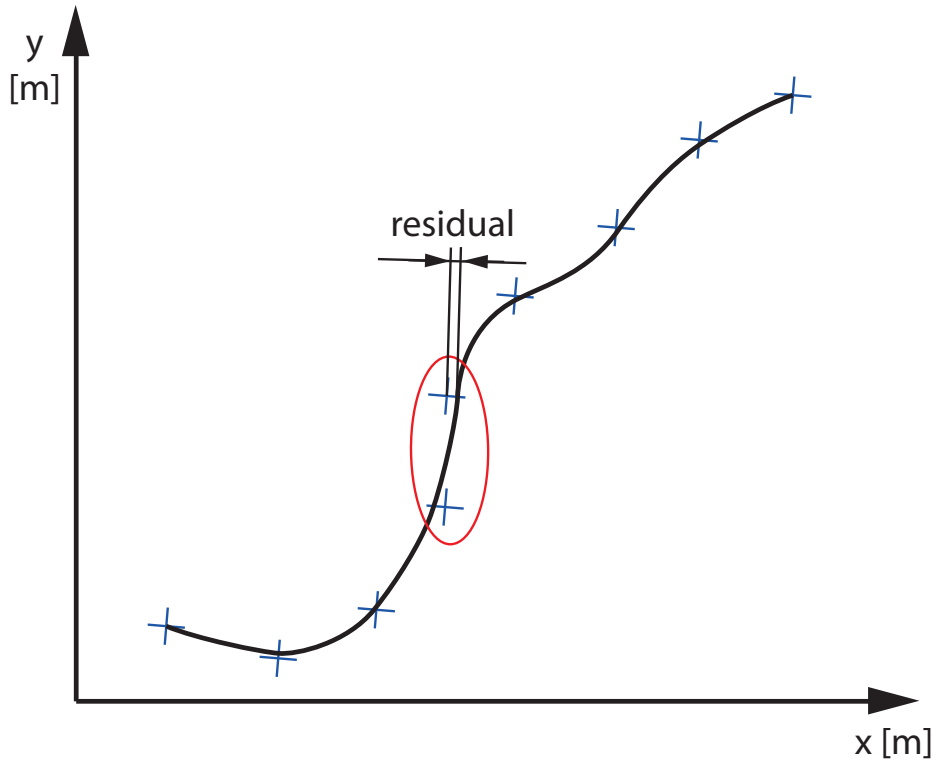

Figure 4.9: Fitting a road with a hermetic cubic spline and a certain error.

Spline fitting is made by a function that takes three arguments. The x and y coordinates of the points to be fitted and a smoothing parameter. In *Matlab*, the smoothing parameter ranges from 0 to 1 where the first one represents a straight line between the first and the n^{th} point. A specified value of 1 indicates that an interpolation (a perfect fit) is applied where every point is part of the fitted curve.

$$spline = f\left(x, y, smoothing\right) \tag{4.6}$$

For some tracks the fitting is not a straight forward task and may require iterative modifications on the smoothing parameter as well on the imported points to obtain a satisfactory approximation of the road track. In the investigated cases, the value of the smoothing parameter has been found between 0.75 and 0.995 by trial and error.

Curvature Calculation

The curvature of a curve can be determined in various ways. Depending on the form of the function given, different formulas apply. For a curve given by a function $y = y(x)$

the curvature κ can be calculated with

$$\kappa = \frac{y''}{(1+y'^2)^{\frac{3}{2}}} \tag{4.7}$$

where the curve radius is given by

$$R = \frac{1}{\kappa} \tag{4.8}$$

It is not possible to describe every planar curve by an equation of the form $y = f(x)$. Let us look at figure 4.10. It shows a piece of road where the value x_i maps to three different y_i values. There exists no possibility to distinguish between each y_i value. That means that a distinct representation of this curve must be taken.

A better suited form in this case is the representation of the curve by a natural parameter. Basically the parameter might be any real number but it is useful to take the arc length s.

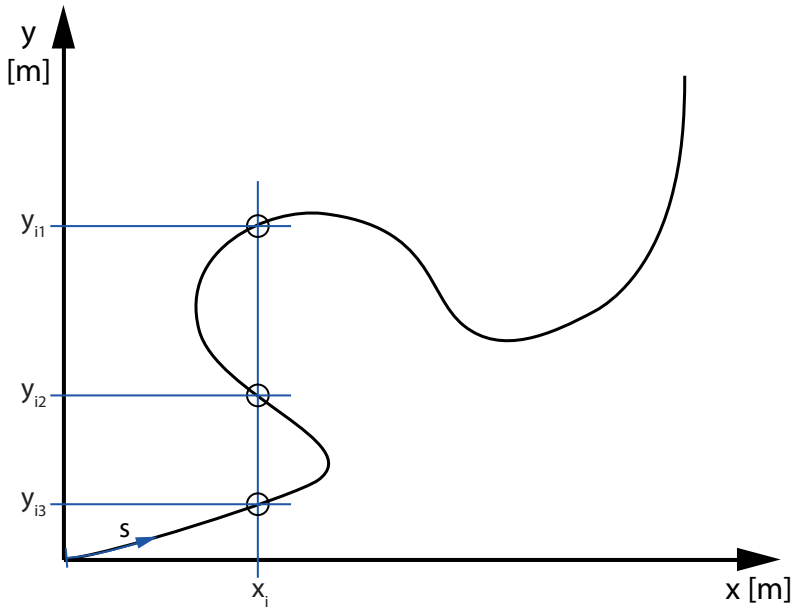

Figure 4.10: A road track that is not representable by a function.

A parameter curve is defined by

$$x = x(t), y = y(t) \tag{4.9}$$

where t denotes the natural parameter, x and y the coordinate tuples. As stated previously it is useful to replace the natural parameter t by the arc length s writting

$$s = t \tag{4.10}$$

The curvature of a curve represented by a parameter function can be written as

$$\kappa = \frac{\dot{x}\ddot{y} - \ddot{x}\dot{y}}{(\dot{x}^2 + \dot{y}^2)^{\frac{3}{2}}} \tag{4.11}$$

and $\dot{x}$ is the derivation of the x coordinate by the parameter t.

The arc length s is given by

$$s = \int_{t_1}^{t_2} \sqrt{\dot{x}^2 + \dot{y}^2}\, dt \tag{4.12}$$

and from this equation it can be seen that s itself is a function of the parameter t. The coordinate functions are further expressed as functions

$$x = x\left(s\left(t\right)\right), y = y\left(s\left(t\right)\right) \tag{4.13}$$

where the parameter is defined $t \in \mathbb{R}_0^+$.

4.1.3 Curve Radii Calculation

In road construction circles are used and those are connected with Euler spirals. A Euler spiral, also commonly referred to as clothoids or Cornu spirals, is a curve whose curvature changes linearly with its curve length. It serves as a transition curve between a straight and a circle to avoid sudden steering corrections when entering a curve from a straight run [20, p. 95].

The radius of a parameter function can be calculated as seen in equation 4.11 and taken the reciprocal value of it. For further risk simulation, not the radius function is required but the curve count and its corresponding radii of a whole road track.

The curves need to be calculated from the spline. In figure 4.11 a section of a road is shown. It includes three curves. A straight line has an infinite curve radius ($R = \infty$). In a smooth spline curve, supposing that no sudden steps or abrupt oscillations are in, when the motorcycle rider enters the curve coming from a straight piece of road, the curve radius begins to decrease until the point with the smallest radius is reached. After

it, the radius increases until a straight piece of road continues or a curve turning onto the other side follows. The radius of the curve changes the sign.

It may occur that a curve is divided into subcurves. This means that a curve closes, opens and closes once more but the second radius is greater than the first one. Mathematically spoken the function has one global minimum and two or more local minima. Figure 4.11 shows schematically the radius plotted as a function of the arc length. The arc length is equal to the distance travelled. Curve 2 has a minimal radius first, the radius increases then and turns into a local minimum.

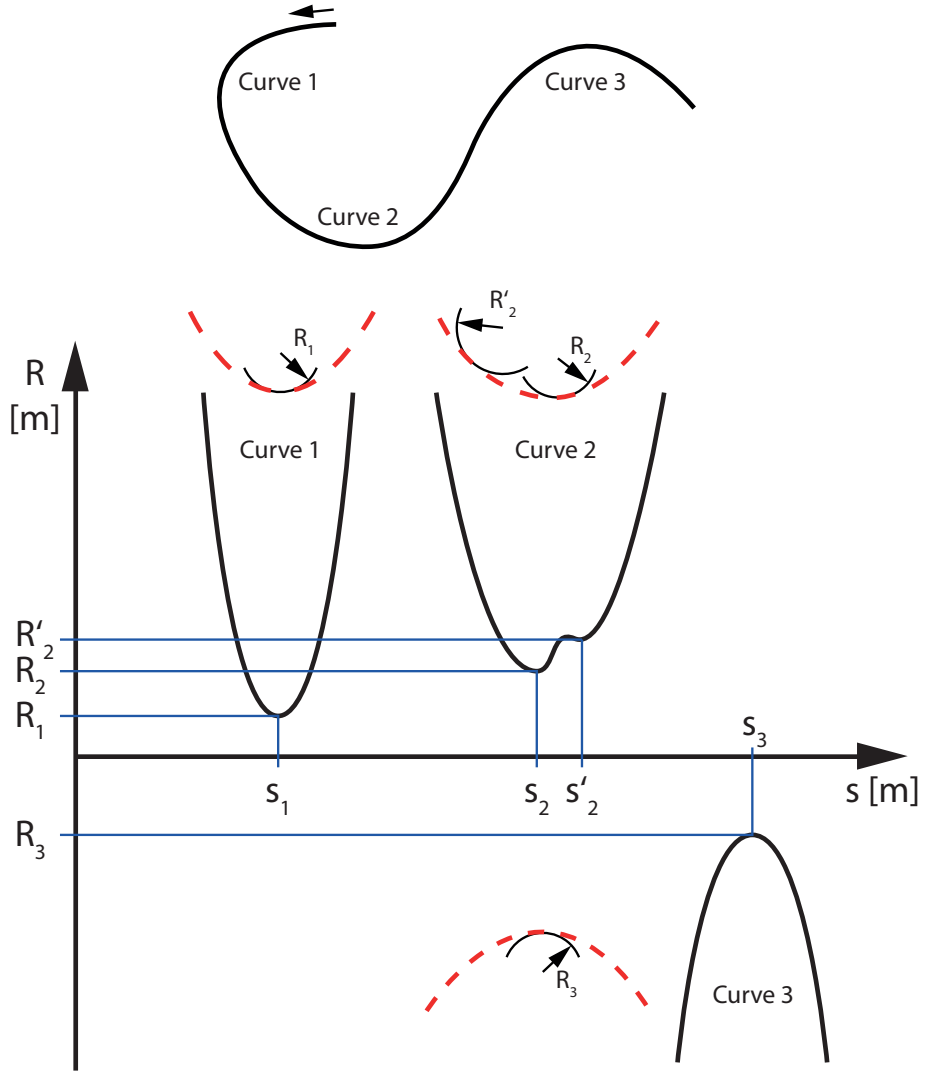

Figure 4.11: A schematic plot of the radius as a function of the arc length.

In this study only the global minimum radius of a curve is considered. The minimal radius is the one that determines how critical a curve is. In more detailed studies it may

be included the progressive closing of a curve but it is omitted for simplicity in this one.

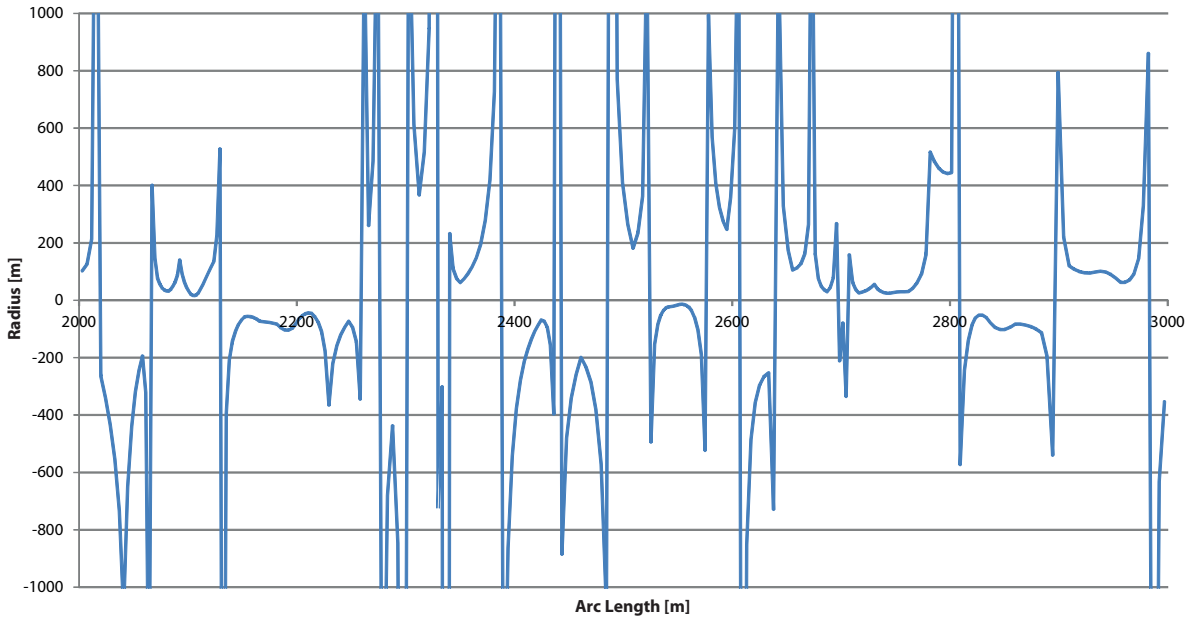

Figure 4.12: The radius plot as a function of the arc length of the road number B27.

The real radius function over the travelled distance varies from the ideal model. From $2000m$ to $3000m$, figure 4.12 shows the radius. The patterns that where assumed in figure 4.11 are reflected in the real road section too but intermediate high-frequency oscillations in the curve show up.

When the road path is copied by marking the points, practice showed that a relatively constant distance between each marked point enhances the quality of the fitted spline. At the change of a straight piece of road into a section with many sharp curves, the point distance should fade slightly into decreased distances.

It is essential for the algorithm to be able to detect curves accurately since minor differences to the real curves may result in totally different final risk prediction values.

4.1.4 Determine Curve Radius Gradients

As described in section 4.2.2, when travelling along a road the single curve radii affect the risk but also the run of the road, generally speaking the gradient of the curve radii.

Those gradients have to be determined. If all single radii are available of the road it is a simple task to calculate the gradients. In this case the gradient is not calculated in

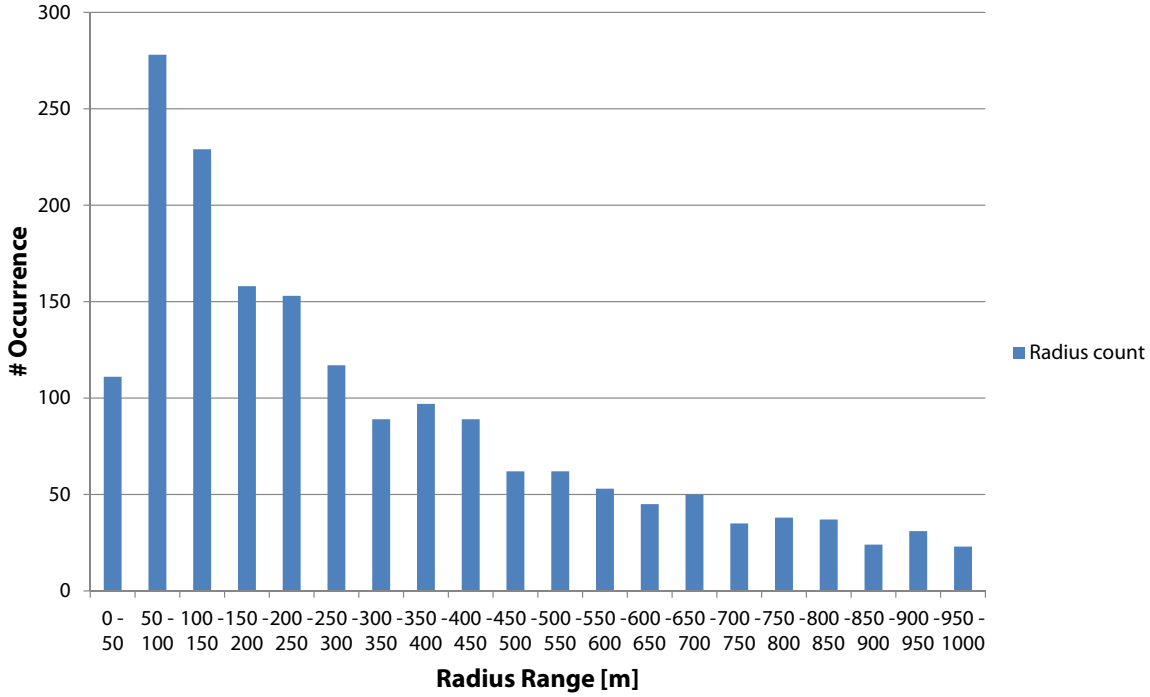

Figure 4.13: The occurrence distribution of the radii of the road number B27 plotted in 50 m steps.

the common sense. It is described by the ratio of the current radius and the following one and can be written as

$$r = \frac{R_i}{R_{i+1}}, i = 1, 2, ..., n \tag{4.14}$$

R_i denotes the radius of the current visited curve, R_{i+1} is the radius of the following curve and r is the ratio. A value greater than one ($r > 1$) means that the following curve is sharper. The index i is the curve number and n is the curve count. At the n^{th} curve, the ratio is not defined by definition because no $i + 1$ radius value is available.

The gradient depends on the direction of the curve visited. The road needs to be traversed twice in the forward and backward direction and corresponds to real-life situations with a two-way road.

4.2 Statistical Model

This modelling approach is taken to investigate the ability to simulate the accident risk based on statistical reports. Reports provide much distinct data material of accident happenings. Statistic analysis on accident occurences on rural roads evidence that significant parameters exist and seem to correlate. A closely related dependency to the risk of motorcycle accidents is hypothesized.

Let $\{(p_1, y_1), ..., (p_i, y_i), ..., (p_n, y_n)\}$ be a set of collected accident data. p_i is a vector of accident related characteristics - causal factors of an accident - at a location i and y_i is the number of crashes reported at the location i.

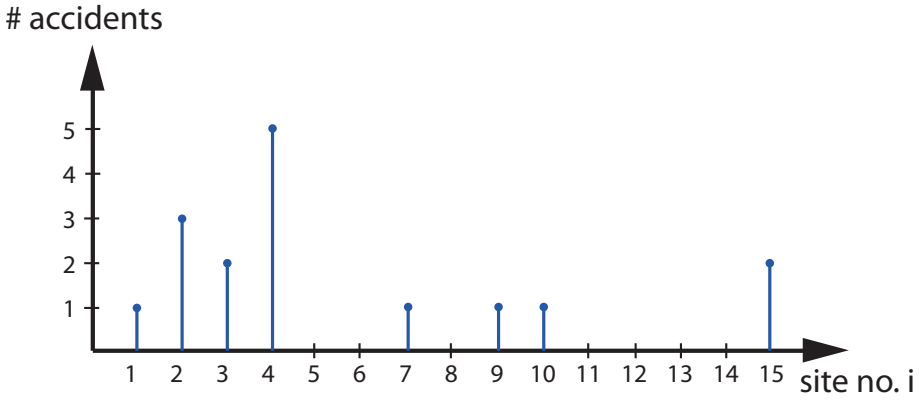

Figure 4.14: The accident count per site illustrated schematically.

The occurrence of an accident at an arbitrary location i can be seen mathematically as an "success" or "failure" event. There are only two choices whether an accident takes place or not.

An essential task is to find a few parameters that are able to forecast the risk of an accident taking place in a certain curve. How well/badly the risk can be foretold lacks the evaluation of the model and shall be derived out of the results.

The risk is going to be defined as a real number starting from zero ($risk \in \mathbb{R}_0^+$). Because of the dependency on variables it can be written

$$h = f(p_1, p_2, p_3, ...) \tag{4.15}$$

where h denotes the hazard and p_i a risk parameter. The hazard is a function that is

dependent on the risk parameters but those are related to the location. The function can be expanded to

$$h = f\left(p_1\left(x,y\right), p_2\left(x,y\right), p_3\left(x,y\right), ...\right) \tag{4.16}$$

where x and y is the cartesian coordinate grid the virtual road is embedded into.

The hazard value is a value that should represent the riskiness of a curve on a road. As shown, it can be written as a function. It is not bounded within a certain range such as 0 to 100%. A single risk number of a curve is not meaningful until it is related to other values from the same road track. Whether a curve is considered hazardous in this model has to be investigated with simulation tests. A comprehensive data basis may improve determining an even more appropiate threshold value.

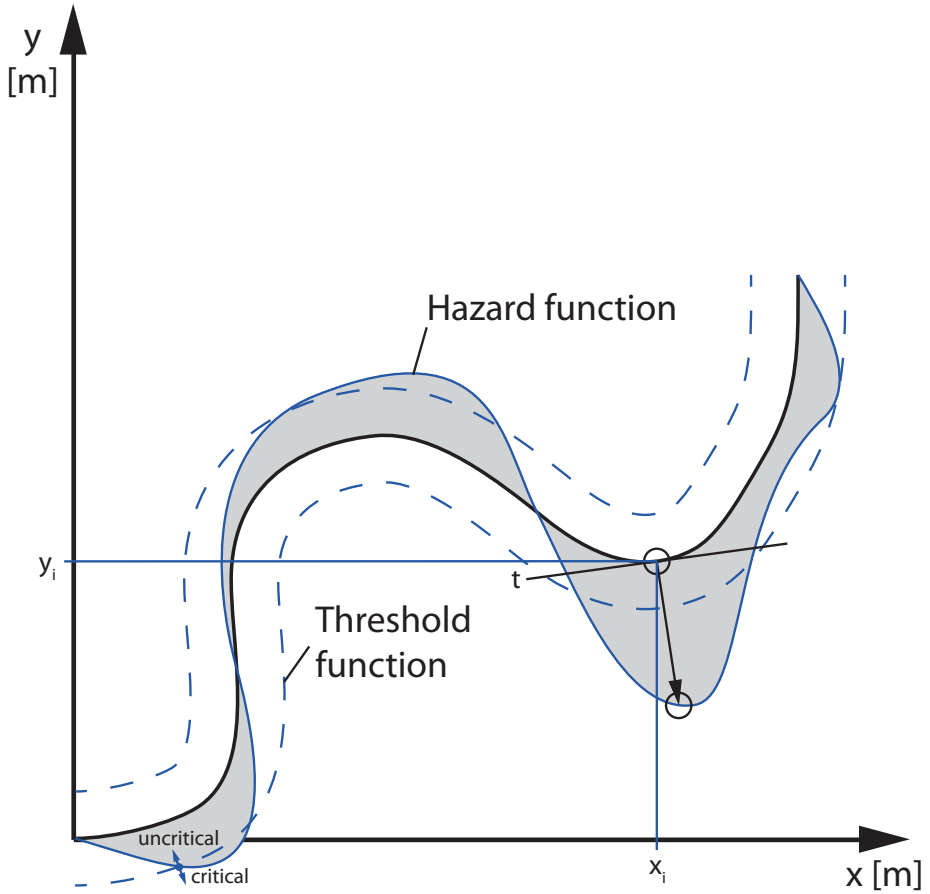

Figure 4.15: A schematic plot of the continuous hazard function on a road piece.

Figure 4.15 schematizes a piece of a road with a fictitious hazard as a function of the travelled distance. From that function an valuable conclusion should be able to be

taken.

Statistic data is not available in a continuous form. Accident locations are divided into sectors and majorly looked at in curves. So it is advantageous to discretize the hazard function according to the curves. Such a discretized hazard function schema is illustrated in figure 4.16. The abscissa shows the number of the curves and the ordinate shows the hazard value. After a certain value is passed the hazard is considered dangerous in terms of this model. A threshold value is introduced and divides the graph into a non-dangerous and into a dangerous zone. The line named as "threshold value" schematizes the level-crossing. The value itself has to be defined by using a methodology. In this case a trial-and-error method is used to determine the number approximately. Accident data is available for known road sections by means of two tracks the model is tuned by varying the risk threshold value. The output that said the prediction probability on those roads is intended to be maximized manually and might be considered as a manual emulation of a model tuning algorithm.

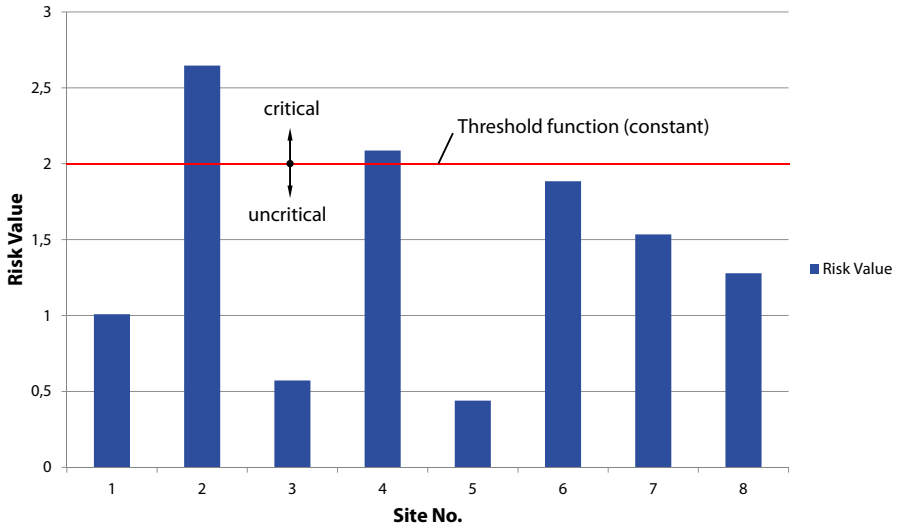

Figure 4.16: A schematic plot of the calculated hazard values.

The hazard is a function. Nevertheless, in order to calculate the risk, the function must be given. The simplest function that can be taken is a linear one. The total risk is a linear combination of each parameter introduced. Mathematically it can be put into

$$h = \lambda_1 \cdot p_1 + \lambda_2 \cdot p_2 + ... + \lambda_n \cdot p_n = \sum_{i=0}^{n} \lambda_i \cdot p_i \tag{4.17}$$

where λ is a conversion factor. The conversion factor enables to scale the parameter. It can be set to one that no scaling will be done.

A linear function is easy to manage in terms of tuning the model. In the model that is carried out in this study, a linear function approach is going to be used with the scaling factors of one.

In the following chapters, the details of the parameters are going to be worked out.

4.2.1 Curve Radius

Curves are trouble spots for vehicles of every type on rural roads. Speeds that exceed the limit of keeping the vehicle on the track may result in accidents. It is easier to reach the technical capabilities of a vehicle and bad environmental conditions can worsen the situation for a driver.

How can the riskiness of a curve be characterized with a simple geometric parameter? The radius qualifies how sharp a curve is starting from zero radius (a point) to an infinite radius (straight line). As described in chapter 3, Hartmann [1] conducted a detailed survey on motorcycle accident statistics on rural roads as a function of the geometric parameters of a road.

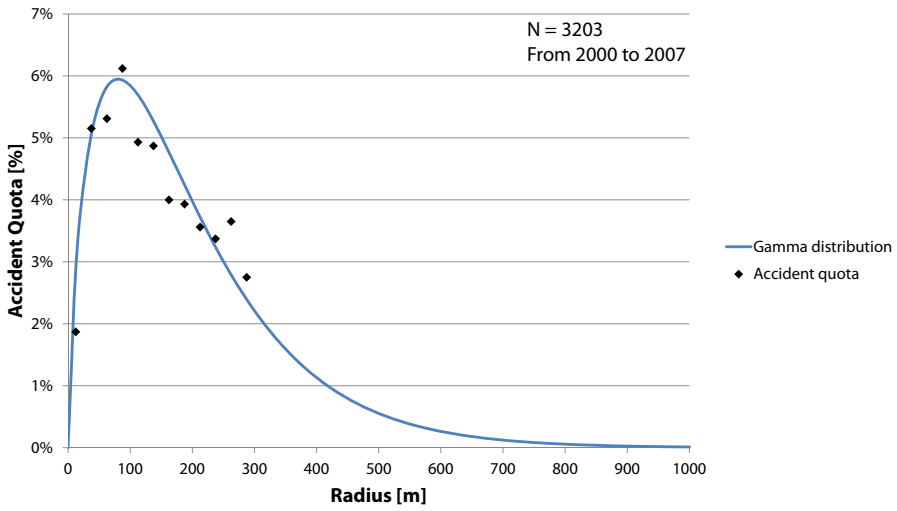

Figure 4.17: Accident percentage as a function of the curve radius [1, p. 67].

Accident quotas as a function of the curve radius can be seen in figure 4.17. The black line with its corresponding junctions are the accident quotas in percent of the

total accident count. The radius ranging from 50 m to 150 m has an elevated accident quota. More accidents happen and it is assumed that the risk is higher.

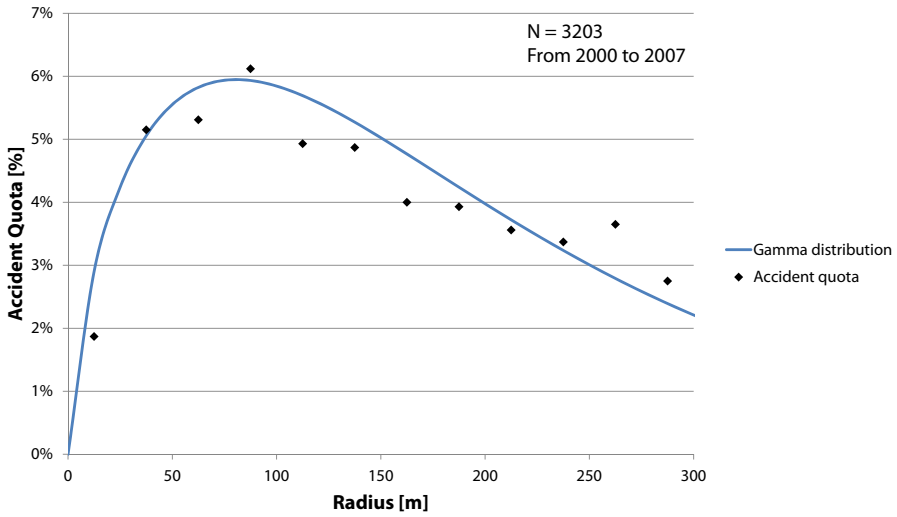

Figure 4.18: Accident percentage as a function of the curve radius zoomed into [1, p. 67].

Because no statistic analysis exist for radii above 300 m and to be able to determine the accident quota for higher radii, a probability density function is fitted into the discrete accident quotas. An adequate probability distribution needs to be found that can fit the supposed accident quotas above 300 m.

The gamma distribution [2] is a continuous probability distribution and is given by

$$f(x) = \frac{b^c}{\Gamma(c)} x^{c-1} e^{-bx} \quad , \quad x > 0 \tag{4.18}$$

where in our case the variable x is the radius. c and b are two parameters of the function and $\Gamma(c)$ denotes the Gamma function of c which is defined by

$$\Gamma(c) = \int_0^\infty t^{c-1} e^{-t}\, dt \tag{4.19}$$

The interval of x ranges from 0 to 1000 m. The function cannot be fitted into the quotas if the radius is not scaled. Thus it is introduced

$$f(x) = \frac{b^c}{\Gamma(c)} \left(\frac{x}{u}\right)^{c-1} e^{-b\frac{x}{u}} \tag{4.20}$$

b	0.12896
c	1.7038
u	16.04

Table 4.2: The gamma density function parameters.

R [m]	**p_1 [%]**	**R [m]**	**p_1 [%]**	**R [m]**	**p_1 [%]**	**R [m]**	**p_1 [%]**
0	0.000	275	2.586	550	0.382	825	0.046
25	4.240	300	2.210	575	0.317	850	0.038
50	5.552	325	1.880	600	0.262	875	0.031
75	5.937	350	1.592	625	0.217	900	0.025
100	5.845	375	1.344	650	0.179	925	0.021
125	5.498	400	1.131	675	0.148	950	0.017
150	5.025	425	0.949	700	0.122	975	0.014
175	4.503	450	0.794	725	0.101	1000	0.011
200	3.977	475	0.663	750	0.083		
225	3.474	500	0.553	775	0.068		
250	3.008	525	0.460	800	0.056		

Table 4.3: p_1 values at certain radii extracted out from statistic data material.

with a scaling factor u. The three parameters b, c, u are identified by fitting the curve with the least square error method. The blue lines in figure 4.17 and 4.18 show the fitted result function.

In table 4.3, the values in percent of the Gamma probability density function in an interval of 25 m are shown. The function decreases fast towards the positive abscissa. According to this function, the percentage of the happening of an accident at 1000 m is only one-hundredth of one percent of the total accident count. Further studies including a big data basis might shed more light on this issue and could verify or disprove this assumption.

The overall hazard function is extended with the probability value of the radius at a certain location x and y in the coordinate grid. It is expected that the hazard is influenced by the radius and write

$$p_1\left(R\left(x,y\right)\right) = f\left(R\left(x,y\right)\right) \tag{4.21}$$

where the x variable of the gamma density function is replaced by the radius.

The overall hazard function h can be written now as

$$h = p_1 + ... \tag{4.22}$$

with the scaling factor λ equal to 1.

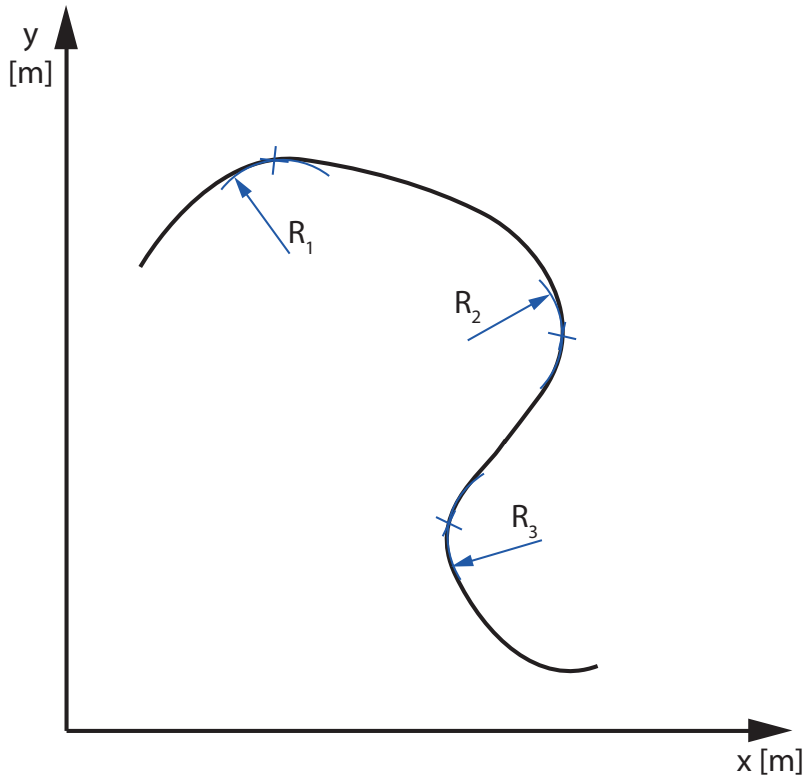

Figure 4.19: p_1 maps to each radius of a road track.

Each radius of a curve is mapped to a equivalent risk value p_1

$$R \mapsto p_1 \tag{4.23}$$

and forms an array of risk values. Table 4.4 contains an example mapping of the radius to the risk value.

4.2.2 Curve Radius Ratio

As outlined the previous chapter, the radius seems to affect the risk directly. When designing a road, not also the radii of the curves are taken care of but also the run of

R [m]	**p_1 [%]**
83	5.47
-22	3.55
-128	5.17
35	4.41
-349	1.77
-88	5.48
495	0.7

Table 4.4: A real road section example of the radius mapped to the risk parameter p_1.

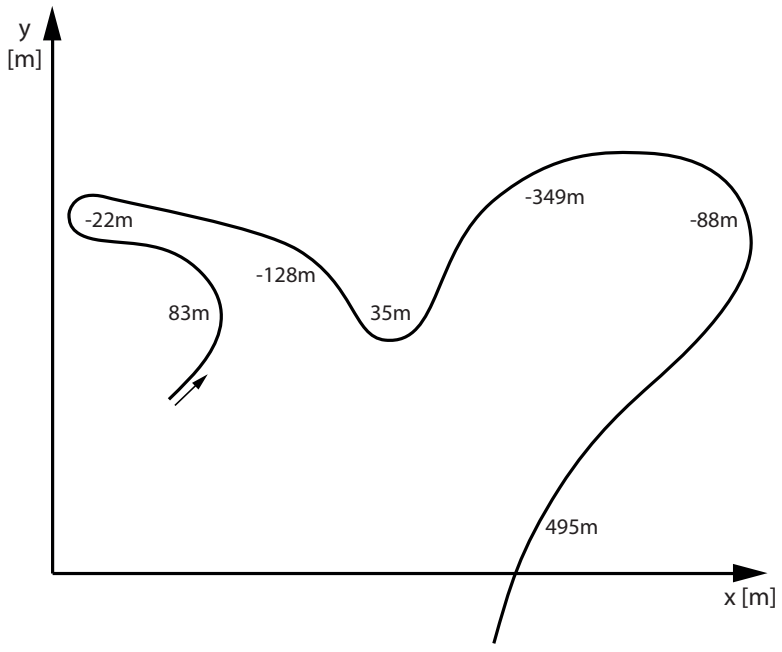

Figure 4.20: The schematic road run of the risk variable in table 4.4.

the whole road. An possible affect on the driving risk has been expected already for a long a time. Out of studies [1] in this field, it appears to confirm that the curves before the actual accident happens, are crucial for the risk of having a crash. A motorcycle rider may get towards his personal or the physical limits, is able to sustain the run but may crash in one of the following curves although the actual cause of the accident was in the curves before.

That is the reason why road designers usually consider, if environmental conditions afford it, to not introduce sharp curves after curves with big radii. The road run shall be harmonic from the driver's point of view. Such a map is shown in figure 4.21. Given the radius of a curve, this map indicates the range of the radius of the following curve so that a harmonic run between two curves is achieved.

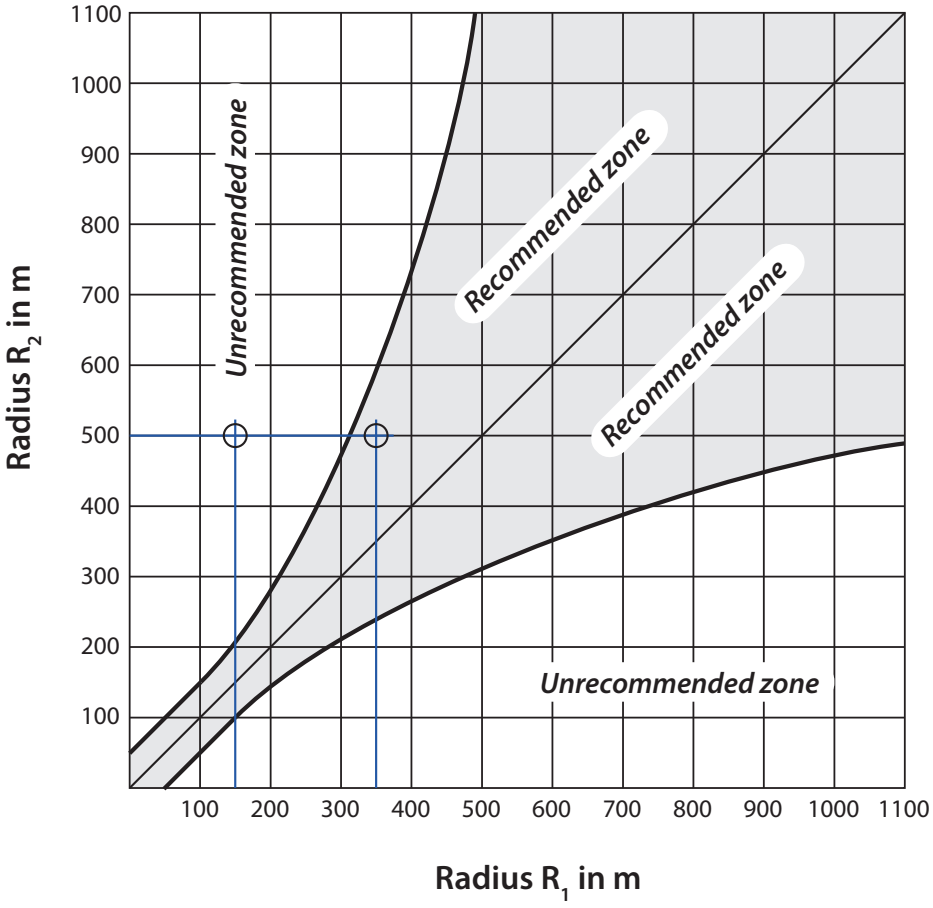

Figure 4.21: Radius ratio map for road curve design [1, p. 66].

Let us suppose the first radius is 150 m and the second is 500 m, then the junction of the two lines lays in the "unrecommended" area. The gradient from 150 to 500 m

is demanding. In contrast, if the first radius is 350 m and the second is 500 m, it is a smoother change and that is why the latter road design is advisable. The same applies on road sections that decrease the radius from curve to curve. The radius map is an recommendation and cannot be applied in every situation since the terrain hinders the construction or would not be affordable.

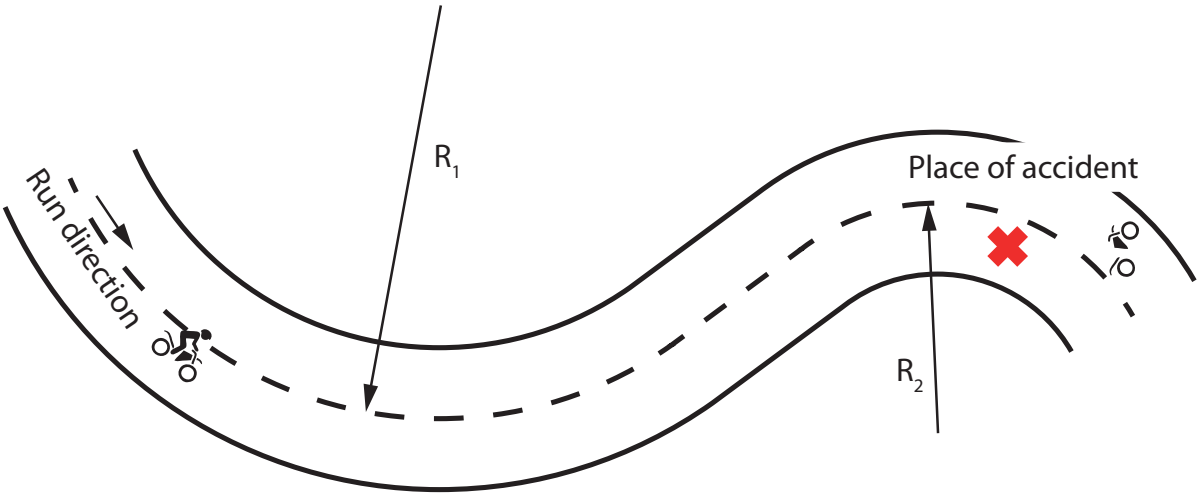

Figure 4.22: Illustration of the accident site. [1, p. 75]

Figure 4.23 charts accidents as a function of the radius ratio. Only accidents one direction are shown. The radius R_2 where the accident was detected and the previous curve radius R_1 are also shown. 16 accidents took place at a radius ratio less than 1 ($\frac{R_1}{R_2} < 1$) and 40 accidents were detected at a radius ratio greater than 1 ($\frac{R_1}{R_2} > 1$). The road must be traversed in two-ways if it is a two-lane road and outputs two risk result values.

Figure 4.24 also chart accidents as a function of the radius but in the opposed direction compared to the previous figure. Here, 8 accidents took place at a radius ratio less than 1 ($\frac{R_1}{R_2} < 1$) and 19 accidents were detected at a radius ratio greater than 1 ($\frac{R_1}{R_2} > 1$).

The highlighted area marked with an ellipse in both figures shows analogies in respect of the accumulation of accidents at a radius ratio greater than 1. It allows to construe that a road section where the radius decreases in each curve, the risk of accidents goes up.

Table 4.5 summarizes the accident count upon the radius ratio greater and less than

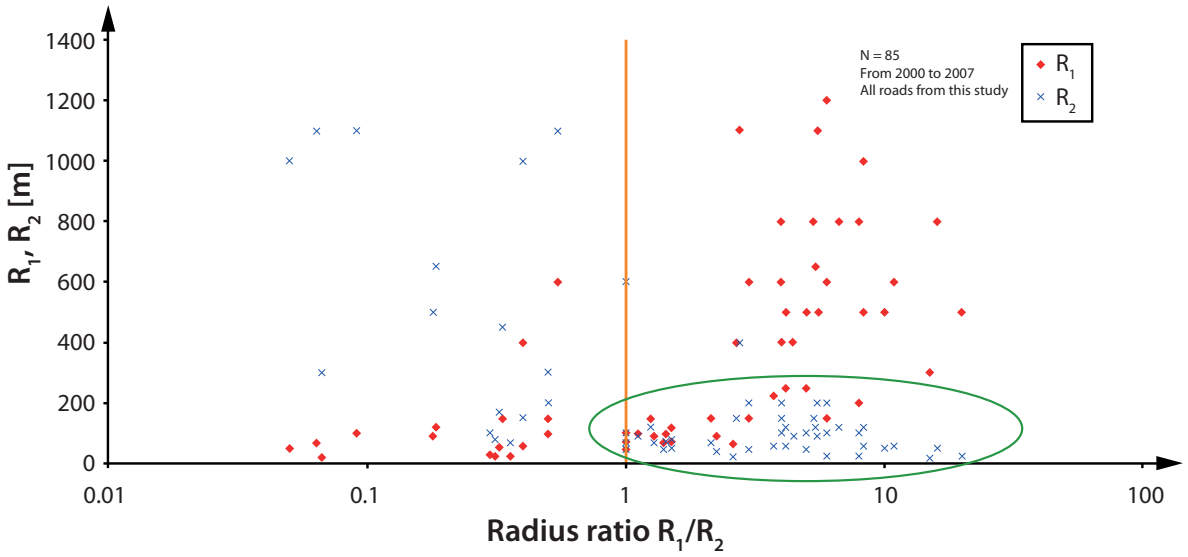

Figure 4.23: Accidents (increasing km) plotted regarding the radius ratio R_1/R_2 [1, p. 93].

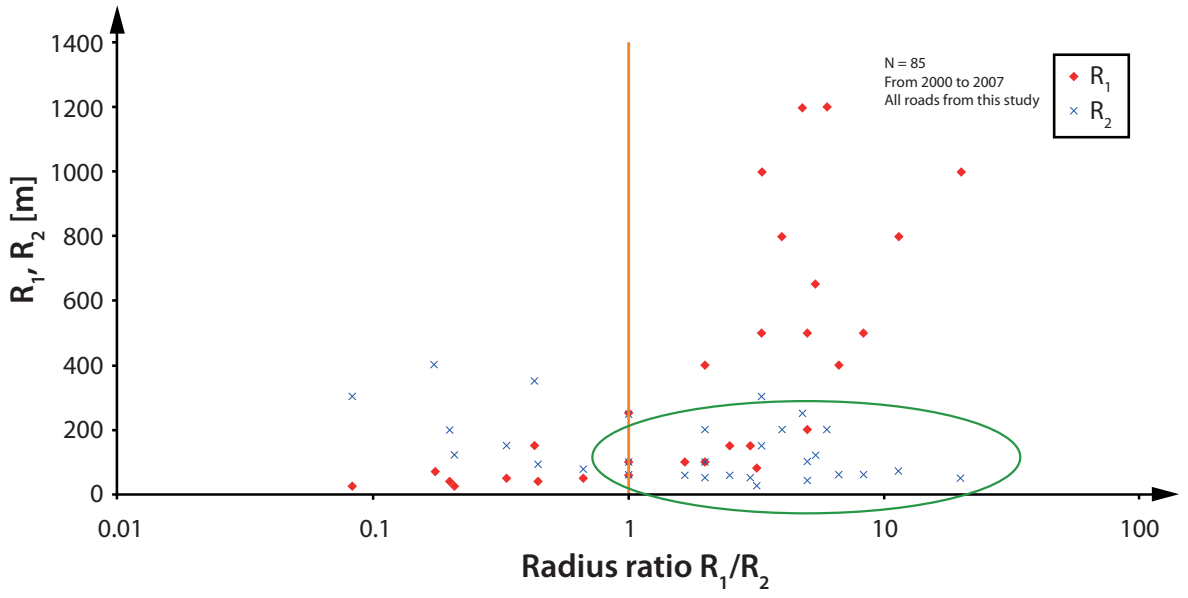

Figure 4.24: Accidents (decreasing km) plotted regarding the radius ratio R_1/R_2 [1, p. 94].

	$\left\lvert\frac{R_1}{R_2}\right\rvert < 1$	$\left\lvert\frac{R_1}{R_2}\right\rvert > 1$
increasing km	16	40
decreasing km	8	19

Table 4.5: A comparision of the accident count upon the radius ratio.

one. "Increasing and decreasing km" denominates a two-lane street that owns a number to be able to identify the direction of a run. The street has a start and an end point starting from zero kilometers. An apparent tendency towards decreasing curve radii can be noticed. Enlarging curve radii in a road run might not be as risky as sharpening curve radii. This may be argued that speed is not adapted to sharper curves in many cases and may lead to losing control of the motorbike.

From the findings about the radius ratio, the ratio is converted into a risk number to be aggregated to the total hazard function h. The risk in this chapter is written as a function of the radius ratio

$$p_2 = f\left(\frac{R_1}{R_2}(x, y)\right) \tag{4.24}$$

According to the values in table 4.5, it is presumed that radius ratios greater than 1 have twice as much accidents compared to radius ratios less than 1. The risk parameter p_2 for the radius gradient is going to be defined as following

$$p_2 = \begin{cases} 0 & R_1 = undef. \rightarrow \left|\frac{R_1}{R_2}\right| = undef. \\ 0.5 & \left|\frac{R_1}{R_2}\right| < 1 \\ 1 & \left|\frac{R_1}{R_2}\right| \geq 1 \end{cases} \tag{4.25}$$

It assesses a doubled risk to a curve ratio that is greater or equal than 1. This may vary from road to road but is a starting point for the roads that are going to be simulated. The absolute value of the ratio is taken to eliminate the influence of the curve direction to the left or to the right.

The radius gradient risk parameter p_2 is further appended to the total hazard function h and written as

R [m]	$\left\lvert\frac{\mathbf{R_1}}{\mathbf{R_2}}\right\rvert$	$\mathbf{p_2}$
83	undef.	0
-22	3,6964	1
-128	0,1756	0,5
35	3,6180	1
-349	0,1013	0,5
-88	3,9634	1
495	0,1780	0,5

Table 4.6: A real road section example of the radius mapped to the risk parameter p_2.

$$h = p_1 + p_2 + ... \tag{4.26}$$

In every curve where the radius ratio is defined, the curve ratio maps to the risk parameter p_2 written as

$$\left|\frac{R_1}{R_2}\right| \mapsto p_2 \tag{4.27}$$

4.2.3 Road Roughness

The International Roughness Index (IRI) is an international used index for comparing the pavement smoothness of roads and represents the reaction of a single tire on a vehicle suspension (quarter-car) traveling at 80 km/h to describe the roughness of the pavement's surface. The higher the IRI gets the rougher the road is [18, p. 1].

[1, p. 114] did a study on the dependency between the IRI, the occurrence in Austrian's road network and the accident count. In figure 4.25, the left bar shows the accidents in percent of all occurred accidents as a function of the IRI. The right bar describes the occurrence of the IRI in the whole road network of Austria.

Especially interesting are the IRI values where the accident percentage exceeds the occurrence percentage of the IRI in the road network. It might indicate that the road's roughness is a causal factor for motorcycle accidents.

To retrieve a continuous accident function depending on the IRI, the Gamma density function is used to approximate the accident quota continuously. Figure 4.26 illustrates

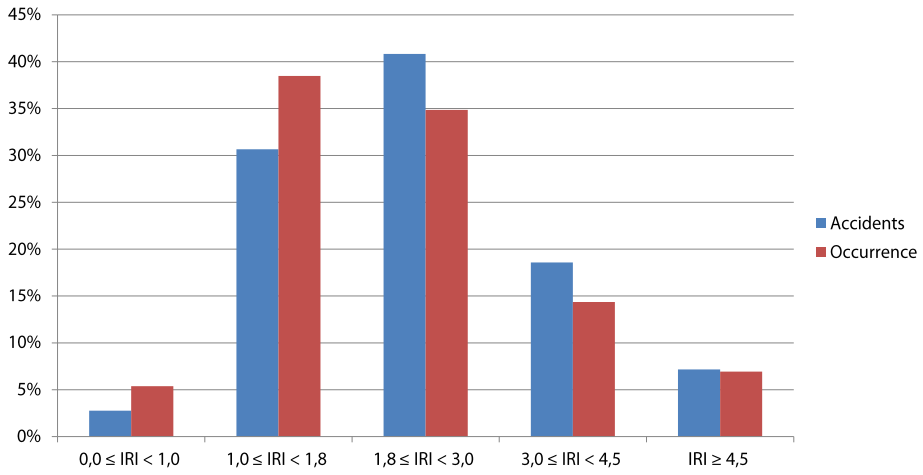

Figure 4.25: The accident percentage plotted as a function of the IRI and the occurence of it in the road network [1, p. 114].

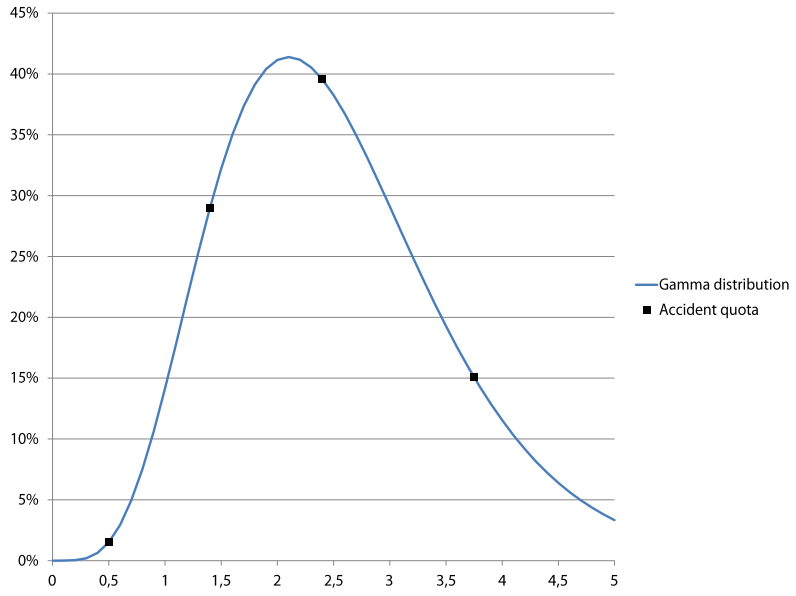

Figure 4.26: The approximated Gamma density function and grouped real accident quota based on the IRI.

b	2.33979
c	5.91651

Table 4.7: The gamma density function parameters for the accident quota as a function of the IRI.

the Gamma distribution fit compared to the real accident quota marked as rectangles. The parameters of the Gamma density function are determined by minimizing the sum of least square errors. Details about the Gamma function see equation 4.20. In this case the scaling parameter u can be ommitted since moderate x values ranging between zero and five permit to scale the seek function correctly.

The IRI influence is embedded into the risk function as in the previous section 4.2.2 with an additional scaling factor λ.

4.2.4 Road Profile Depth

The Mean Profile Depth (MPD) characterizes the road's superficial structure. The value varies depending on the material used in road construction as well as on the construction process itself. Traffic load and the weather has a significant long-term influence on it [1, p. 114].

[1, p. 114] collected 3,070 motorcycle accidents and classified them by MPD value ranges and furthermore outlines the occurrence of the MPD value ranges in Austrian's road network as shown in figure 4.27.

4.2.5 Longitudinal Road Plane

Roads are embedded into the environment and are usually aligned to the terrain in certain ways. In road constructions it is not possible to avoid up and downhill grades although they should be minimized. The longitudinal plane is the parameter that describes the up or downhill grade in percent [1, p. 112].

3,188 motorcycle accidents are classified by the longitudinal plane by [1, p. 112] and can be seen in figure 4.28.

More than 64% of all accidents took place at sites within one or two percent. It

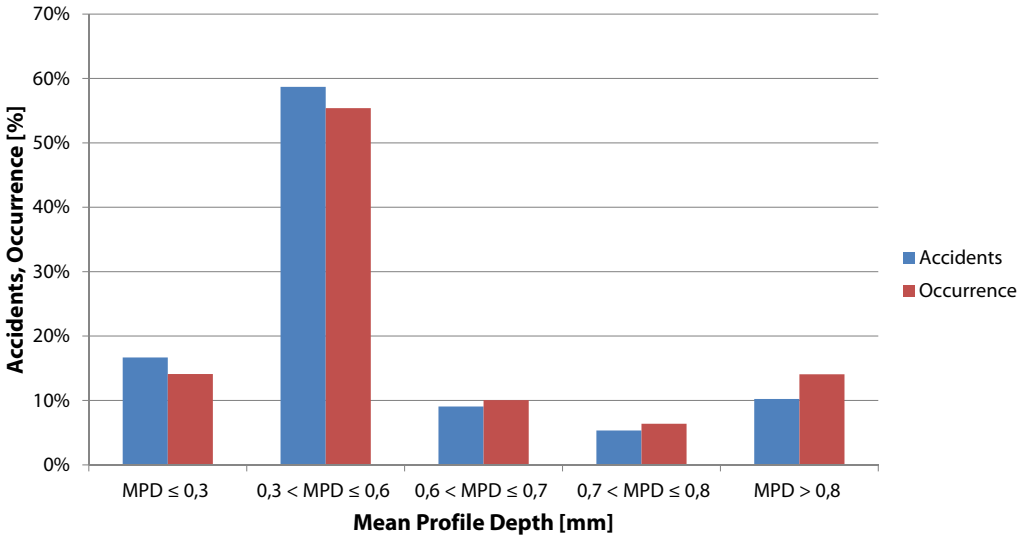

Figure 4.27: The accident percentage plotted as a function of the mean profile depth and the occurence of it in the road network [1, p. 114].

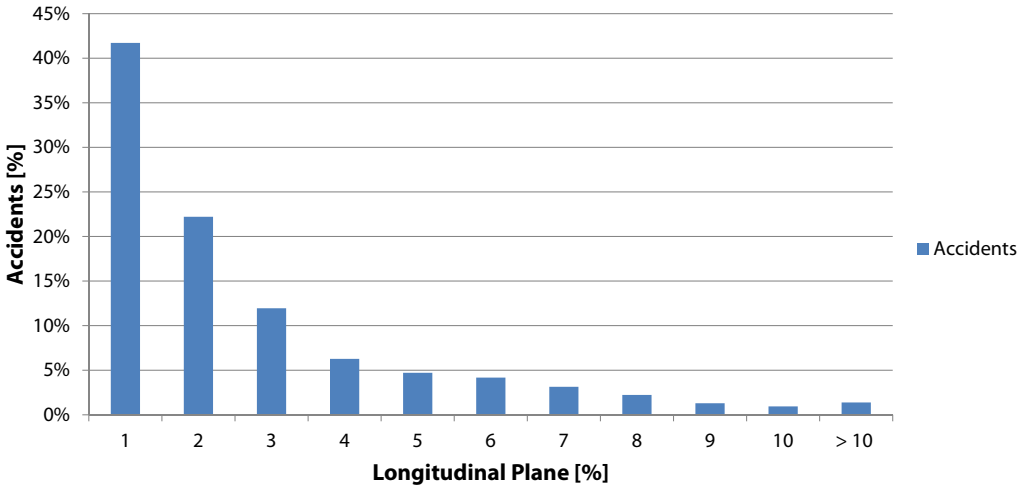

Figure 4.28: The accident percentage plotted as a function of the longitudinal plane and the occurence of it in the road network [1, p. 112].

may be concluded that the longitudinal plane has an insignificant causal influence on accidents.

4.2.6 Transversal Road Gradient

As stated in 4.2.5 terrain often does not enable to construct straight roads. The transversal plane of a road has several tasks. Primarily, due to an transversal inclination of the road the water can drain off. Additionally in a curve, a part from the centrifugal force is induced into the ground apart from only being sustained by friction. It is an gradient and measured in percent [1, p. 112].

In figure 4.29 3,188 motorcycle accidents are shown and divided into gradient ranges from one to greater 10% [1, p. 112].

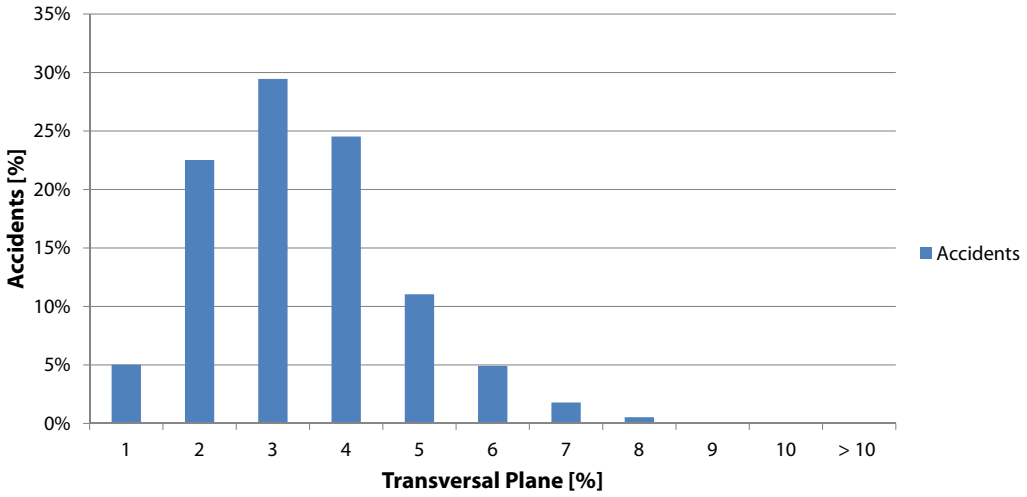

Figure 4.29: The accident percentage plotted as a function of the transversal road plane and the occurence of it in the road network [1, p. 113].

The majority of the accidents happens at little gradients and shows that straight pieces of roads and curve in and outgoings are the main sites of motorcycle accidents.

4.2.7 Road Friction Coefficient

3,182 motorcycle accidents are classified by friction coefficient ranges. The occurrence of those friction coefficients in the Austrian's road network are overlapped and shown in figure 4.30 [1, p. 113].

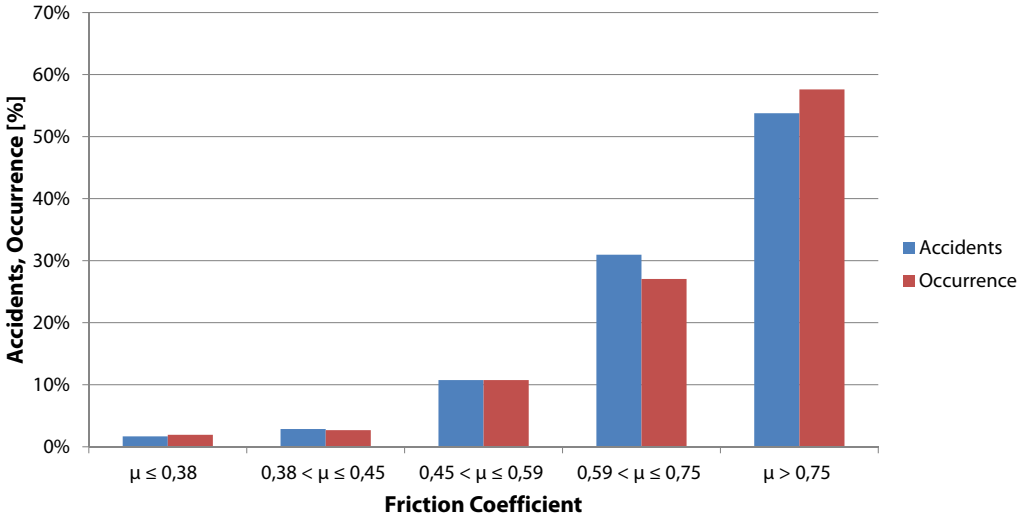

Figure 4.30: The accident percentage plotted as a function of the friction coefficient and the occurence of it in the road network [1, p. 113].

More than 80% of all accidents happen under very good and good conditions regarding the friction coefficient. Abrupt changes of the road's surface that said friction loss or gain may have a significant influence on accident counts but demands a closer study to verify the statement. From 0.59 to 0.75 a superproportional percentage of accidents took place compared to the occurrence in the road network.

4.2.8 Road Rut Depth

The rut depth on a road is measured transversally to the road with a rod and can be seen as the deviation in millimeters from the ideal plane [1, p. 115].

[1, p. 115] categorizes 3,181 motorcycle accidents into rut value ranges. The occurrence of the rut depth values in the road network are shown combined with the accident percentage in figure 4.31.

In the range from 5mm to 10mm and from 10mm to 15mm is a superproportional occurrence of accidents outlined. It may be concluded that ruts after certain value influence the accident number negatively.

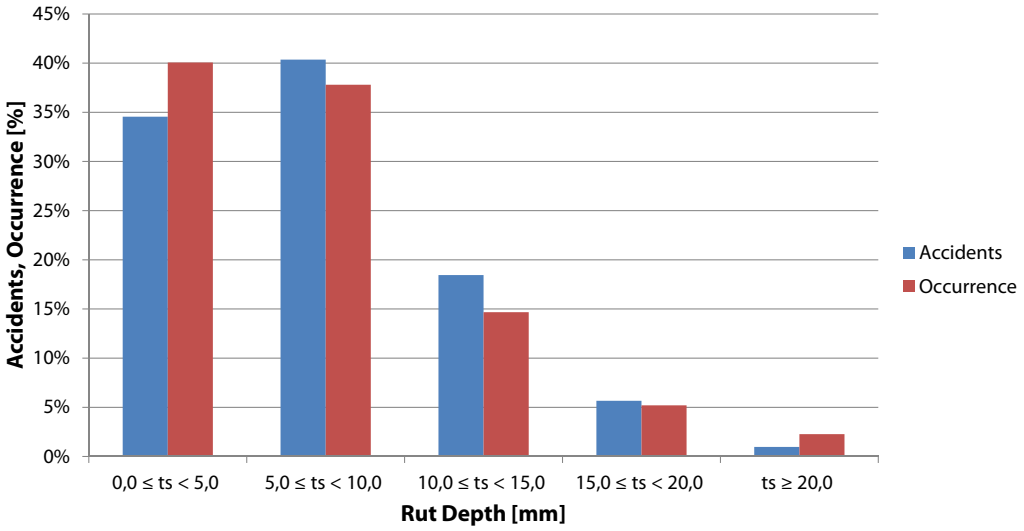

Figure 4.31: The accident percentage plotted as a function of the rut depth and the occurence of it in the road network [1, p. 115].

4.2.9 Road Water Film Depth

The theoretical water film depth on a road is related to the rut depth described in 4.2.8. Water on the road forms a film that depth depends on the transversal road profile and gradient [1, p. 116].

[1, p. 116] puts 3,181 motorcycle accidents into several categories regarding the theoretical water film depth and shows the occurence of those categories in the Austrian's road network.

The accident percentage and the occurence of the theoretical water film depth differs vastly compared to the other previously looked at parameters. Between 1 and 2.5mm occurence is low but the accident quota is relatively high. This may lead to the conclusion that this parameter plays a role in accident causalities.

A statistical model is taken to model a risk value and based on that a decision of hazard severity of a track is made. In the following chapter a physical model is going to be derived that aims to point up the variable dependency of velocity, friction and roll angle. Those physical values are looked at in all curves and compared with the output of the statistical model.

Next, the risk results of the simulation of real road sections in Austria are shown.

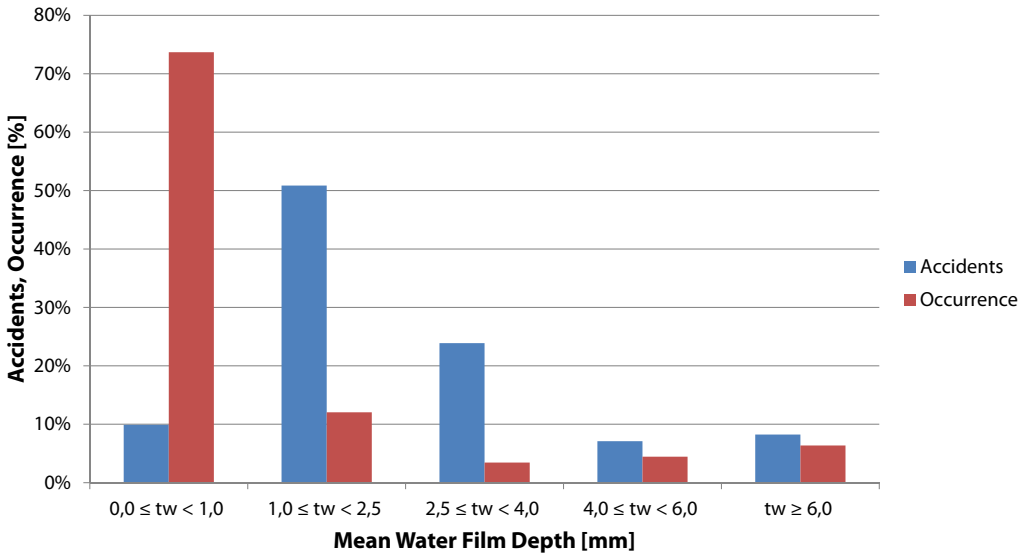

Figure 4.32: The accident percentage plotted as a function of the water film depth and the occurence of it in the road network [1, p. 116].

5. Simulation Results

The simulation model that has been worked out in the chapters before is applied on six real road sections in Austria. They are known as high risk sections for motorcycle riders and in the last years a considerable motorcycle accident density is noticed.

Various parameters for feeding the risk simulation have been worked out in the previous chapter 4.2. Currently two parameters are used within the simulation. In future extensions the other presented parameters may be appended and implemented into the model.

In this case a risk threshold value of two is taken and applied to the other four road sections. The individual results are presented in the coming sections.

5.1 Roads for Model Tuning

The two roads B27 and B20 (Reith to Mitterbach) are taken to tune the model. The tuning is done by hand and consists of determining the risk threshold value. This process has space for further improvement by applying a multidimensional optimization technique to find a solution for the risk parameter constants and the risk threshold value.

5.1.1 Road - B27

The map of the road number B27 from Klostertal to Hirschwang is shown in figure 5.1. The crosses mark the start and the end point of the simulated road part.

The radii distribution is shown in figure 5.2. All radii of the road section are counted, divided into 50m step categories and put into a graph. It presents a similiar figure as in figure 4.18.

The result sites are marked in figure 5.3 with a square. The critical curves that were determined with the physical model are marked with diamonds.

Road	Used for Tuning	Used for Validation
B27 - Klostertal to Hirschwang	X	-
B20 - Reith to Mitterbach am Erlaufsee	X	-
B72 - St. Kathrein to Krieglach	-	X
B95 - Reichenau to Turracherhoehe	-	X
B127 - Rottenegg to Lacken	-	X
B164 - Bischofshofen to Muehlbach	-	X
B20 - Tuernitz to Annaberg	-	X

Table 5.1: The gamma density function parameters for the accident quota as a function of the IRI.

Figure 5.1: Map of the road number B27 from Klostertal to Hirschwang.

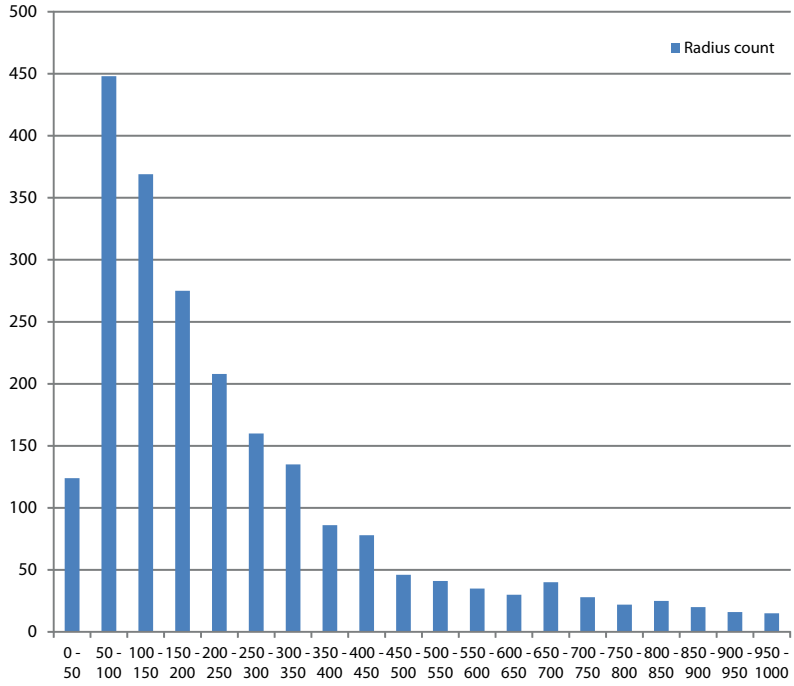

Figure 5.2: The radius distribution of the B27 road in 50m steps.

# real accidents	33
# real accidents at distinct sites	24
# predicted risk sites	35
# successfully predicted accidents	17
Accident prediction probability	**52%**
Site prediction probability	**71%**

Table 5.2: Summary of the B27 road's prediction results.

Table 5.2 sums up the results and shows the prediction probabilities of the site and the accident.

Table 5.2 sums up the predicted sites of the B27 road section. 33 accidents happened in total on that road from 2000 to 2007. 24 of them took place at distinct sites. The model's forecast is 35 risky sites and 17 are predicted correctly. "Correctly" in this case denotes accidents that happened in the same curve and is used throughout all coming results too. Refering the results to the real accident count leads to a prediction probability of accidents of 52%. The value results from dividing 17 by 33. It is possible that the percentage is over 100%. An overfit of the model would be the case and

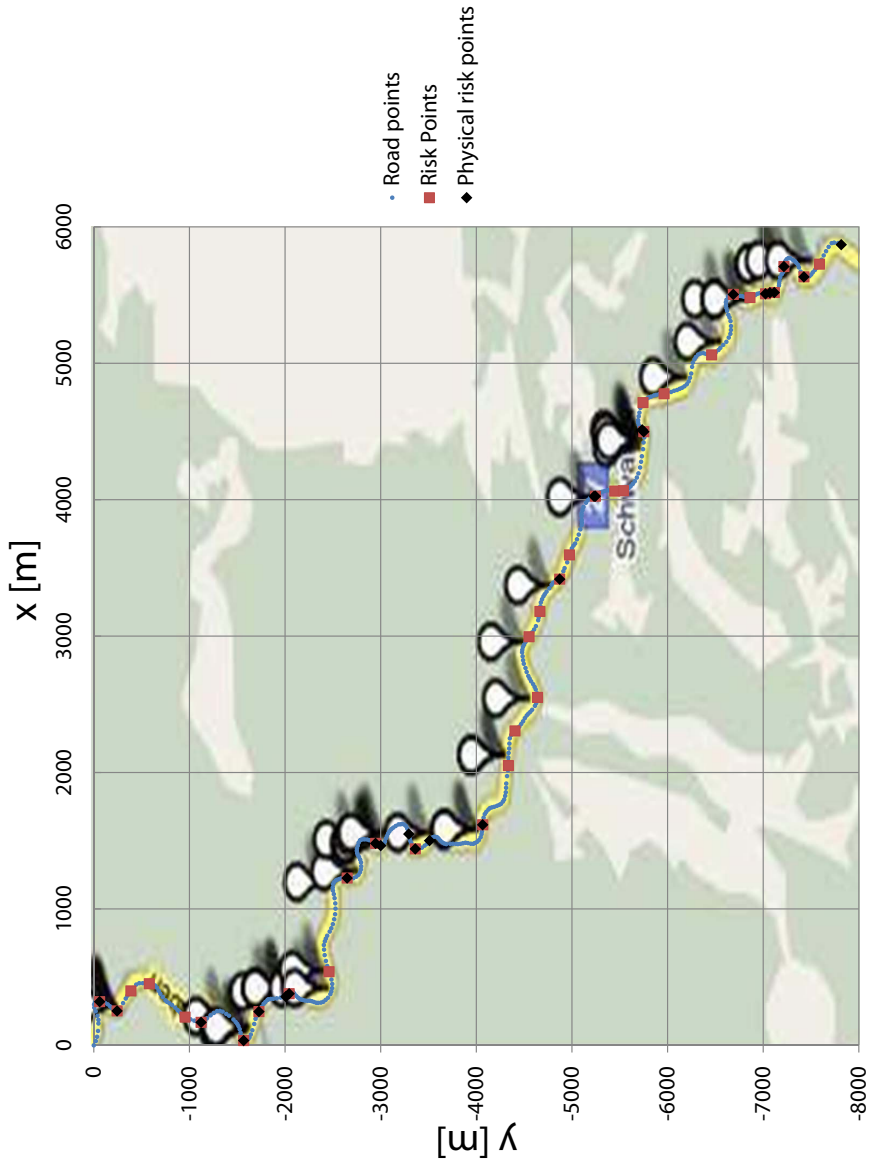

Figure 5.3: The B27 road's accident prediction sites results overlayed with the map.

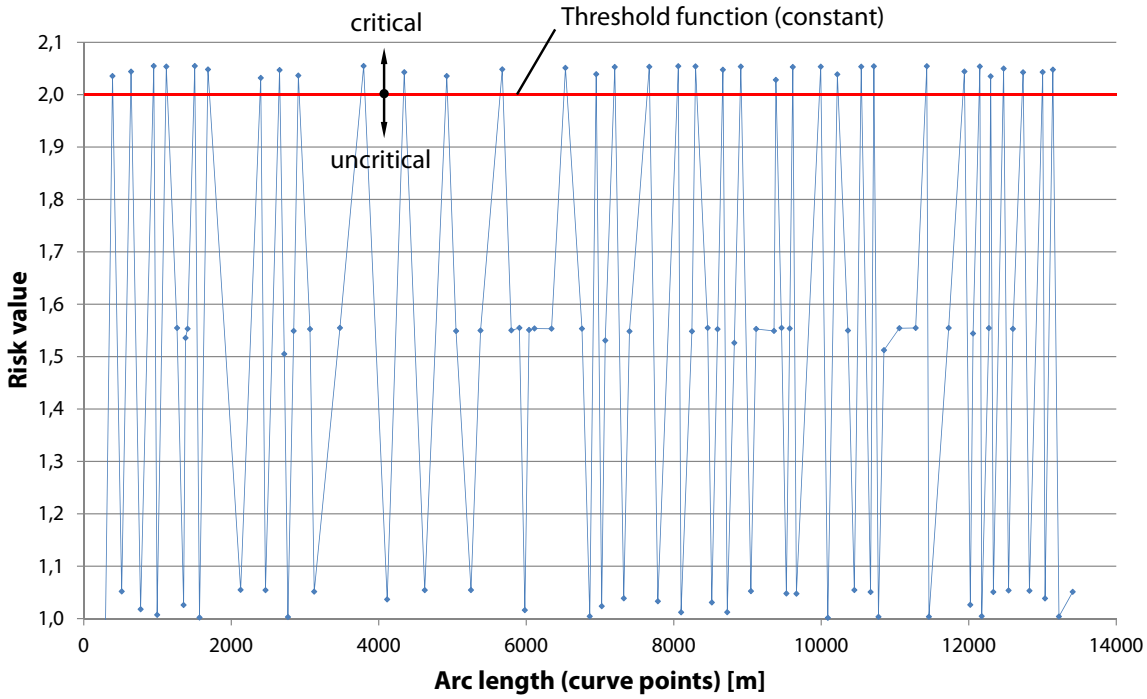

Figure 5.4: The B27 road's risk values as a function of the arc length in m.

practically means that more accidents are predicted than occurred. Another value gained from the model is the probability of predicting the site where an accident takes place. It is gained by dividing the successfully predicted accidents, 17, by the real accidents at distinct sites, 24.

5.2 Roads for Prediction

5.2.1 Road - B72

In figure 5.5 the map of the road number B72 from St. Kathrein to Krieglach is shown marking the start and the end point of the simulated road part with crosses.

Figure 5.7 presents the radii distribution of the B72. It follows the same distribution scheme as shown in figure 5.2.

The results of the forecast are shown in table 5.3. With the previously tuned model parameters the simulation is carried out on the other roads. The accident prediction probability is about 28%. The probability of forecasting the site is higher at 36%. The

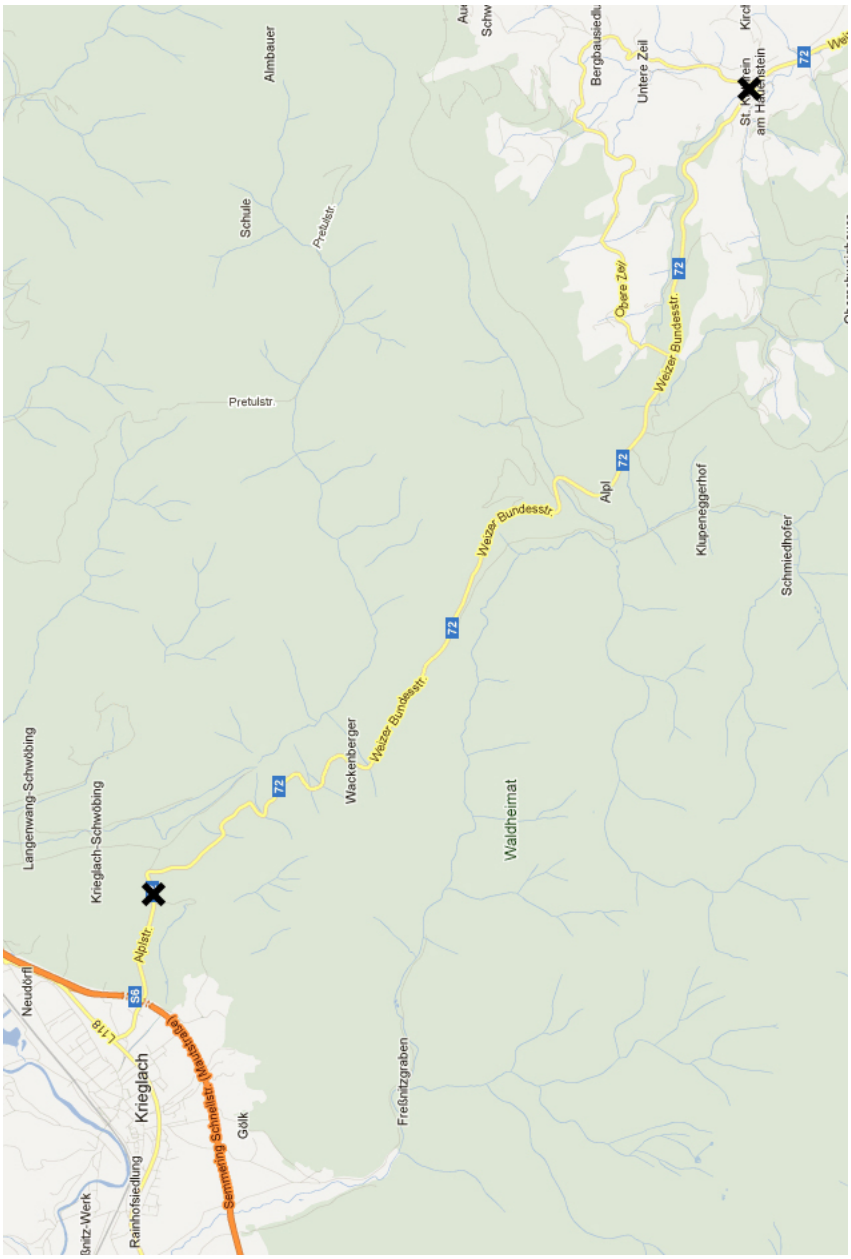

Figure 5.5: Map of the road number B72 from St. Kathrein to Krieglach.

# real accidents	14
# real accidents at distinct sites	11
# predicted risk sites	20
# successfully predicted accidents	4
Accident prediction probability	**28%**
Site prediction probability	**36%**

Table 5.3: Summary of the B72 road's prediction results.

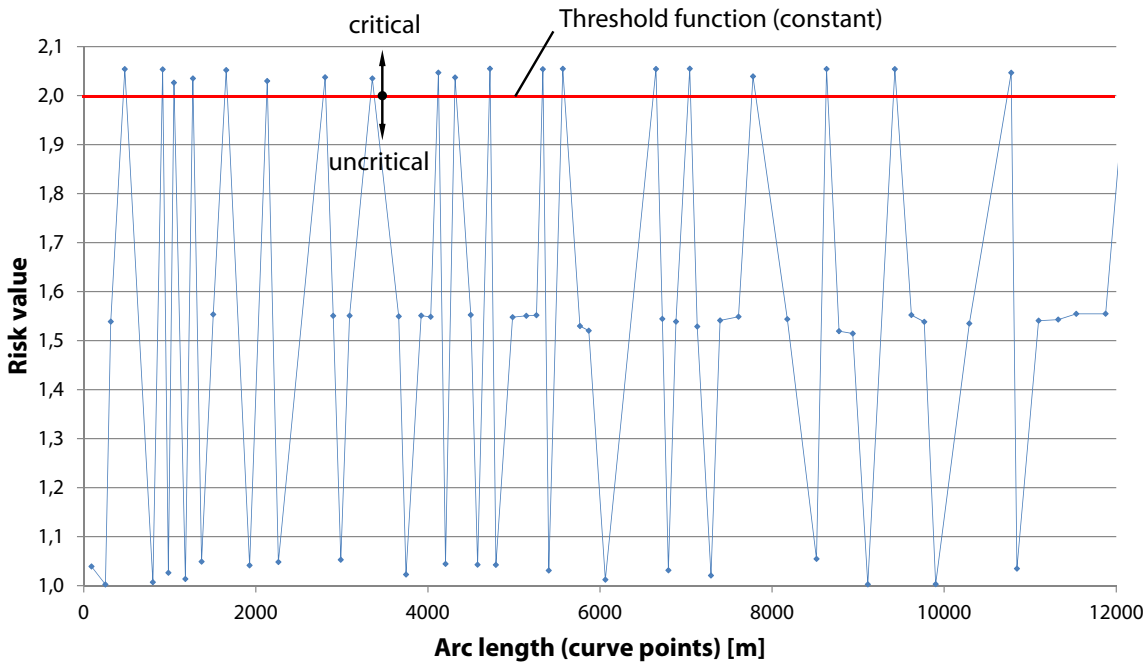

Figure 5.6: The B72 road's risk values as a function of the arc length in m.

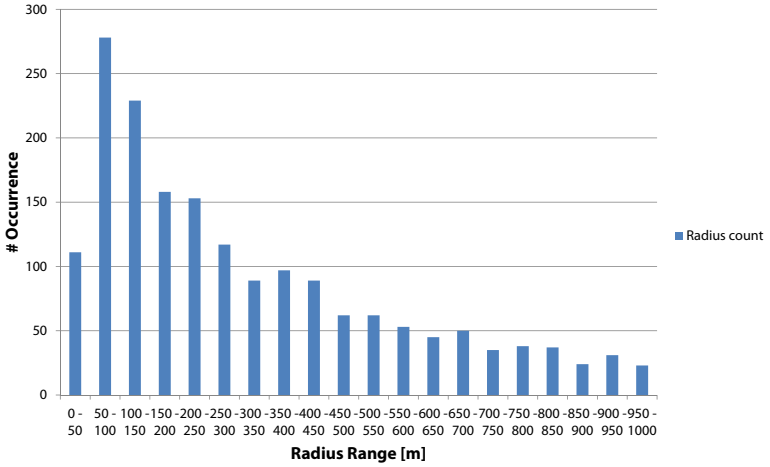

Figure 5.7: The radius distribution of the B72 road in 50m steps.

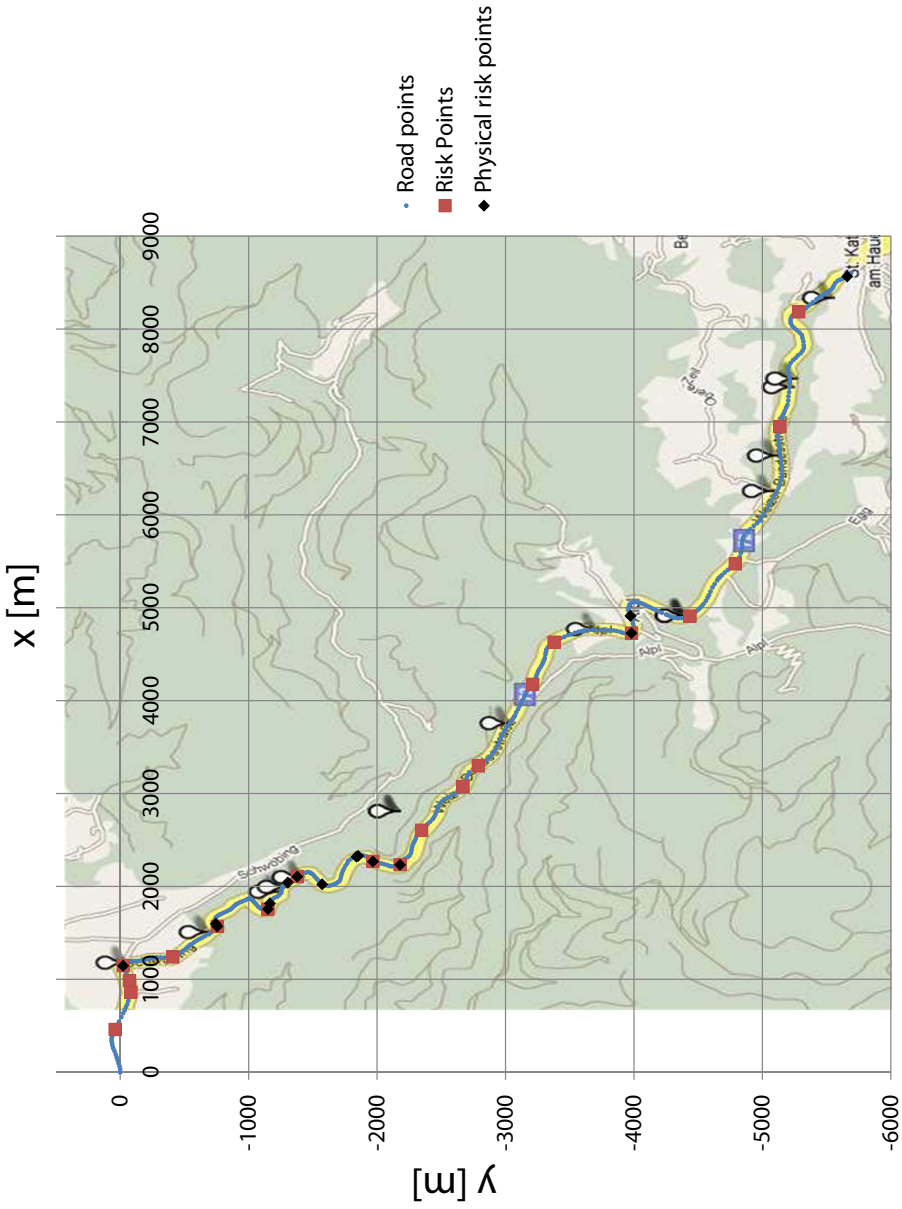

Figure 5.8: The B72 road's accident prediction sites results overlayed with the map.

B20 (Reith to Mitterbach) - accident prediction probability	73%
B20 (Reith to Mitterbach) - site prediction probability	122%
B20 (Tuernitz to Annaberg) - accident prediction probability	23%
B20 (Tuernitz to Annaberg) - site prediction probability	33%
B164 - accident prediction probability	34%
B164 - site prediction probability	37%
B127 - accident prediction probability	41%
B127 - site prediction probability	63%
B95 - accident prediction probability	26%
B95 - site prediction probability	28%

Table 5.4: Prediction percentages of the remaining roads.

forecast result probabilities are the half of the model output on the roads that are used for tuning the model.

5.2.2 Remaining Roads

The results of the roads that are shown more detailed in the appendix are listed compactly in table 5.4.

Mean accident prediction probability	**40%**
Standard deviation	**16%**
Mean site prediction probability	**56%**
Standard deviation	**31%**

Table 5.5: Mean prediction values of all roads' results.

5.3 Summary

The prediction results of every road is further statistically summarized. The mean values of the accident and the site prediction probability are calculated. In table 5.5 those values are listed. The mean accident forecast is 40% and can be interpreted as 40% of the accidents that occurred on the roads are foreseen by the simulation model. It is underfitted and infers that less accidents are predicted than happened actually. The standard deviation is 16% and can be seen as the statistical dispersion of the values. A less random component in the model also leads to lower standard deviation values.

6. Discussion and Outlook

[1] put up statistics about the radius influence on motorcycle accidents. The single radius is presented as an apparent causal factor as well as the radius ratio between two subsequent curves.

The accident quota as a function of the single radius practically recurs in all road sections that are studied. It could be the case that the accident quota correlates with the occurence of the single curve radius because those radii are the most common ones. This model set up with other parameters than the used ones might bring insight in the dependency of the single radius and the accident quota.

The radius ratio two subsequent curve radii describe show accumulated accidents for ratios higher than one. The superposition of the single radius and the radius ratio built up the current simulation model. The threshold value of two that is taken for deciding whether a site is considered to be hazardous to motorcycle riders or not was determined manually. Two (B27 and B164) out of six existing road sections are used to tune the threshold parameter by trying to find the maximum prediction probabilities.

This model configuration outputs accident prediction probabilities between 23% and 73%. The probability of predicting the site of an accident ranges from 28% to 122% and is constantly higher than the accident prediction probability. The reason is that more than one accident can happen at a specific site. If the prediction probability is higher than 100% more potential accidents are predicted than real ones occurred. The mean accident prediction probability is 40% and the mean site prediction probability is 56%.

In future studies multidimensional optimization algorithms can be used to find better tuned constants. The threshold function may not be preset to a constant but transformed into a linear or polynomial function. The other risk parameters presented in the model description may be incorporated into the model. Those require a broader data base to tune the model.

A. Appendix

```
<?xml version="1.0" encoding="UTF-8"?>
<kml xmlns="http://www.opengis.net/kml/2.2"
 xmlns:gx="http://www.google.com/kml/ext/2.2"
 xmlns:kml="http://www.opengis.net/kml/2.2"
 xmlns:atom="http://www.w3.org/2005/Atom">
 <Document>
  <name>KmlFile</name>
  <Style id="s_ylw-pushpin_hl2">
   <IconStyle>
    <scale>1.3</scale>
    <Icon>
     <href>http://maps.google.com/...</href>
    </Icon>
    <hotSpot x="20" y="2" xunits="pixels"
    yunits="pixels"/>
   </IconStyle>
  </Style>
  <StyleMap id="m_ylw-pushpin1">
   <Pair>
    <key>normal</key>
    <styleUrl>#s_ylw-pushpin</styleUrl>
   </Pair>
   <Pair>
    <key>highlight</key>
    <styleUrl>#s_ylw-pushpin_hl2</styleUrl>
   </Pair>
  </StyleMap>
```

```
  <Style id="s_ylw-pushpin">
   <IconStyle>
    <scale>1.1</scale>
    <Icon>
     <href>http://maps.google.com/...</href>
    </Icon>
    <hotSpot x="20" y="2" xunits="pixels"
    yunits="pixels"/>
   </IconStyle>
  </Style>
  <Placemark>
   <name>B27-2</name>
   <styleUrl>#m_ylw-pushpin1</styleUrl>
   <LineString>
    <tessellate>1</tessellate>
    <coordinates>
     15.72930425368495,47.78782291918012,0
     15.72971310040831,47.78763236429659,0
     ...
     ...
     ...
    </coordinates>
   </LineString>
  </Placemark>
 </Document>
</kml>
```

Listing A.1: KML file format structure.

Figure A.1: Map of the road number B27 from Reith to Mitterbach.

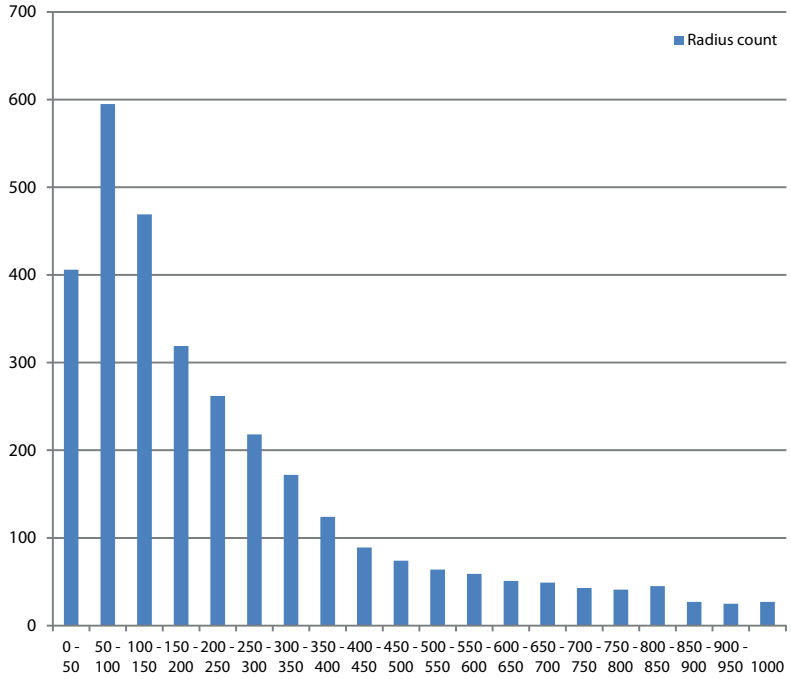

Figure A.2: The radius distribution of the B20 (Reith to Mitterbach) road in 50m steps.

# real accidents	15
# real accidents at distinct sites	9
# predicted risk sites	19
# successfully predicted accidents	11
Accident prediction probability	73%
Site prediction probability	122%

Table A.1: Summary of the B20 (Reith to Mitterbach) road's prediction results.

# real accidents	29
# real accidents at distinct sites	27
# predicted risk sites	16
# successfully predicted accidents	10
Accident prediction probability	34%
Site prediction probability	37%

Table A.2: Summary of the B164 road's prediction results.

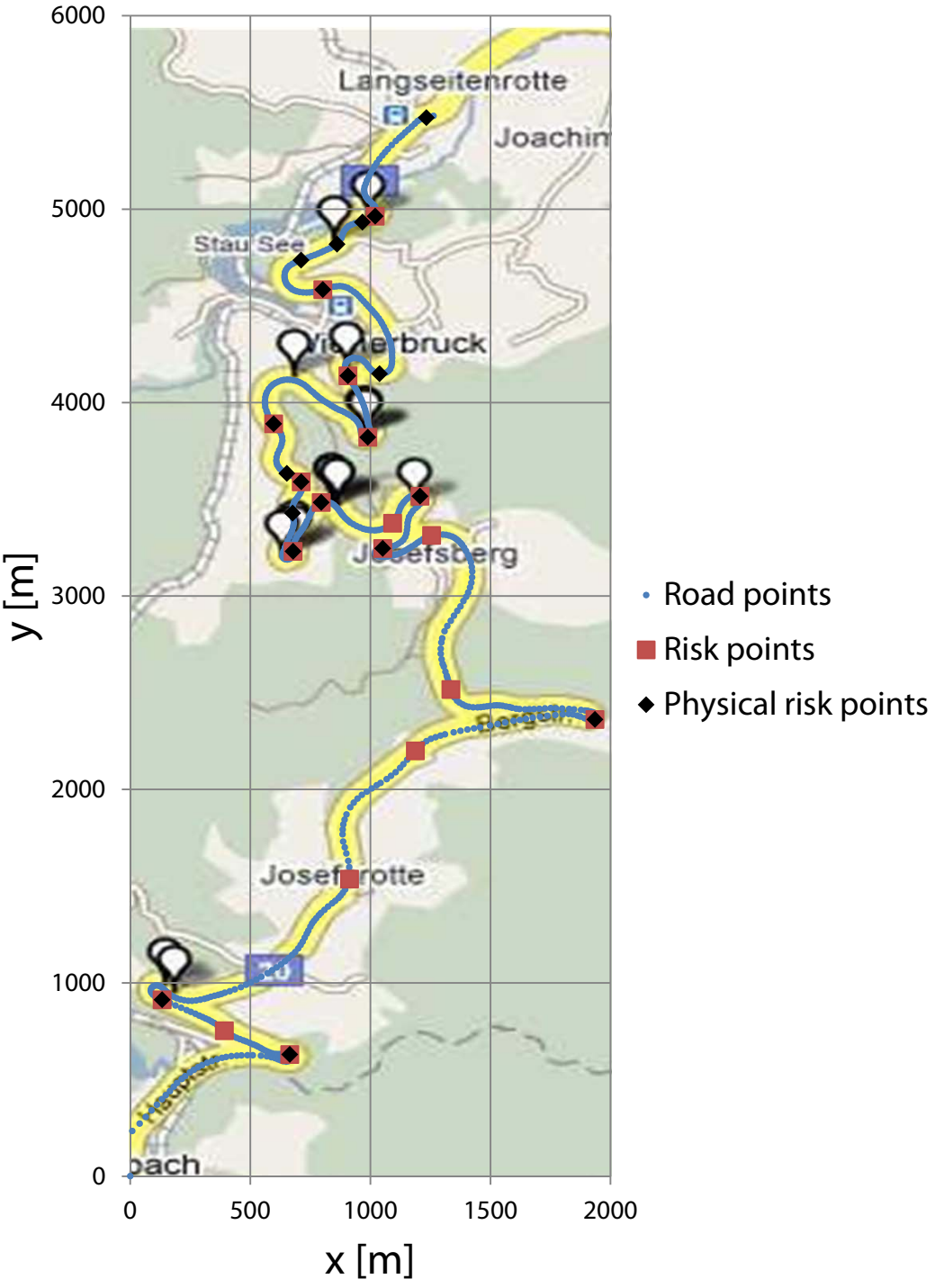

Figure A.3: The B20 (Reith to Mitterbach) road's accident prediction sites results overlayed with the map.

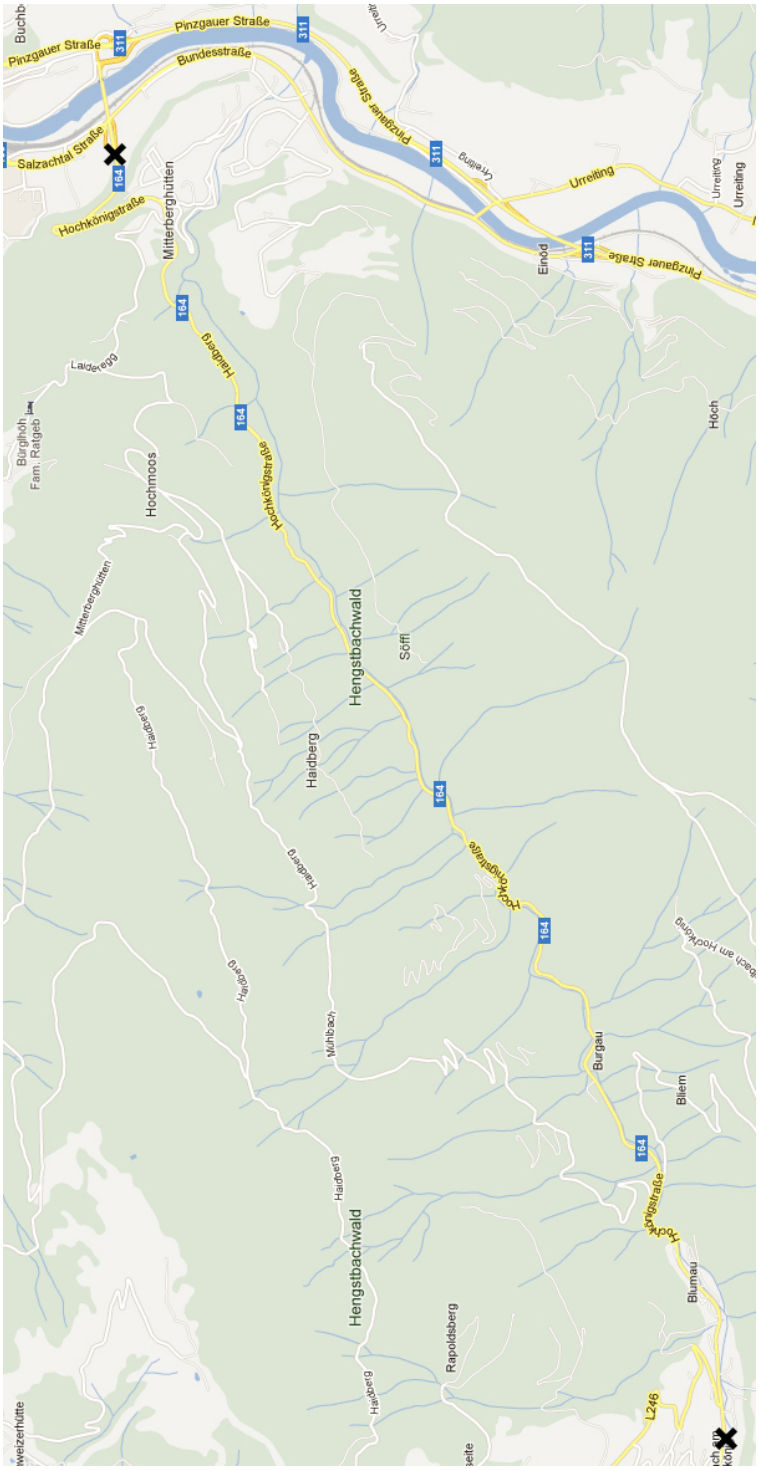

Figure A.4: Map of the road number B27 from Bischofshofen to Muehlbach.

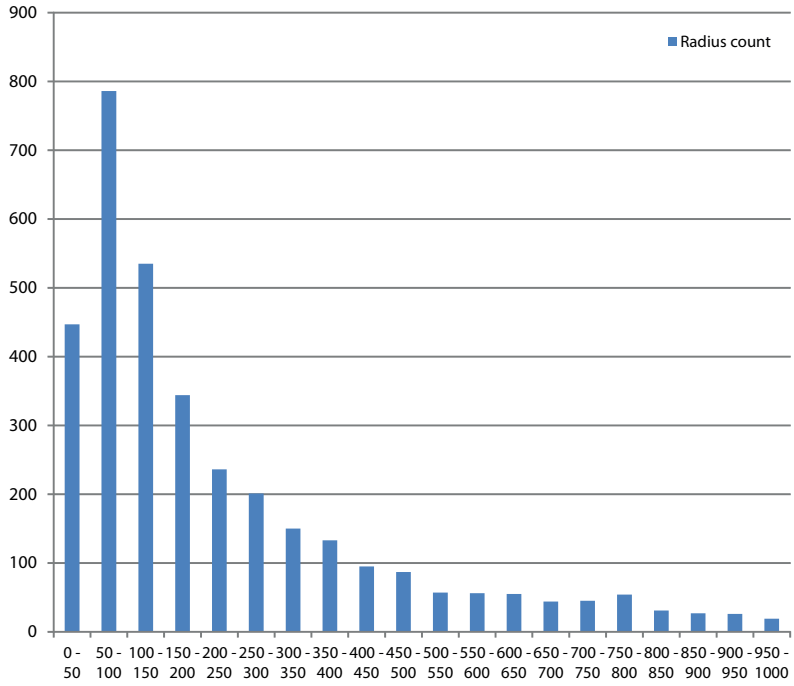

Figure A.5: The radius distribution of the B164 road in 50m steps.

# real accidents	13
# real accidents at distinct sites	9
# predicted risk sites	9
# successfully predicted accidents	3
Accident prediction probability	23%
Site prediction probability	33%

Table A.3: Summary of the B20 (Tuernitz to Annaberg) road's prediction results.

A.0.1 Road - B20 Reith to Mitterbach am Erlaufsee

A.0.2 Road - B164

A.0.3 Road - B20 Tuernitz to Annaberg

A.0.4 Road - B95

A.0.5 Road - B127

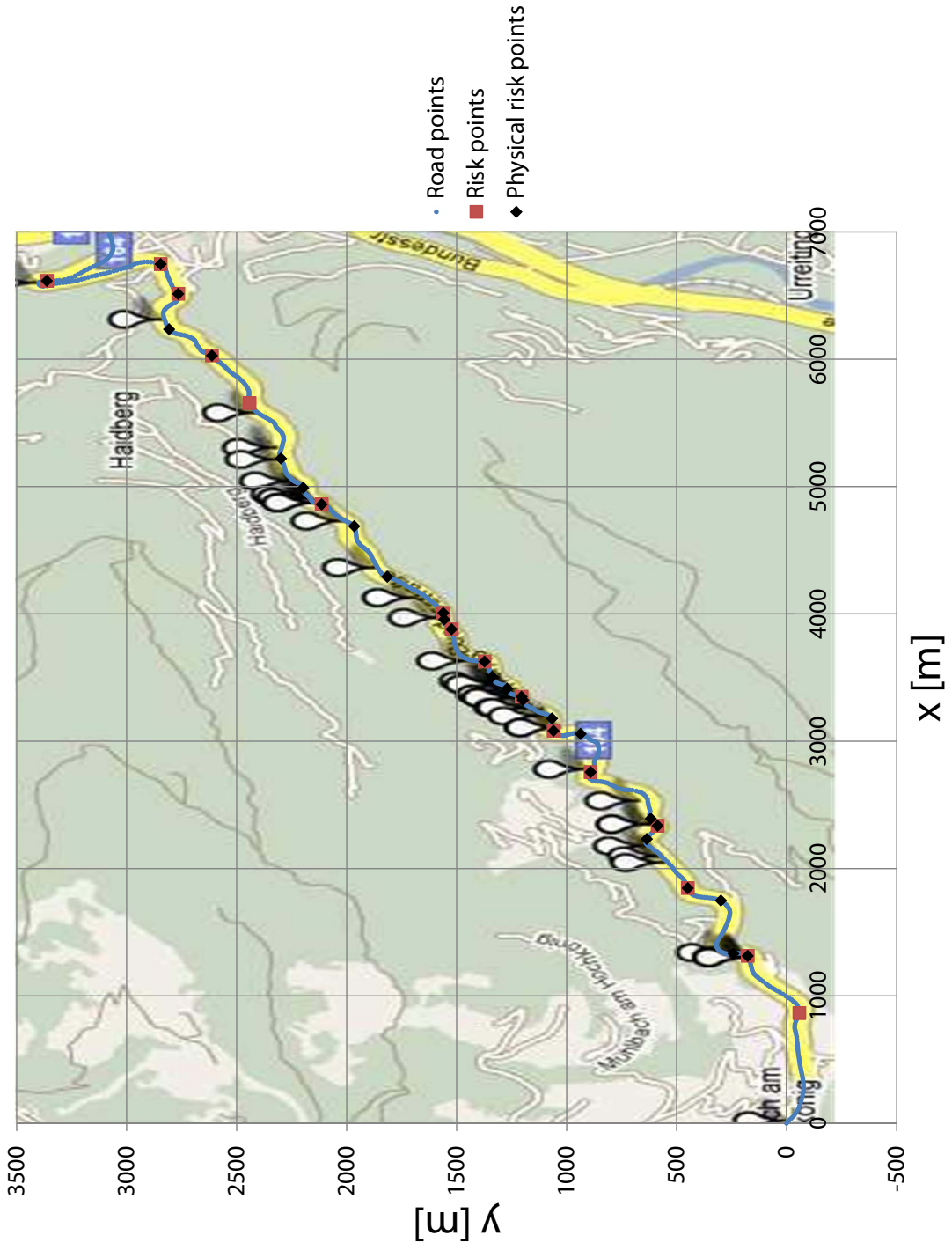

Figure A.6: The B164 road's accident prediction sites results overlayed with the map.

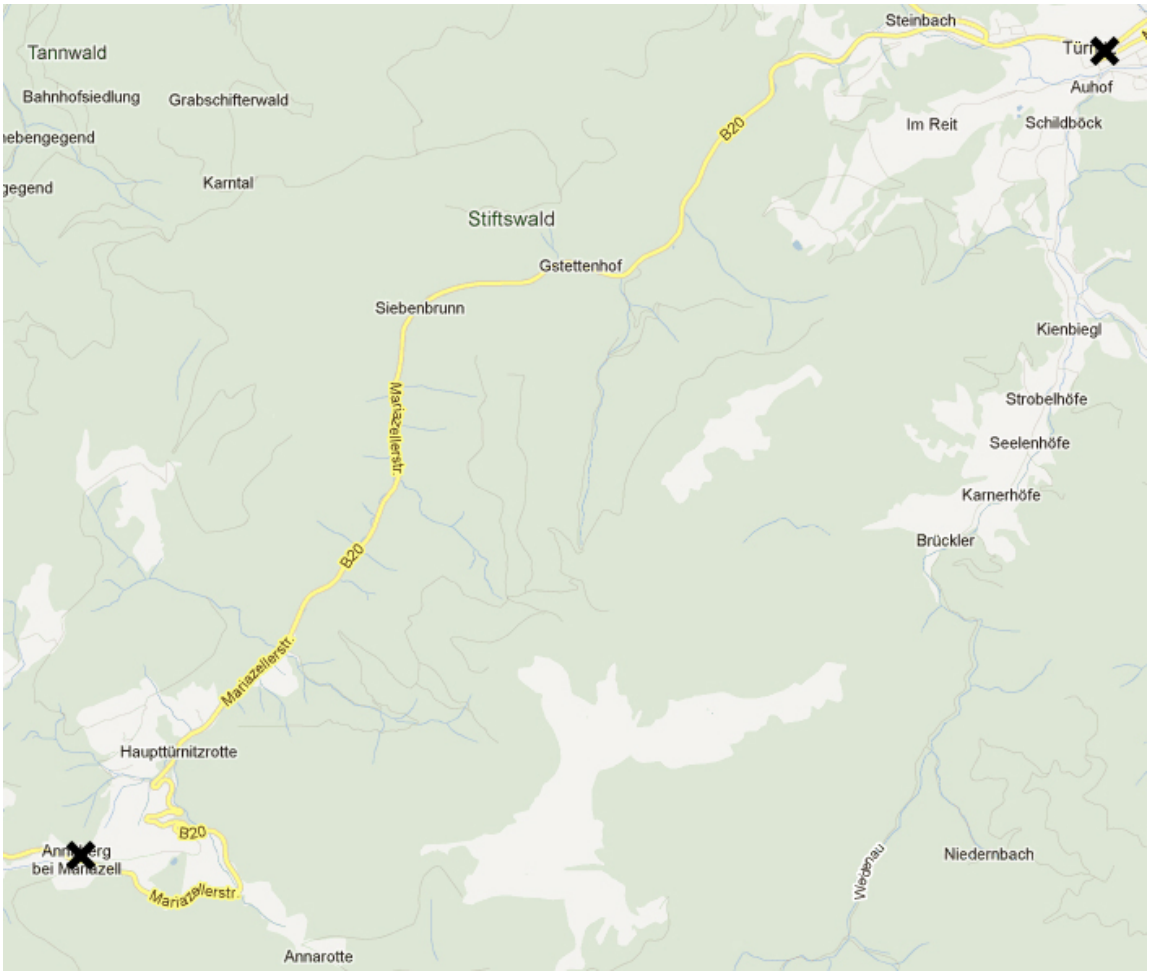

Figure A.7: Map of the road number B27 from Tuernitz to Annaberg.

# real accidents	19
# real accidents at distinct sites	18
# predicted risk sites	9
# successfully predicted accidents	5
Accident prediction probability	26%
Site prediction probability	28%

Table A.4: Summary of the B95 road's prediction results.

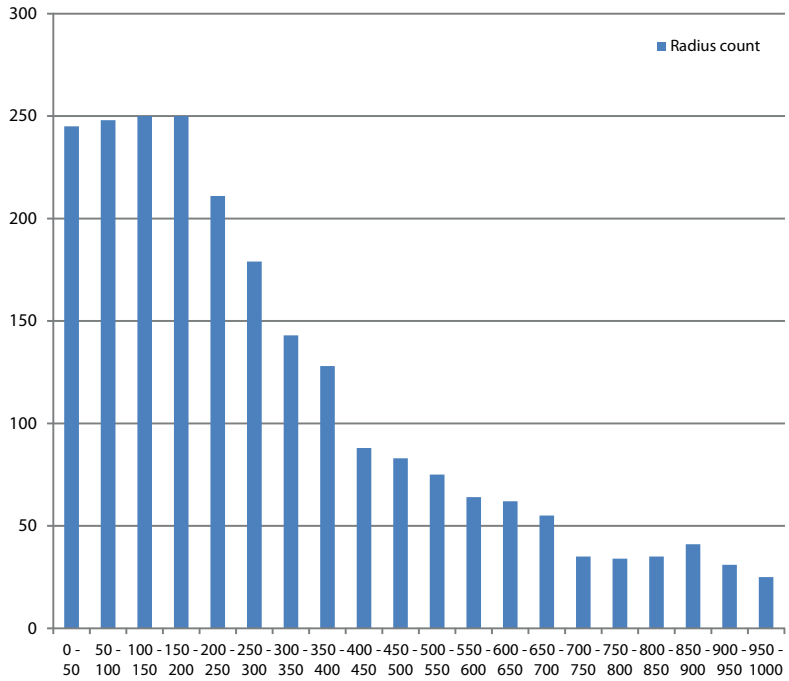

Figure A.8: The radius distribution of the B20 (Tuernitz to Annaberg) road in 50m steps.

# real accidents	12
# real accidents at distinct sites	8
# predicted risk sites	6
# successfully predicted accidents	5
Accident prediction probability	41%
Site prediction probability	63%

Table A.5: Summary of the B127 road's prediction results.

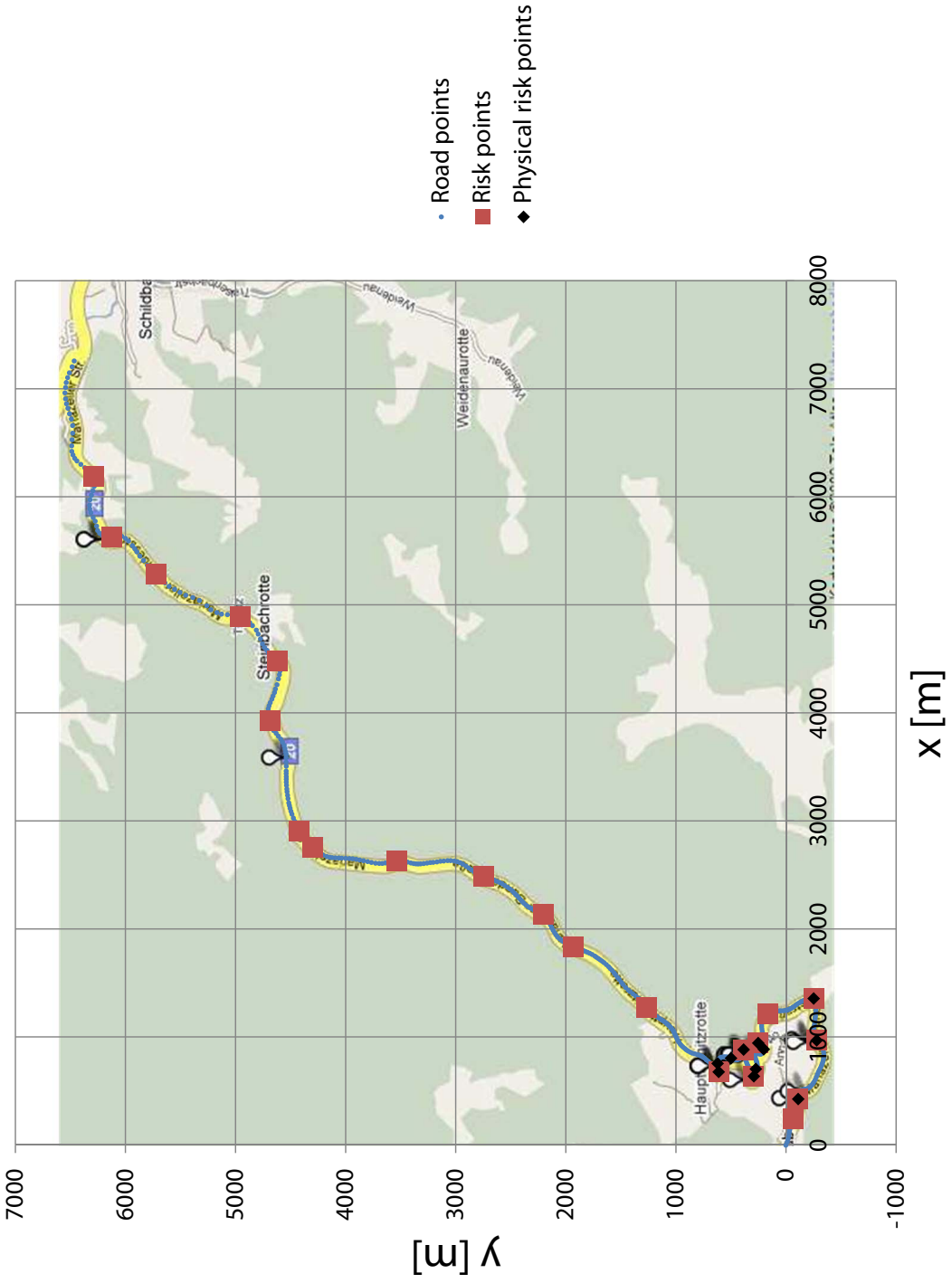

Figure A.9: The B20 (Tuernitz to Annaberg) road's accident prediction sites results overlayed with the map.

Figure A.10: Map of the road number B95 from Reichenau to Turracherhoehe.

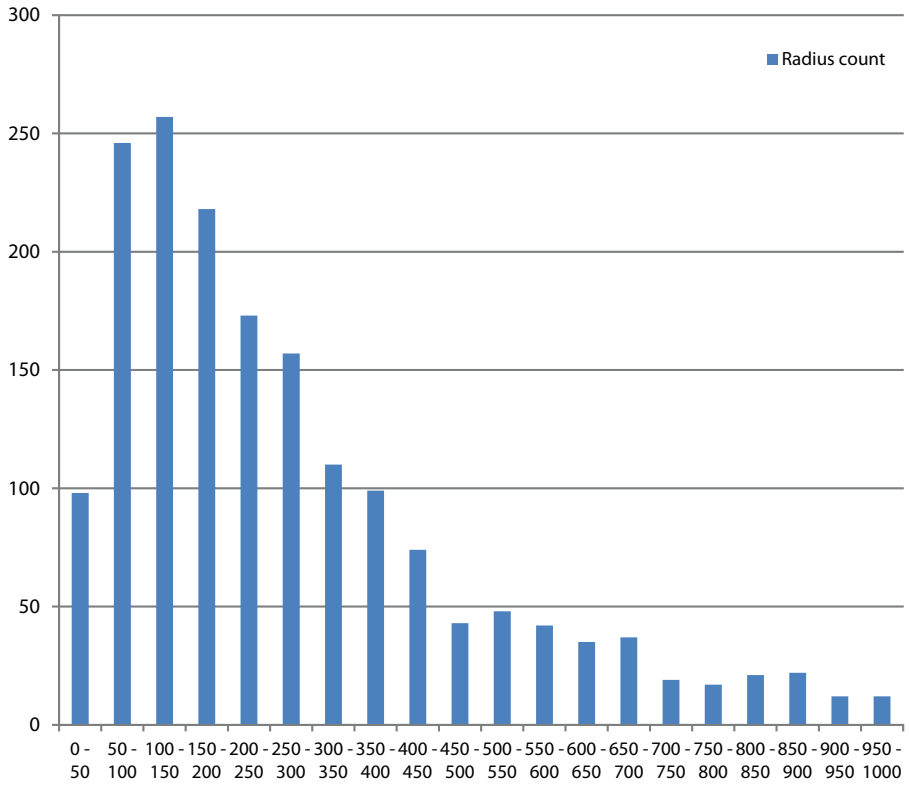

Figure A.11: The radius distribution of the B95 road in 50m steps.

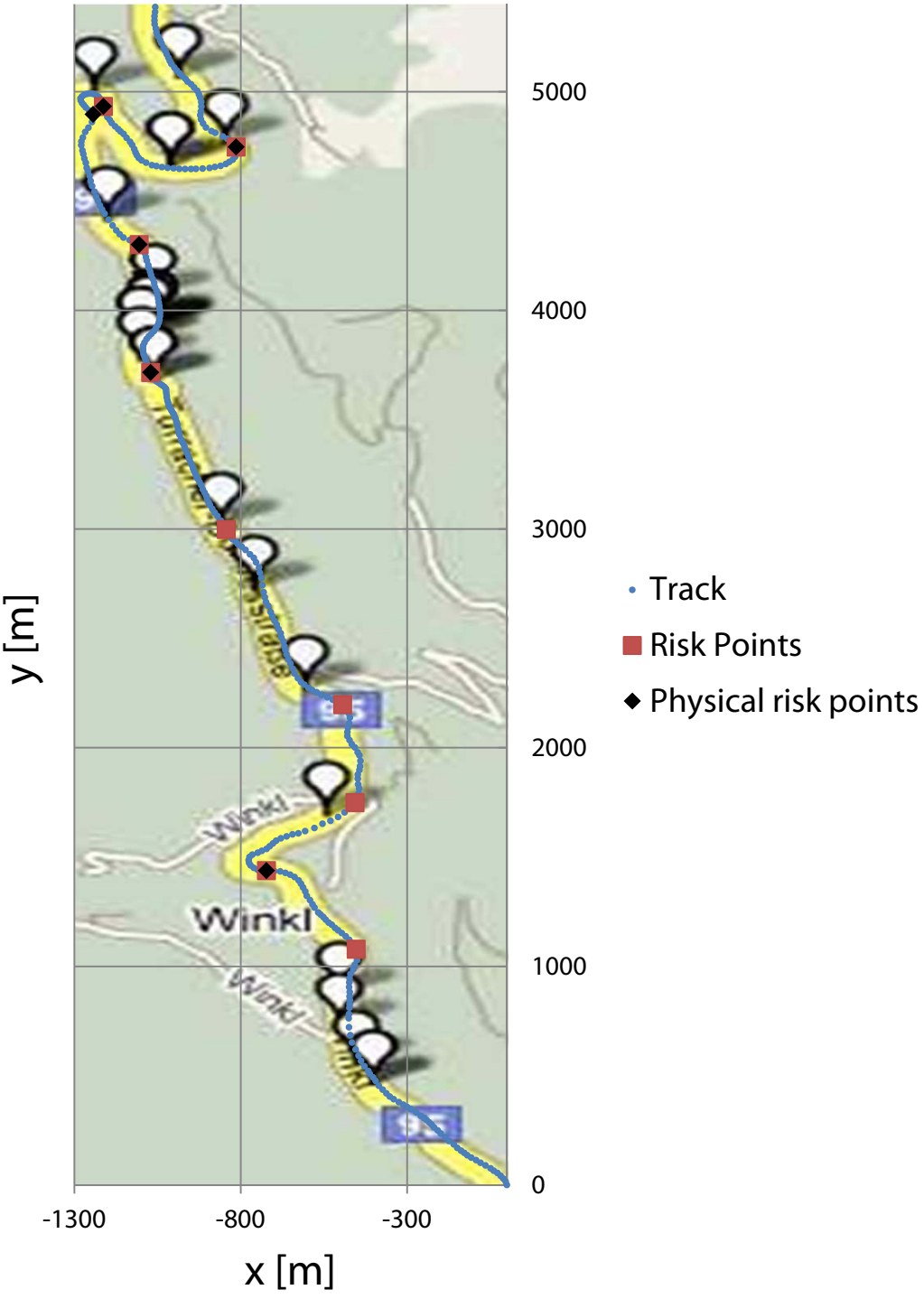

Figure A.12: The B95 road's accident prediction sites results overlayed with the map.

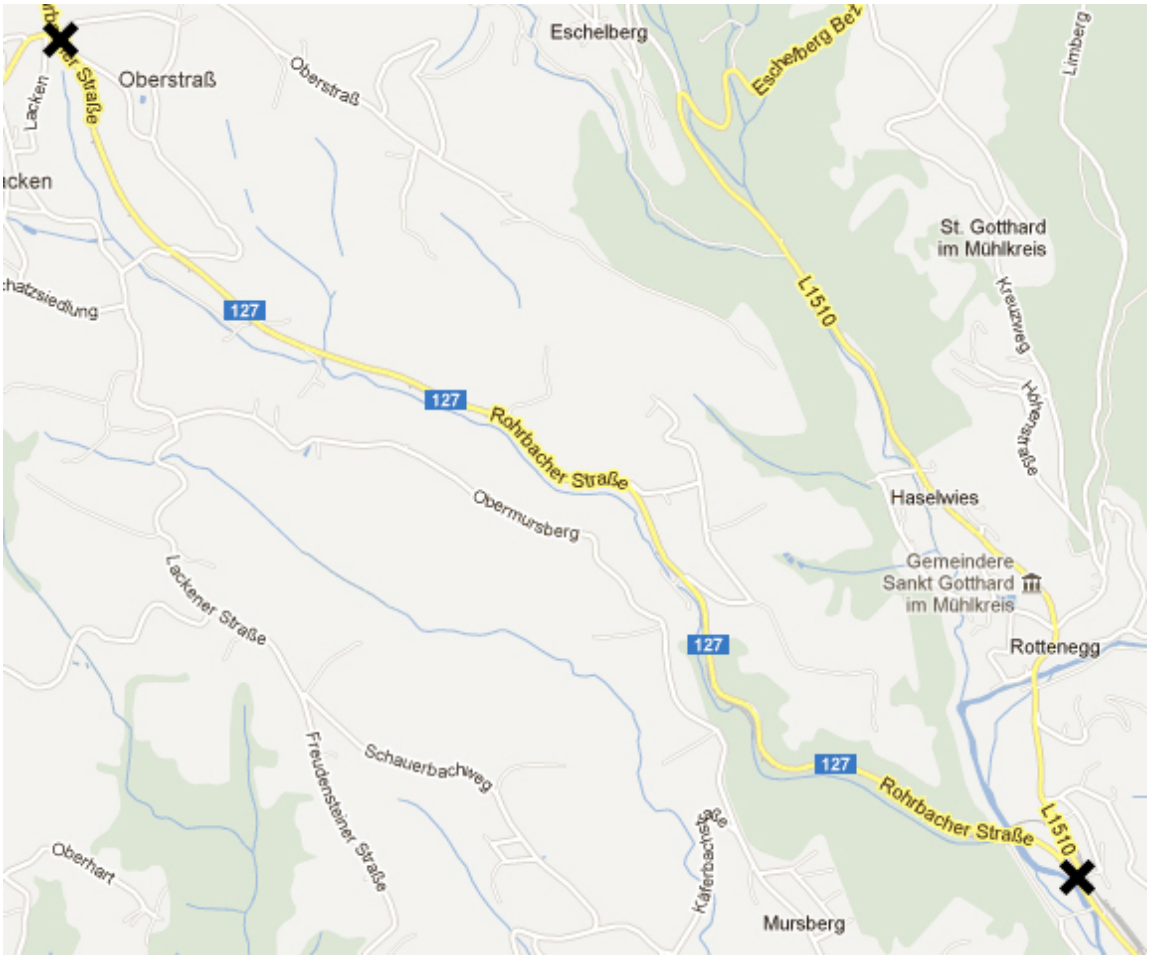

Figure A.13: Map of the road number B127 from Rottenegg to Lacken.

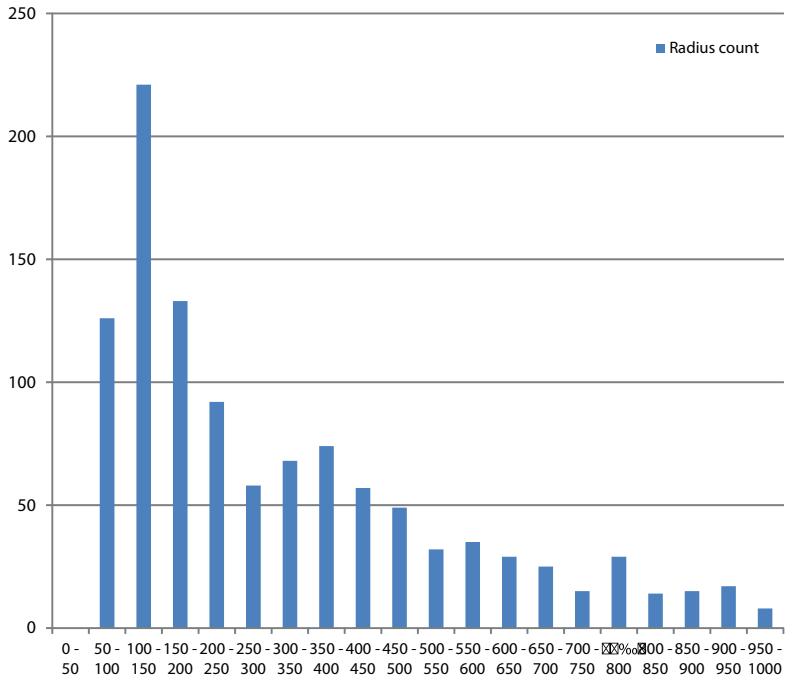

Figure A.14: The radius distribution of the B127 road in 50m steps.

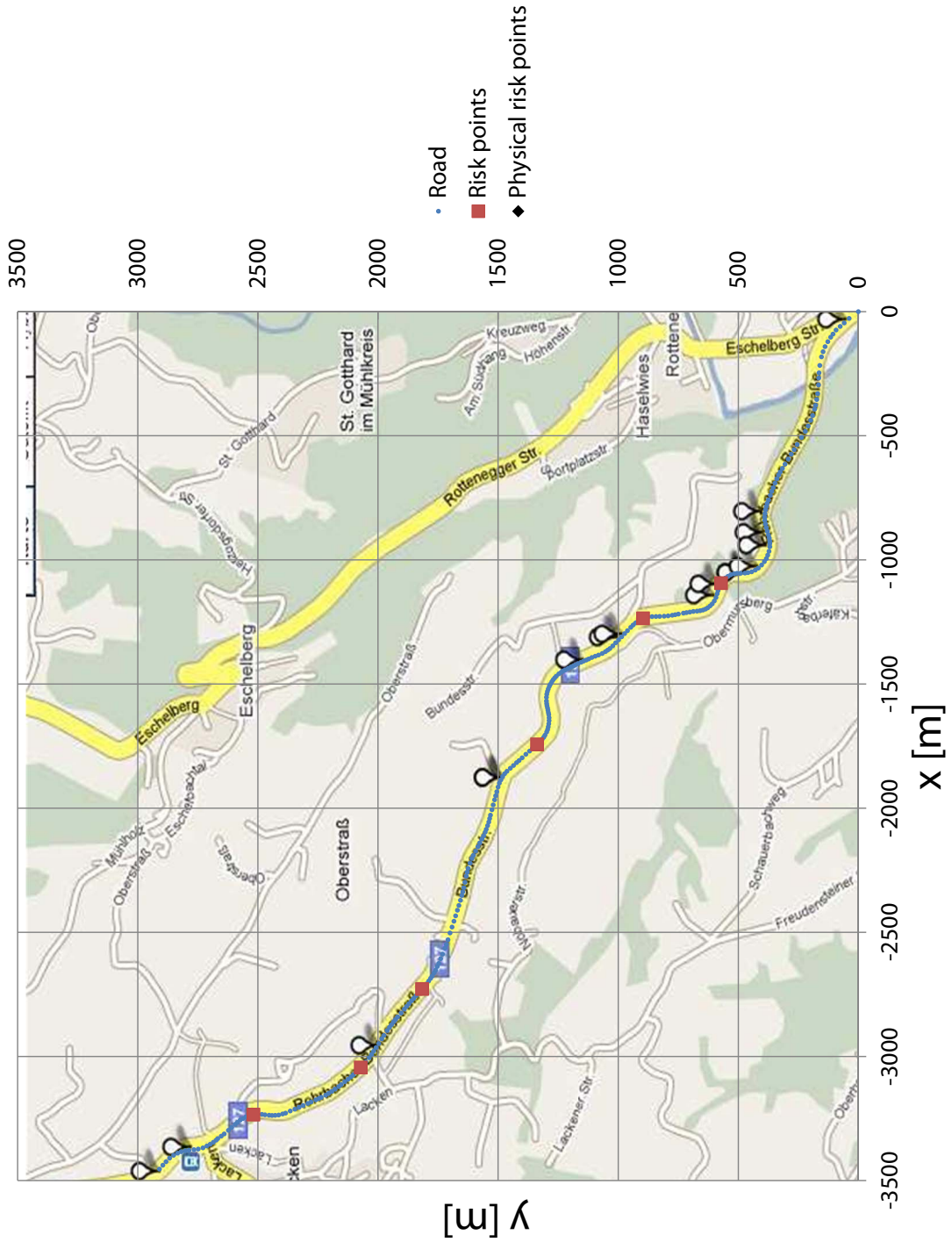

Figure A.15: The B127 road's accident prediction sites results overlayed with the map.

Bibliography

[1] Hartmann C. Analyse von unfallkausalen Zusammenhaengen von Motorradunfaellen in Abhaengigkeit der Radienrelation [master thesis]. Vienna: University of Natural Resources and Life Sciences; 2010. [cited 2012 Jan 15]. Available from: University of Natural Resources and Life Sciences Vienna E-Library.

[2] Schlittgen R. Einfuehrung in die Statistik. 10th ed. Munich: Oldenbourg; 2003. p. 225.

[3] Allgemeiner Deutscher Automobil-Club e.V. (ADAC). Motorrad fahren auf sicherer Straße! Ein Leitfaden für die Praxis [report on the internet]. Munich: ADAC; 2010. Available from: `http://www.ifz.de/Publikationen/Praxishefte\%20DVR.pdf`. [Accessed 05/13/2012].

[4] Statistisches Bundesamt. Unfallentwicklung auf deutschen Straßen 2010 [report on the internet]. Wiesbaden: Statistisches Bundesamt; 2011. Available from: `https://www.destatis.de/DE/Publikationen/Thematisch/TransportVerkehr/Verkehrsunfaelle/Unfallentwicklung5462401109004.pdf?__blob=publicationFile`. [Accessed 05/15/2012].

[5] Kuratorium für Verkehrssicherheit. Verkehrsunfallstatistik 2011 [database on the internet]. Available from: `http://www.kfv.at/unfallstatistik/index.php?id=57`. [Accessed 05/15/2012].

[6] Limebeer D. J. N, Sharp R. S. Bicycles, Motorcycles, and Models: Single-track vehicle modelling and control [magazine on the internet]. IEEE Control Systems Magazine; 2006.

[7] Gross D., Hauger W., Schröder J., Wall W. A. Technische Mechanik 3: Band 3 - Kinetik. 9th ed. Berlin Heidelberg: Springer; 2006.

[8] DellAcqua G., Russo F. Accident prediction models for road networks [report on the internet]. Naples: University of Naples Federico II. Available from: www.4ishgd.valencia.upv.es/index_archivos/38.pdf. [Accessed 06/04/2012].

[9] Eenink R., Reurings M., Elvik R., Cardoso J., Wichert S., Stefan C. Road Safety Impact Assessment [report on the internet]. Available from: http://ec.europa.eu/transport/roadsafety_library/publications/ripcord_d02_road_safety_impact_assessment.pdf. [Accessed 06/04/2012].

[10] Abel R. E. Evaluation of crash rates and causal factors for high risk locations on rural and urban two-lane highways in Virginia [report on the internet]. Richmond: University of Virginia. Available from: http://www.vhb.com/SiteObjects/published//4FCC5B454FF7253000FE9B66206DA365/C156E3A7569BAF6E31D5A699DF169E65/file/BAbel_VTC_07.pdf. [Accessed 06/04/2012].

[11] Moghaddam F. R., Afandizadeh Sh., Ziyadi M. Prediction of accident severity using artificial neural networks. International Journal of Civil Engineering. 2011 March; 9(1): 41-49.

[12] Lester A. H., Garber N. J., Adel, W. S. Transportation Infrastructure Engineering: A Multimodal Integration. SI ed. Virginia: Thomson Learning; 2010.

[13] Aworemi, Remi J., Abdul-Azeez, Adegoke I., Olabode, Oluwaseun S. Analytical study of the causal factors of road traffic crashes in southwestern Nigeria. International Research Journals. 2010 May; 1(4): 118-124.

[14] Bundesministerium für Inneres. Aus dem Inneren: Verkehrsdienst der Bundespolizei: Fachgespräch mit Innenministerin Maria Fekter am 22. Juni 2010 [report on the internet]. Available from: http://www.bmi.gv.at/cms/BMI_Service/Aus_dem_Inneren/Verkehrsdienst_der_Bundespolizei.pdf. [Accessed 05/15/2012].

[15] Abel R. E. Evaluation of crash rates and causal factors for high risk locations on rural and urban two-lane highways in Virginia [report on the internet]. Virginia: M.S. Civil Engineering, the University of Virginia. Available from: http://www.vhb.com/SiteObjects/published//4FCC5B454FF7253000FE9B66206DA365/C156E3A7569BAF6E31D5A699DF169E65/file/BAbel_VTC_07.pdf. [Accessed 06/24/2012].

[16] Bayer B. Das Pendeln und Flattern von Krafträdern. 2th ed. Bochum: Institut für Zweiradsicherheit GmbH; 1987.

[17] Stamatelatos M., Vesely W., Dugan J., Fragola J., Minarick J., Railsback J. Fault Tree Handbook with Aerospace Applications [report on the internet]. 1.1 ed. Washington D.C.: NASA Office of Safety and Mission Assurance, NASA Headquarters; 2002. Available from: http://www.hq.nasa.gov/office/codeq/doctree/fthb.pdf. [Accessed 08/15/2012].

[18] American Concrete Pavement Association. The International Roughness Index (IRI): What is it? How is it measured? What do we need to know about it? [report on the internet]. Skokie: American Concrete Pavement Association; 2002. Available from: http://www.acpa.org/Downloads/RT/RT3.07.pdf. [Accessed 09/25/2012].

[19] Cossalter V., Lot R. A Motorcycle Multi-Body Model for Real Time Simulations Based on the Natural Coordinates Approach. Vehicle System Dynamics. 2002; 37(6): 423-447.

[20] Taner A. Vergleich verschiedener Systeme zur Sichtverbesserung bei Nacht in Personenkraftwagen. 1st ed. Goettingen: Cuvillier Verlag; 2007